THE USE OF MICROBIAL IRON CHELATORS AND POLYAMINE
ANALOGUES AS ANTINEOPLASTICS

By

MICHAEL JOSEPH INGENO

A DISSERTATION PRESENTED TO THE GRADUATE SCHOOL
OF THE UNIVERSITY OF FLORIDA IN PARTIAL FULFILLMENT
OF THE REQUIREMENTS FOR THE DEGREE OF
DOCTOR OF PHILOSOPHY

UNIVERSITY OF FLORIDA

1988

This work is dedicated to my family, with love.

ACKNOWLEDGMENTS

TABLE OF CONTENTS

Abstract of Dissertation Presented to the Graduate School
of the University of Florida in Partial Fulfillment of the
Requirements for the Degree of Doctor of Philosophy

THE USE OF MICROBIAL IRON CHELATORS AND POLYAMINE
ANALOGUES AS ANTINEOPLASTICS

By

Michael Joseph Ingeno

December 1988

Chairman: Raymond J. Bergeron
Major Department: Medicinal Chemistry

This research focuses on the development of compounds which are
effective in controlling the growth of cancer cells. The two classes
of agents studied are the microbial iron catecholamide chelators
(siderophores) and the N-alkyl polyamine analogues.

The biological activity of the catecholamide chelators, parabac-
tin and vibriobactin, has been assigned, at least in part, to their
ability to chelate iron and inhibit the iron dependent enzyme ribonuc-
leotide reductase. These siderophores are potent inhibitors of neo-
plastic cell growth, with 50% inhibitory concentrations in the micro-
molar range. The ligands have pronounced effects on cell cycle kinet-
ics producing a G_1-S cell cycle block. On short term exposure to the
chelators, this block in DNA synthesis is reversed simply by washing
the chelator away. The cells remained synchronized for at lease three
cycles after release of the block. The cell cycle block and synchroni-
zation induced by the chelators may be exploited to potentially enhance
cytotoxicity when used in combination with other antineoplastics.

v

The biological activity of the N-alkylated polyamine derivatives has been postulated to be a consequence of their similarity to the natural intracellular polyamines, spermidine and spermine in terms of uptake, while functionally they are unable to fulfill or interfere with important roles of the natural polyamines. Inhibition of cell growth may result as a consequence of alterations in the polyamine biosynthetic network. Preliminary studies of the structural boundary conditions required for significant antiproliferative activity of the polyamine analogues have been carried out. The most active analogues, the terminally diethylated tetramines N^1,N^{12}-diethylspermine and N^1,N^{14}-diethylhomospermine, have been shown to be potent inhibitors of neoplastic cell growth, with 50% inhibitory concentrations in the micromolar range in vitro and significant in vivo activity. They have been found to have only incidental effects on nuclear DNA, while having profound effects on mitochondrial DNA.

Results are presented as to the action of these drugs both in vitro and in vivo. From these studies a great deal has been determined about the growth inhibitory effects, mechanisms of actions, broadness of activity against various cell lines, structure activity relationships, and effectiveness of these compounds either alone or in combination with other agents.

INTRODUCTION

This research focuses on the development of compounds which are effective in controlling the growth of cancer cells.

Catecholamide Iron Chelators

The first part of the dissertation is concerned with the evaluation of catecholamide iron chelators as a means of controlling the proliferative processes. Over the past decade there has been a dramatic increase in the attention given to the crucial role which iron plays in proliferative processes. Although iron has oxidation states between -2 and +6, the equilibrium between the +2 and +3 oxidation states, an equilibrium which is very sensitive to both ligation and pH (1), best characterizes the biological use of this metal. This transition metal plays a critical role in a variety of biological redox systems within the cell, e.g., the cytochromes, peroxidases, catalases, and ribonucleotide reductase (2). Even though virtually all organisms are auxotropic for Fe(III), because of the insolubility of ferric hydroxide $(Fe(OH)_3)$, the predominant form of the metal under physiological conditions $(K_{sp}=10^{-38}M^4)$, nature has had to develop rather sophisticated mechanisms for accessing the metal (3).

Microorganisms produce low-molecular weight ligands (siderophores) which chelate and facilitate transport of iron into the cell (2). Most of these siderophores fall into two general structural classes, hydroxamates and catecholamides (4). The catecholamides,

1

typified by enterobactin (Fig. 1-1a), generally form tighter iron complexes (metal-ligand formation constant $(K_f=10^{48}M^{-1})$ (5) than the hydroxamates, exemplified by desferrioxamine (Fig. 1-1b) $(K_f=10^{31}M^{-1})$ (6).

Mammalian cells have developed larger, more complicated molecules, iron binding proteins for the metal's transport and utilization: e.g., the iron shuttle proteins, transferrin (7), lactoferrin (8), uteroferrin (9), and the iron storage protein, ferritin (10). It has been suggested that the virulence of pathogenic bacteria may be partially related to the efficiency with which its siderophore removes iron from these iron binding proteins (11).

Transferrin, the major iron transport protein in animals, binds two iron atoms in the +3 oxidation state, each with a slightly different metal-protein formation constant. This binding is very sensitive to the oxidation state of the metal and to pH with an apparent iron binding constant at physiological pH of $K_f=10^{28}M^{-1}$ (12). Once the transferrin is bound to the transferrin receptor on the cell's surface, it is internalized via endocytotic vesicles. The iron-protein-receptor complex enters a nonlysosomal acidic vacuole where conditions favor release of the iron for utilization or storage as an iron-ferritin complex. The apotransferrin-receptor complex then returns to the cell surface where the apotransferrin is released for further use (13).

The number of transferrin receptors on a cell membrane has been directly linked to the proliferative state of the cell and/or the
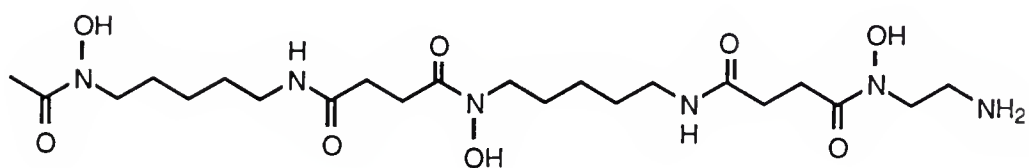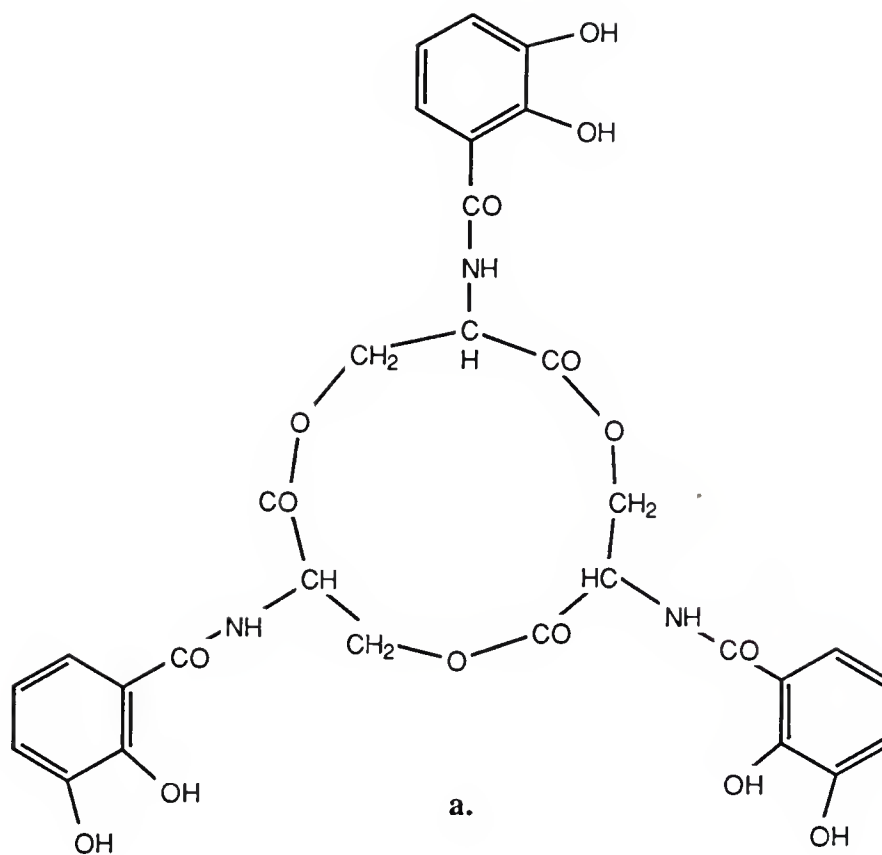
Figure 1-1. The microbial iron chelators

    a.   Enterobactin
    b.   Desferrioxamine

availability of iron (14). For example, it has been observed that highly proliferative cells have significantly greater numbers of transferrin receptors than resting cells (15). Alternatively, if iron is withheld from cells there is a substantial increase in the number of transferrin receptors (16). This increase is due to stimulation of synthesis and translation of the transferrin receptor mRNA, and can be inhibited by the addition of iron (17). Conversely, if iron is added to the cells in a utilizable form there is a dramatic decrease in transferrin receptor expression, and an increase in cellular ferritin iron as a means of defense against bacterial infection and neoplasms.

It is interesting to observe how the body alters iron metabolism in response to a bacterial infection. In the course of an infection, the body attempts to withhold iron from the invading organism by decreasing gastrointestinal absorption of iron, lowering the serum transferrin iron saturation, and increasing liver ferritin levels and iron ferritin storage in reticuloendothelial systems (18). The same response is seen in febrile states, neoplasia, and on injection of various sham substances (19). It has been demonstrated that mice fed a low iron diet developed smaller and slower growing tumors than mice maintained on a normal iron diet (20). Conversely, iatrogenic iron overload as well as idiopathic hemochromotosis, a genetic disease characterized by iron overload, have been associated with increased incidence of neoplasia (21,22). These findings suggest continued study of the role of iron metabolism in malignancy and the possible adverse effects of iron supplementation in patients with cancer.

There is evidence to indicate that activated macrophage cytotoxicity may be mediated by iron removal from the target cells (23). A

selective inhibition of iron dependent DNA replication and mitochondrial respiration is observed. The authors speculate that a macrophage-derived iron chelator could be involved, leading to cytostasis. Later studies (24) found that aconitase, a citric acid cycle enzyme containing iron-sulfur clusters, activity declined simultaneously with arrest of DNA synthesis. The cytotoxic activated macrophage-induced inhibition of aconitase is shown to be due to loss of iron from the iron-sulfer cluster. More recently (25), a newly discovered cyclic hydroxamate siderophore, bisucaberin, was found to render tumor cells susceptible to cytolysis mediated by macrophages and showed specific inhibition by addition of ferric iron.

One of iron's more interesting roles in cells is its association with ribonucleotide reductase (Fig. 1-2), an enzyme which catalyses the production of deoxyribonucleotides in the rate limiting step of DNA synthesis (26). In mammalian cells, ribonucleotide reductase consists of two nonidentical dimer subunits, M1 and M2, analogous to the B1 and B2 subunits of Escherichia coli (E. coli) (27). The M2 dimer contains a nonheme iron center. The metal stabilizes a tyrosyl free radical at the active site and, due to the rapid turnover of the enzyme, a constant supply of iron is essential for the enzyme's activity (28). Ribonucleotide reductase levels are elevated in neoplastic cells and have been shown to be transformation-linked and progression-linked in a series of hepatomas (29).

If the theory that withholding iron as a defense mechanism against neoplasia is correct, then artificially inducing a state of iron deprivation by means of the siderophores may prove to be effective in controlling neoplastic cell growth. Iron chelators could control
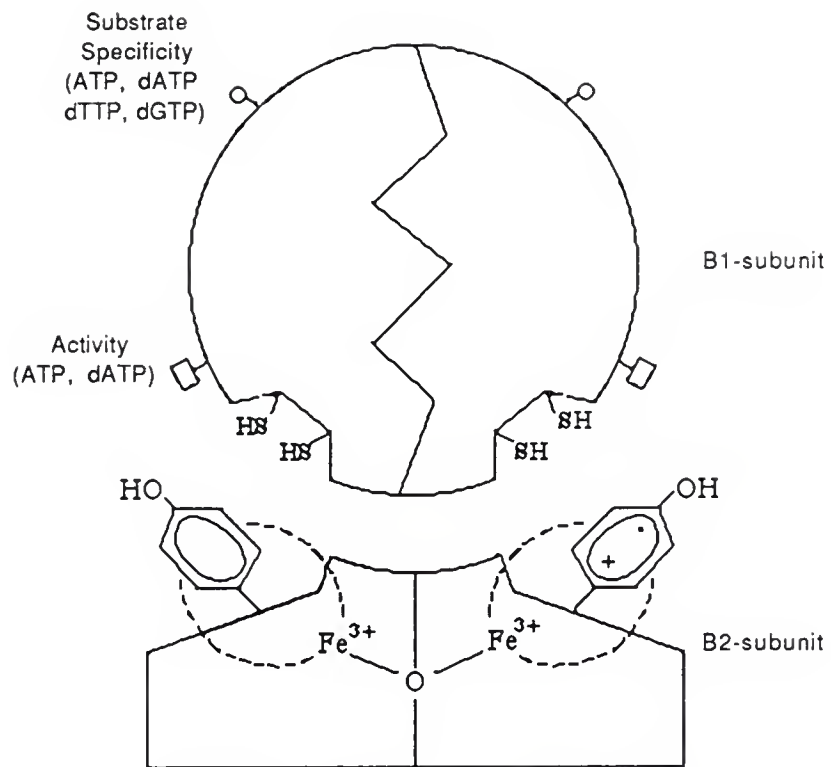
Figure 1-2. Model of _E. coli_ ribonucleotide reductase (from Ref. 26).

cellular proliferation by complexing extracellular iron (including that bound to transferrin), "free" cytoplasmic iron, and/or iron bound to critical proteins or enzymes.

There are several rationales for the use of the microbial catecholamide iron chelators as a means of controlling neoplastic growth.

1. The formation constants for the catecholamide iron complexes ($K_f=10^{46}$-10^{52} M^{-1}) are far greater than those observed for chelators previously used as antiproliferatives (4). Considering how effectively the catecholamide siderophores bind iron, one would expect these chelators to remove iron from several enzyme bound sites, e.g., ribonucleotide reductase, mitochondrial enzymes, as well as from transferrin. However, in spite of the thermodynamic binding advantage these ligands have over various proteins, if the ligand cannot access the protein bound iron, it obviously cannot remove it. Thus, removal of iron is a kinetic problem.

2. Previously low biological yields from microorganisms and tedious isolation procedures of these compounds limited their use. Chemical schemes have now been devised for the efficient synthesis of the catecholamide microbial siderophores as well as a number of synthetic analogues (30-32). The natural products are 2,3-dihydroxybenzoylamide derivatives of polyamines, e.g., N^1,N^8-bis(2,3-dihydroxybenzoyl)spermidine (compound II) and parabactin, first isolated from cultures of Paracoccus denitrificans by Tait (33) and vibriobactin, isolated from Vibrio cholerae by Neilands et al. (34) (Fig. 1-3).

3. It has been postulated that the transferrin receptor is a potential marker for the identification of proliferating cells (35).
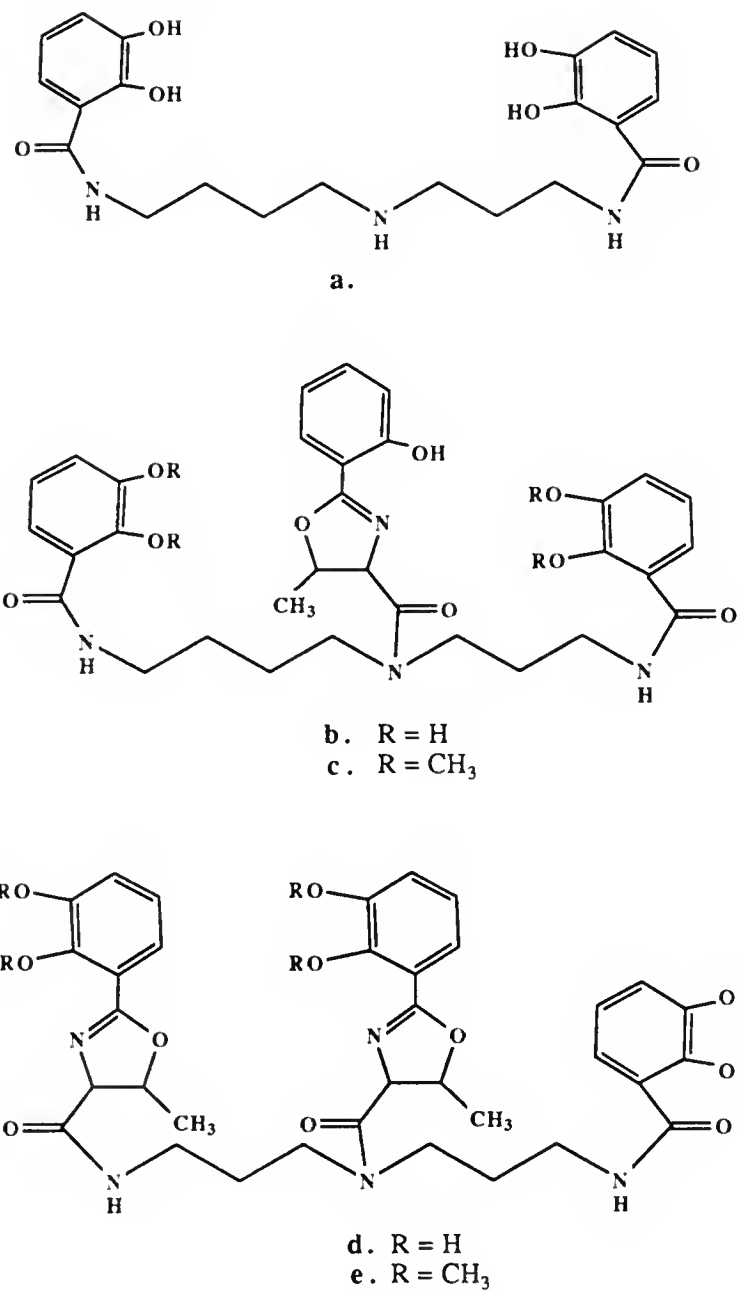
Figure 1-3. The catecholamide iron chelators.

a. Compound II
b. Parabactin
c. Tetramethyl parabactin
d. Vibriobactin
e. Permethylated vibriobactin

In a study using monoclonal antibodies to the transferrin receptor, it was found that in all cases of breast carcinomas transferrin receptors could be detected while in samples of normal breast tissue little or no evidence of staining was exhibited (36). The evidence that neoplastic cells, as indicated by their uninhibited proliferation and increased means of iron acquisition, have higher iron requirements in comparison to host cells provides a rationale for the potential selectivity of iron removal by the microbial iron chelators as a target in antineoplastic strategy.

4. Evidence suggested that the catecholamide chelators could penetrate cellular membranes. A correlation between antiproliferative activity and octanol/saline partition coefficients for a series of siderophores has been established (37). It was found that the ratios of the ligand partition coefficients between octanol and phosphate buffered saline for the catecholamides versus dihydroxybenzoic are closer to the ratios of the ligand's antileukemic activity than are the ratios of their binding constants. This suggested that cellular penetration as well as iron-chelation potential may determine the chelator's antiproliferative activity.

5. Parabactin and compound II have pronounced inhibitory effects on the growth of L1210 cells in vitro with IC_{50} values in the micromolar range (38). These values are in the range of antineoplastics currently being used and are at concentrations attainable as serum levels in vivo.

6. There is good evidence that the catecholamide siderophores, unlike previously studied chelators, are relatively nontoxic to the

host. It has been observed that compound II, the biological precursor
to parabactin, has an LD_{50} in mice greater than 800 mg/kg when given as
a single intraperitoneal (i.p.) injection (39). It has been further
observed that compound II and parabactin at concentrations up to 2 mM
(100 times the 50% inhibitory concentration for murine L1210 leukemia
in vitro) appeared to be nontoxic to a confluent monolayer of monkey
kidney cells (37).

7. The iron dependent enzyme ribonucleotide reductase is a suit-
able target for antineoplastic activity of the catecholamide chelators.
Hydroxyurea, an inhibitor of ribonucleotide reductase (40), has found
clinical usefulness as an anticancer agent. A number of other less
avid iron chelators such as desferrioxamine (41), α-picolinic acid (42)
as well as certain toxic thiosemicarbazones (43) have been shown to
inhibit tumor growth by interfering with ribonucleotide reductase
activity.

Parabactin and compound II have been shown to be potent inhibi-
tors of ribonucleotide reductase activity and to block DNA biosynthesis
at the G_1-S boundary of the cell cycle. However, RNA and protein syn-
thesis were inhibited to a much lesser extent, and DNA polymerase activ-
ity was essentially unaffected (38). Alterations in intracellular deox-
ynucleoside triphosphate levels revealed elevated dTTP pool and lower-
ing of dATP pool size as is characteristic of other ribonucleotide
reductase inhibitors. Cytidine diphosphate (CDP) reductase activity
was inhibited by >97% in L1210 cells treated for 4 h with 5 μM parabac-
tin. The cell cycle block seen in L1210 cells after a 4 h exposure to 5
μM parabactin could be partially reversed by the addition of exogenous

$Fe(Cl)_3$ and the bulk of the cells cascade into S-phase 3 h later. Catecholamide chelators have also demonstrated pronounced effects against the DNA virus Herpes simplex type I (37), another ribonucleotide reductase dependent system, while they were inactive against the RNA virus, Vesicular stomatitis.

It is clear that there is sufficient evidence to suggest that iron withholding should be pursued as a means of controlling the proliferative process. The microbial catecholamide siderophores and their synthetic derivatives may represent an important class of pharmacological agents with potential value in the treatment of proliferative disorders. They may prove useful in cancer chemotherapy as single agents or in combination with other agents.

Polyamine Analogues

The second part of this dissertation deals with the evaluation of the N-alkylated derivatives of the polyamines as potential antiproliferatives. The role of polyamines in proliferative processes has been extensively reviewed in recent years (44-50). The polyamines spermidine, spermine, and the diamine putrescine (Fig. 1-4) are present in all mammalian cells and are required for normal cellular maintenance, proliferation, and differentiation. These basic amines are extensively protonated at physiological pH and capable of electrostatic interactions with a variety of macromolecules including nucleic acids and proteins. Although many roles have been ascribed to the polyamines, their exact functions in cellular physiology are not yet well understood.

The intracellular concentrations of these polyamines are maintained through a highly regulated metabolic system (49,50) (Fig. 1-5).
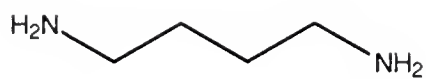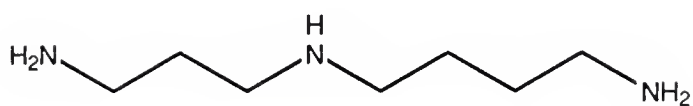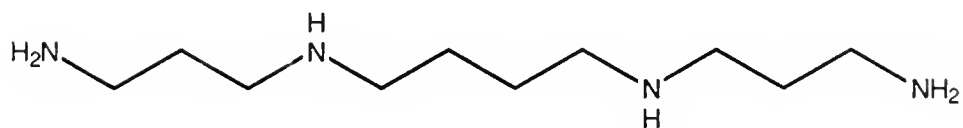
Figure 1-4. The polyamines.

a. Putrescine
b. Spermidine
c. Spermine
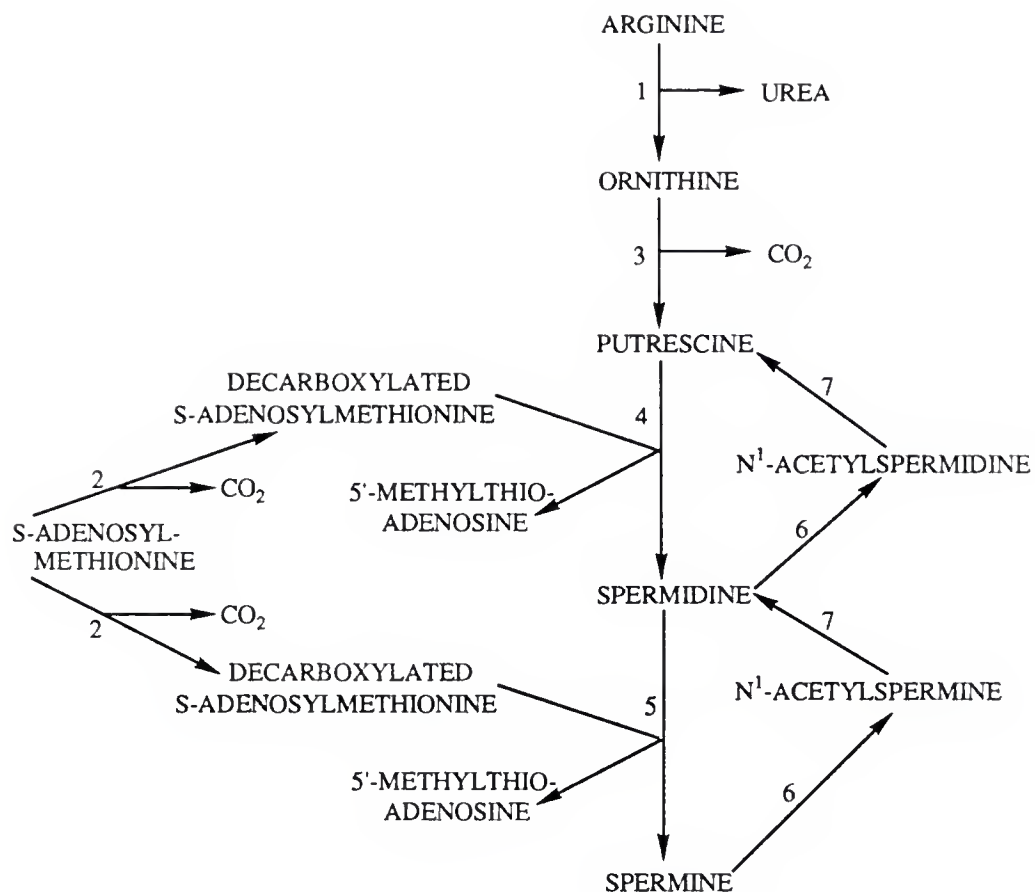
Figure 1-5. Pathway of polyamine synthesis and intercon-
version in mammalian cells. Enzymes involved are: (1) arginase,
(2) S-adenosylmethionine decarboxylase, (4) Spermidine synthase,
(5) Spermine synthase, (6) Spermidine N^1-acetyltransferase, and (7)
Polyamine oxidase (49).

In mammalian cells putrescine is derived from ornithine by the pyridox-
al phosphate-dependent enzyme ornithine decarboxylase (ODC). Ornithine
is available in the plasma or formed from arginine by the action of
arginase. Levels of ODC are normally low in quiescent cells, and its
activity can be increased manyfold within hours after exposure to such
stimuli as hormones, drugs, tissue regeneration and growth factors
(47).

To convert putrescine to spermidine an aminopropyl group must be
added. The aminopropyl moiety is derived from S-adenosylmethionine
(SAM) which is committed to polyamine biosynthesis as an aminopropyl
donor once it is decarboxylated by S-adenosylmethionine decarboxylase
(AdoMetDC). Levels of AdoMetDC are regulated by the cell's need for
spermidine and the availability of putrescine as a substrate for sperm-
idine synthesis. Its activity is also regulated by growth-promoting
stimuli (49).

The transfer of the aminopropyl group from decarboxylated
S-adenosylmethionine to putrescine is catalyzed by the action of the
enzyme spermidine synthase to yield spermidine. In a similar fashion,
a second aminopropyl transfer to spermidine, catalyzed by spermine
synthase, yields spermine. Despite the similarity of these reactions,
spermidine synthase and spermine synthase are substrate specific
enzymes. The two synthases are thought to be regulated by the avail-
ability of their substrates as well as factors stimulating cell growth.
The other product of the aminopropyl transfer reaction is 5'-methyl-
thioadenosine (MTA). The MTA produced by polyamine synthesis is

rapidly degraded and converted by a salvage mechanism into 5'-AMP and methionine (50).

Spermine may also be interconverted into spermidine and spermidine into putrescine by the action of the enzymes N^1-acetyltransferase and polyamine oxidase. The acetyltransferase uses acetyl-CoA to convert spermine into spermidine and spermidine into putrescine. The N^1-acetylated polyamines are good substrates for polyamine oxidase, which cleaves at the internal nitrogen yielding 3-acetamidopropanal and putrescine or spermidine. Normally, only small amounts of the acetylated derivatives are present due to the much greater activity of polyamine oxidase (49).

An active transport system distinct from those for amino acids is also present (49,50). It is unclear why cells would maintain a polyamine transport system since intracellular synthesis is normally used to provide polyamines and extracellular polyamine levels are normally low. However, uptake and efflux may be important mechanisms by which cellular polyamine levels are maintained. The uptake pathways for the polyamines have not been fully characterized at the biochemical level and there may be multiple transport mechanisms (50).

Rapidly proliferating tissues have high levels of polyamines and their biosynthetic enzymes (47), and increased quantitites of polyamines are found in the urine and serum of humans and animals bearing tumors (51). These facts suggest the potential of impacting on polyamine metabolism as a useful target for antiproliferative therapy.

Interruption of the polyamine biosynthetic network has been partially successful as a means of controlling the proliferative process

including the growth of cancer cells (52-54). The antineoplastic drugs, α-difluoromethylornithine (DFMO) and methylglyoxyal-bis(guanyl hydrazone) (MGBG) (Fig. 1-6), are both potent inhibitors of enzymes which are critical to polyamine biosynthesis. DFMO is an enzyme-activated irreversible inhibitor of ODC which causes depletion of intracellular polyamine pools (55). It is postulated that DFMO is recognized by ODC as a substrate and that its decarboxylation yields a highly reactive intermediate which binds irreversibly to the active site of the enzyme. The action of MGBG, however, is not specific. MGBG induces spermine/spermidine acyl-transferase, inhibits diamine oxidase and AdoMetDC, and has other effects (50). Although it is not clear which of MGBG's roles is most important in inhibiting the growth of cancer cells, uptake of the drug by the polyamine transport apparatus seems critical. The drug has been regarded as a structural analogue of spermidine, and since its uptake involves an active transport mechanism cells, can actually concentrate the drug so that millimolar quantities of MGBG can accumulate intracellularly (56).

Although DFMO and MGBG have shown impressive results against transplantable murine tumor models, the success of both in a clinical setting, unfortunately, has been somewhat marginal (50,57). The action of DFMO on most neoplasms is cytostatic, and the rapid rate of synthesis of new ODC (half-life of less than 1 h in many cell lines) makes it essential to maintain high drug concentrations since enzyme levels and cell growth are restored rapidly once drug is removed (49). MGBG has produced unacceptable host toxicity in early trials.
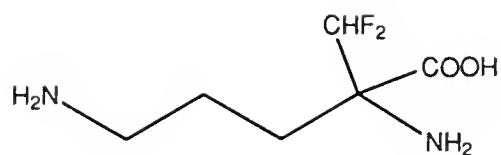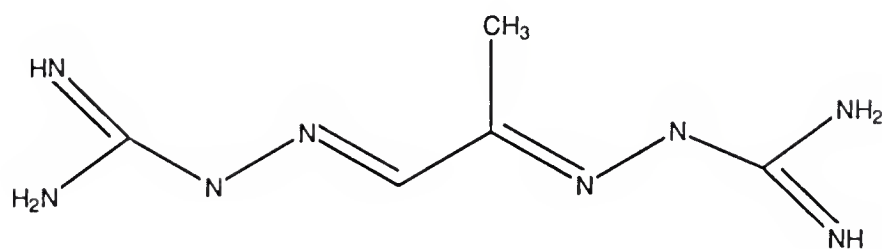
a.

b.

Figure 1-6. The inhibitors of polyamine biosynthesis.

a. DFMO
b. MGBG

The combination of MGBG and DFMO has been reported to have synergistic activity (57). It was speculated that the simultaneous inhibition of AdoMetDC by MGBG and reduction of ODC levels by DFMO treatment would enhance tumor cell kill. Furthermore, DFMO depletion of intracellular polyamine pools increases uptake of MGBG by the polyamine uptake apparatus (58). Since DFMO is relatively nontoxic (53), it was hoped that potential tumor cell selectivity would be increased while decreasing MGBG's host toxicity. This does not seem to be the case in several trials (50). However, the fact that these agents do have anticancer activity, albeit limited, supports the aim of impacting on polyamine metabolism as a rational approach for controlling the proliferative process.

The initial design, synthesis and testing of polyamine derivatives which utilize the polyamine uptake apparatus and exhibit antiproliferative properties was conducted by Porter, Bergeron and Stolowich (59). There are several properties which may be desirable for the design of polyamine analogues as antiproliferatives: (1) the analogues may utilize the polyamine uptake apparatus as a means of delivery, and such uptake may be enhanced by polyamine depletion, (2) the analogues may fulfill some but not all of the functions of polyamines and thereby interfere with normal polyamine metabolism and/or function, and (3) the analogues may act to regulate the polyamine-biosynthetic pathway leading to depletion of cellular polyamines and their biosynthetic enzymes.

In a systematic approach, a number of spermidine analogues were synthesized and studied for their structure/function relationships

(59-65) and some were found to meet the above requirements. It was found that, in terms of uptake, retention of charge is of major importance since N-acetylation as opposed to N-alkylation at either the central or the terminal nitrogens decreased the ability of the analogue to compete with spermidine for uptake into the cell (65). While the N^1,N^8-alkyl derivatives (65) were poorer competitors for spermidine uptake than N^4-alkyl derivatives, they accumulated to high concentrations during longer incubations (66). The antileukemic activity of several N^4-alkyl spermidine analogues was enhanced by pretreatment of cells with DFMO (67). Structural analogues of spermidine differing in aliphatic chain length separating the amines were also studied (68). Several of the homologues were found to support cell growth and no more than a one-carbon extention was tolerated for biological activity.

Certain of the N^1,N^8-alkyl spermidine derivatives, particularly N^1,N^8-diethylspermidine (BESPD), were found to inhibit L1210 cell growth, diminish ODC activity, reduce AdoMetDC, and deplete intracellular polyamine pools (65,66,69). It has been concluded that BESPD affects polyamine biosynthesis, at least, at one critical point by regulating ODC at a translational and/or post-translational level in a manner similar to the natural polyamines. However, the analogue is apparently incapable of fulfilling certain critical functions of natural polyamines necessary for normal cellular function and proliferation (65). Depletion of intracellular polyamine pools by BESPD may also occur by displacement of the natural polyamines from their intracellular binding sites. In addition, potent induction of the spermidine/ spermine acetyl transferase activity by BESPD (70) could lead to the

back-conversion of spermine and spermidine to putrescine and efflux of the polyamines from the cell.

The effects of these polyamine analogues may vary considerably from one cell type to another depending on the cellular requirements for polyamines. Despite inhibition of cell growth, BESPD was not toxic towards L1210 cells (69). However, BESPD at concentrations of greater than 5 μM was found to be cytotoxic to human large-cell lung cancer cells normally quite resistant to DFMO (71).

The design, synthesis, evaluation, and study of the biochemical and physiological effects of this new class of antiproliferatives is currently the area of intense investigation.

CHAPTER II
CATECHOLAMIDE CHELATORS

Materials and Methods

The catecholamide chelators and methylated analogues were synthesized by methods previously described (30-32,72). Stock solutions (2 mM) of the catecholamide chelators were made in 50% (v/v) ethanol and water. Stock solutions of Adriamycin and ara-C were prepared in water. BCNU was prepared in 50% (v/v) ethanol and water. All solutions were passed through a 0.2 μm filter prior to use. Reagents for cell culture were obtained from Gibco (Grand Island, NY). Cell culture flasks, 25 and 75 cm^2, were purchased from Corning (Corning, NY). Adriamycin was obtained from Adria (Columbus, OH), carmustine (BCNU) from Bristol (Syracuse, NY), hydroxyurea from Aldrich Chemical Co. (Milwaukee, WI) and cytosar (ara-C) from UpJohn (Kalamazoo, MI). Diamidino-phenylindole (DAPI) and propidium iodide (PI) were obtained from Sigma (St. Louis, MO). Desferrioxamine was provided by Ciba-Geigy (Basel, Switzerland). Iron atomic absorption standard solution, 1003 μg/mL Fe in 2% HNO_3 (Aldrich) was used as an Fe(III) source. Cremophore RH-40 was provided by BASF-Wyandot Corp. (Parsipany, NJ). Rhodamine-123 (Rh-123) was purchased from (Eastman Kodak Company, Rochester, NY). [methyl-^{3}H]Thymidine was obtained from New England Nuclear (Boston, MA). DBA/2 mice were obtained from Jackson Laboratories (Bar Harbor, ME).

Cell Culture.--Murine L1210 leukemia cells and human Burkitt lymphoma (Daudi) cells were maintained in exponential growth as suspension cultures at 0.3×10^4 to 1.5×10^6 cells/mL and 1×10^5 to 2×10^6 cells/mL, respectively. Chinese hamster ovary (CHO) cells and murine B-16 melanoma cells were grown as monolayers to near confluency in 48 h after reseeding at 2.5×10^5 cells/25 cm^2 flask. Human foreskin fibroblasts (HFF) cells were grown as monolayers to near confluency in 96 h after a 1:4 dilution of cells in fresh medium. Monolayer cells were lifted as single cell suspensions with 0.05% trypsin and 0.02% ethylenediaminetetraacetic acid tetrasodium salt (2 mL/25 cm^2) and diluted with Hanks' balanced salt solution. All cells were grown in complete medium containing RPMI-1640, 2% 4-(2-hydroxyethyl)-1-piperazinethanesulfonic acid/3-(N- morpholino)propanesulfonic acid (HEPES--MOPS buffer), and 10% fetal bovine serum unless otherwise stated. Cells were grown in 25 cm^2 tissue culture flasks in a total volume of 10 mL under a humidified 5% CO_2 atmosphere at 37°C.

IC_{50} Value Determinations.--Cultures in logarithmic growth were treated with compounds of interest at concentrations ranging from 10^{-3} to 10^{-7} M. Cells were counted by electronic particle analysis (Coulter Counter, Model ZB1, Coulter Electronics, Hialeah, FL) and confirmed periodically with hemocytometer measurements. Cell viability was assessed by trypan blue dye exclusion.

The percentage of control growth was determined as follows:

% of control growth = 100 x [Final treated cell no.-initial inoculum]/[Final untreated cell no.-initial inoculum]

The 50% inhibitory concentration (IC_{50}) value is defined as the concentration of compound necessary to reduce cell growth to 50% of control growth after defined intervals of exposure. The IC_{50} values were determined as the chelator concentration necessary to inhibit cell growth to 50% of the control growth at 48 h for all cell lines except HFF cells, for which the IC_{50} values were determined at 96 h.

Preformed chelator-iron chelates were formed by the addition of equimolar amounts of chelator and iron to the media 30 min prior to the addition of the cells.

A 50% ethanol and water solution in appropriate amounts was used to treat cells in all control flasks. Addition of iron and ethanol alone in the concentrations used had no significant effect on growth studies.

Stock suspensions of L1210 cells were maintained for 48 h, with normal 10-12 h doubling times, in complete mediums containing 5%, 10%, and 20% fetal bovine serum. The IC_{50} value of parabactin was determined for cells grown in each medium.

Drug Combinations.--L1210 cells in suspension culture were incubated in the presence of parabactin and antineoplastics at various concentrations and combinations. Two types of experiments were performed for each drug combination.

a. To obtain median effect plots for simultaneous drug combinations, cells at 3×10^4 cells/mL were exposed to a constant ratio of chelator to antineoplastic, a ratio in which absolute concentrations were varied. The absolute concentrations of the drugs were chosen in the neighborhood of their IC_{50} values. This gave the ratio of

parabactin to ara-C of 100:1, of parabactin to Adriamycin of 100:1, and of parabactin to BCNU of 1:1. The growth was monitored at 48 h, and an IC_{50} value was determined. A separate experiment was run to determine the IC_{50} value of parabactin, ara-C, Adriamycin, and BCNU.

b. In a second experiment, cells at 3×10^5/mL were first incubated with 5 μM parabactin for 5 h at 37°C, then washed twice with fresh medium, resuspended at 3×10^4 cells/mL, allowed to incubate at 37°C for 3 h (allowing the cells to cascade into S phase), and then treated with varying concentrations of the antineoplastic. Growth was monitored every 12 h for 96 h.

Additional experiments were carried out with various combinations of parabactin and Adriamycin, ara-C or BCNU treatments.

c. Cells at 3×10^5 cells/mL were treated with 5 μM parabactin for 3 h, and then BCNU was added at varying concentrations. The flasks were allowed to incubate for an additional 5 h. The cells were next washed with fresh medium and resuspended at 3×10^4 cells/mL, then their growth was monitored for up to 96 h.

d. Cells at 3×10^5 cells/mL were treated with 5 μM parabactin for 4 h, and then Adriamycin was added. The flasks were allowed to incubate for an additional 2 h. The cells were next washed with fresh medium and resuspended at 1×10^5 cells/mL, then their growth was monitored for 48 h.

e. Cells at 3×10^5 cells/mL were treated with 2 μM parabactin for 4 h, and then ara-C was added and the flasks were allowed to incubate for an additional 12 h. The cells were next washed with fresh medium and resuspended at 5×10^4 cells/mL, then their growth was monitored for up to 120 h.

f. Cells at 3×10^5 cells/mL were simultaneously treated with 5 µM parabactin and ara-C. The cells were allowed to incubate for 5 h, washed with fresh medium, resuspended at 5×10^4 cells/mL, and their growth was monitored for up to 96 h.

In each case, the drug concentrations and treatment times are indicated on the figure legends.

Data Analysis for Simultaneous Drug Combinations.--Briefly, this procedure involves (a) determination of an IC_{50} value for each drug and (b) determination of an IC_{50} value for a constant ratio of two drugs. The molar ratio of the drugs is maintained while the absolute concentration of the drugs is changed. The cell growth data from these experiments are plotted as $\log F_a/F_u$ versus concentrations ($\log [c]$), where F_a is fraction of cells affected, F_u is fraction of cells unaffected, and c is molar concentration. The data from the median effect plots were analyzed by the method of Chou and Talalay (73) according to the following equation.

$$A/D_A + B/D_B = CI \qquad\qquad (A)$$

The D values are the IC_{50} concentrations of each of the drugs alone, the A and B values are the concentrations of each drug at the IC_{50} value of the constant ratio combination, and CI is the combination index. When the CI is in excess of 1, the combination is "antagonistic." When it is less than one, the combination is "synergistic"; and when the CI is equal to 1, the combination is "additive."

Regrowth Studies.--L1210 cells in suspension culture at approximately 3×10^5 cells/mL were incubated in the presence of chelator for 5 h at 37°C. The cells were then washed twice in fresh complete medium, resuspended at a final concentration of 5×10^4 cells/mL, and incubated at 37°C. Cell samples during logarithmic growth were counted for up to 60 h after ligand treatment and compared to controls.

Cloning Assay.--Cells at 3×10^5 cells/mL were incubated with 5 μM parabactin for 5 h and washed with fresh medium. Treated cells were then plated in triplicate 96-well microtiter plates at 0.4 cells/well with each well containing 100 μM of sample. The plates were incubated at 37°C in a humidified incubator in an atmosphere of 5% CO_2 and 95% air. The plates were examined with an inverted phase microscope at X100 magnification. The final number of colonies per plate was quantitated at 7 days after plating. Groups of 50 or more cells per well were identified as having been cloned from a single viable cell.

Viability Assay.--Cell viability was assayed by two dye exclusion methods. In one method cells were diluted 1:1 with 0.4% trypan blue in phosphate-buffered saline and counted in a hemacytometer using a light microscope. In the second method 10^6 cells were diluted in 1 mL of a 1.12% sodium citrate solution of propidium iodide (50 μg/mL) and counted on a fluorescent microscope.

Viability determination by Rh-123 uptake (74) was assayed by adding the mitochondrial dye Rh-123 (10 μg/mL) to a aliquot of 10^6 cells. The samples were incubated at 37°C for 10 min and washed once with medium. Trypan blue was added, prior to counting, to give a final concentration of 0.2 μg/mL. Rh-123 and trypan blue stained cultures were

observed in a hemocytometer using a Zeiss epifluorescence Axioscop microscope. The excitation wavelength was 485 nm.

Flow Cytometric Analysis.--Cell analysis was performed with a RAT-COM flow cytometer (RATCOM, Inc., Miami, FL) interfaced with a microcomputer (IBM-XT). Cell samples of 10^6 cells were taken at various intervals and stained with DAPI (10 μg/mL) in a nuclear isolation media (NIM-DAPI) (75). DNA distributions were obtained from the fluorescence and analysis of the DAPI-stained cells.

Alternately, cell analysis was performed with a FACS II flow cytometer (Becton Dickinson FACS Systems, Sunnyvale, CA) interfaced with a microcomputer (Hewlett Packard 45B, Fort Collins, CO). Samples of 10^6 cells were removed and stained with PI and then exposed to RNase. DNA distributions were obtained from analysis of the red fluorescence from the PI-stained DNA (76).

Effect of Percent Fetal Bovine Serum in the Medium on Cell Cycle Kinetics.--Stocks of L1210 cells were maintained for 48 h with normal 10-12 h doubling times in complete mediums containing 5%, 10%, 15% and 20% fetal bovine serum. The time course for the effect of 5 μM parabactin on the cell cycle kinetics of cells grown in each of the mediums was followed for up to 8 h.

Bromodeoxyuridine (BrdUrd) Incorporation Studies.--Cultured L1210 cells were treated with 10 μM vibriobactin, washed, resuspended, and incubated as in the regrowth studies. At times, 0, 5, 10, 15 and 20 h of regrowth cell samples were removed for dual parameter flow cytometric measurements of cellular DNA content and amount of BrdUrd incorporated into cellular DNA by methods presented elsewhere (77,78).

Radiolabeled Thymidine Incorporation.--Cells treated with 5 μM

parabactin for 5 h were washed, resuspended in fresh complete medium,

and incubated at 37°C for 30 min with [^{3}H]thymidine (specific activ-

ity, 80.9 Ci/mmol; 1 μCi/mL) in triplicate tubes containing 10^6

cells in a total volume of 1 mL of complete medium. Labeling was

halted by the addition of 0.5 mL of ice-cold Hanks' balanced salt

solution (HBSS) containing thymidine (1 mg/mL) to each tube. The cells

were washed, resuspended in 1 mL of 10% trichloroacetic acid in HBSS

containing thymidine (1 mg/mL), and allowed to sit on ice for 30 min.

The acid-precipitable material was filtered and the filter washed.

Then filters were air dried and counted in Biofluor (New England

Nuclear) scintillation fluid. Background labeling was evaluated in

cell samples pulsed for 30 min with [^{3}H]thymidine at 5°C.

% of control incorporation = $\dfrac{\text{treated cpm - treated background cpm}}{\text{control cpm - control background cpm}} \times 100$

Cr^{51}Release Assay.--L1210 cells were treated with vibriobactin

(10 μM) for 5 h, washed with fresh media and regrown for 20 h. Approx-

imately 2 x 10^6 cells were centrifuged and 150 μCi Cr^{51} added to the

pelleted cells. The pellet was incubated for 45 min at 37°C in a 5%

CO_2 atmosphere. Sample radiation was counted with an automatic gamma

counter (LKB-Wallac RiaGamma 1274, Wallac Oy, Finland).

A microwell assay using triplicate samples of 200 μL containing

1 x 10^5 cells was employed as described elsewhere (79). The percent

Cr^{51} release for the control cells was compared to that for the vibrio-bactin treated cells.

Animal Studies.--The murine L1210 leukemia cells were maintained in DBA/2J mice. Cells from a single mouse which was injected i.p. with 1.25×10^4 cells 7 days earlier were harvested and diluted with cold saline so that an inoculum of 10^5 cells could be administered by a 0.25 mL i.p. injection. In each study, mice were injected with L1210 cells on day 0.

The catecholamide chelators were first solubilized in 20% Cremophor RH-40 in 0.9% saline with sonication and gentle heating ($<60°C$) and then diluted with an equal volume of 0.9% saline. The chelator was administered by i.p. injection according to the appropriate dosing schedule. Concentrations of chelator were adjusted so that the mice were injected with a volume of 1-2 mL/100 g of animal/dose (i.e.: a 25 g mouse was injected with 0.25-0.5 mL of drug solution).

The in vivo effectiveness of parabactin alone and combinations of parabactin with ara-C or Adriamycin against the L1210 ascites tumor were studied. Ara-C and Adriamycin were diluted in 0.9% saline so that the mice were injected i.p. with a volume of 1 mL/100 g of animal/dose. Due to the possible toxicity or antitumor activity of Cremophor RH-40, groups of mice treated with 10% Cremophor RH-40 as well as untreated mice served as controls. Groups of 6 mice were used in each treatment schedule.

One parameter used for treatment evaluation was mean animal survival time (percent increased life span, % ILS).

%ILS = 100 x [mean survival time treated animals-
mean survival time controls]/[mean survival time controls]

Another parameter used for treatment evaluation was tumor burden.
The L1210 cells were harvested from the animal's peritoneum by two
washings with 5 mL of 0.9% saline. The total number of cells recovered
was determined by counting on a hemocytometer.

The in vivo effect of a single i.p. injection of parabactin (100
mg/kg) on L1210 cell cycle kinetics was studied in mice which had been
injected i.p. with 1×10^5 L1210 cells 6 days earlier. Mice were sac-
rificed by cervical dislocation each hour after injection of the che-
lator and the cells were harvested from the peritoneum with HBSS. The
cells were stained with NIM-DAPI and DNA content measured by flow cyto-
metric analysis.

Results

Inhibition of Cell Growth

The effectiveness of various iron chelators as inhibitors of
L1210 cell growth was assessed by comparison of their IC_{50} values
(Table 2-1). The bidentate compound, dihydroxybenzoic acid, while
being a good iron chelator ($K_f = 10^{36}M^{-1}$) (5,37) is not very effective
cell growth inhibitor, requiring millimolar concentrations. Hydroxy-
urea, which structurally resembles a bidentate hydroxamate chelator,
was only fair at inhibiting cell growth, with an IC_{50} value of 40 μM.
The hexacoordinate hydroxamate iron chelator, desferrioxamine, and the
tetracoordinate catecholamide chelator, compound II, showed similar
activity against L1210 cell growth with IC_{50} values of 8 μM and 7 μM
respectively. The most effective of the compounds tested were the
hexacoordinate catecholamide chelators, vibriobactin and parabactin,

TABLE 2-1
IC_{50} VALUES OF VARIOUS CHELATORS AGAINST
CULTURED L1210 LEUKEMIA CELLS

Chelators	IC_{50} Values at 48 H
Dihydroxybenzoic Acid	2.8 mM
Hydroxyurea	40 μM
Desferrioxamine	8 μM
Compound II	7 μM
Vibriobactin	2 μM
Parabactin	1.5 μM

having IC_{50} values of 2 μM and 1.5 μM respectively. The dose-effect curves generated in these studies indicate linear inhibitory effects for parabactin and vibriobactin within a very narrow range of ligand concentrations (Fig. 2-1). For example, at concentrations of greater than 5 μM, cells uniformly grow to only about 10% of controls, while below 1 μM approximately 90% control growth is obtained.

The time dependence of growth inhibition of cultured L1210 cells by the siderophores is shown in Figures 2-2 and 2-3. The concentration of 10 μM was selected for both parabactin and vibriobactin as a value at approximately 5 times their IC_{50} values. The onset of growth inhibition by both siderophores was almost immediate. Both chelators eventually caused a total cessation cell growth. In either case, the growth inhibition could be prevented with the addition of an equimolar amount (10 μM) of Fe(III) to the culture medium at the same time as the chelator.

Methylation of the ligand catechol hydroxyl groups, as in tetra-methyl parabactin (Fig. 1-3c) and permethylated vibriobactin (Fig. 1-3e), greatly reduced the growth inhibitory activity of both chelators. Total methylation of the three catechol groups of vibriobactin completely eliminated its activity at a concentration 10 μM (Fig. 2-2). In fact, it showed no inhibitory activity at concentrations of up to 50 μM. Tetramethyl parabactin (10 μM), while having greatly reduced inhibitory activity, did have some effect on L1210 growth (Fig. 2-3). In fact, it had an IC_{50} value of 30 μM.

The IC_{50} values for parabactin were determined against L1210 cells grown in culture mediums with varying concentrations of fetal
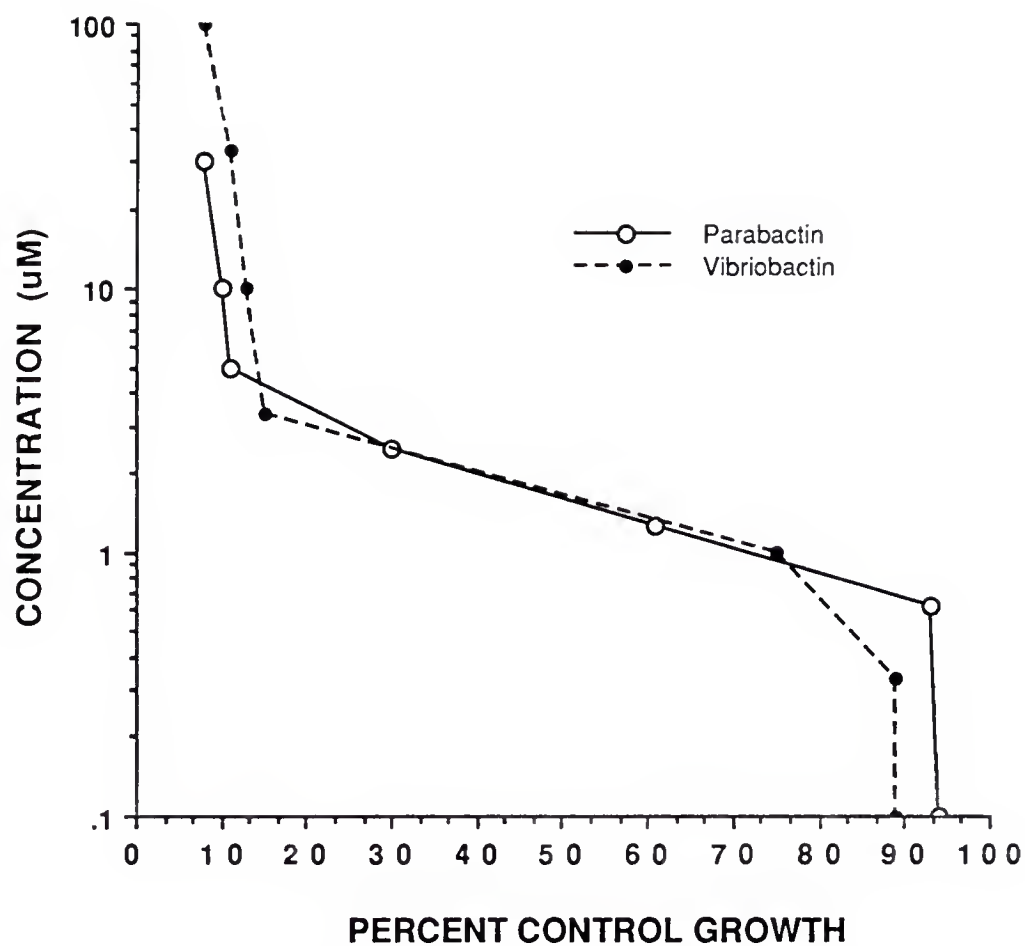
Figure 2-1. Dose-response curves illustrating the effects of increasing concentrations of parabactin and vibriobactin on the growth of L1210 cells.
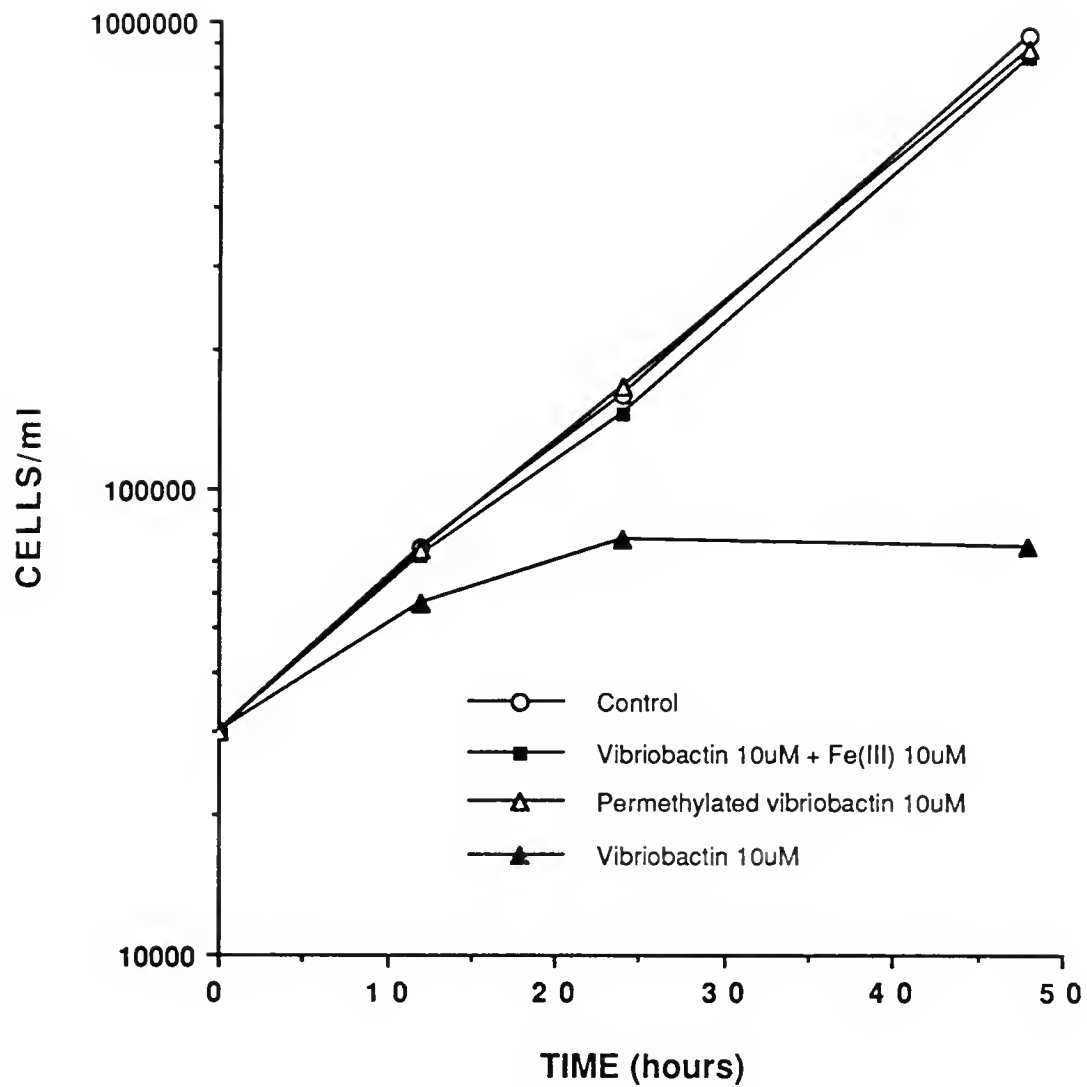
Figure 2-2.   Comparison of the effects of 10 μM vibriobactin, in the presence or absence of Fe(III), and 10 μM permethylated vibriobactin on the growth of L1210 cells.
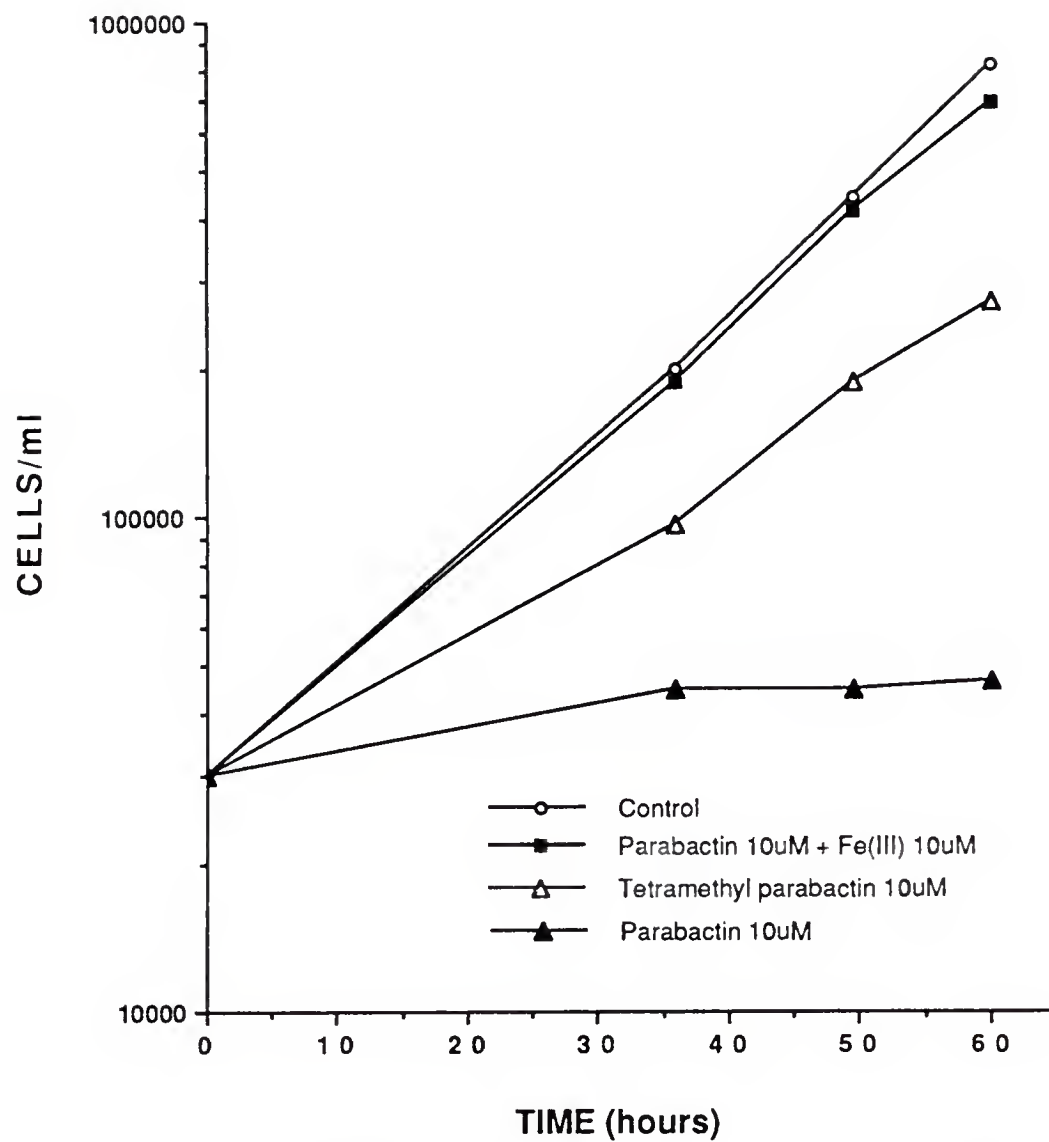
Figure 2-3. Comparison of the effects of 10 μM parabactin, in the presence or absence of Fe(III), and 10 μM tetramethyl parabactin on the growth of L1210 cells.

bovine serum (Fig. 2-4). Cells grown in 5, 10 and 20% FBS had IC_{50} values of 0.8, 1.2, and 1.6 μM respectively.

Parabactin was also found to have potent growth inhibitory effects on cultured B16-melanoma and CHO cells exhibiting a 48 h IC_{50} value of 1.5 μM for both cell lines. Both vibriobactin and parabactin exhibited a 48 h IC_{50} value of 2 μM for Daudi cells and parabactin was active, with a 96 h IC_{50} value of 2 μM, against HFF cells. The IC_{50} value for HFF cells was determined at 96 h due to their relatively slow doubling time (45-50 h) compared to the other cell lines studied (12-24 h).

Treatment Reversibility

When cells were treated for 5 h with 5 μM parabactin, the growth-inhibitory effects of parabactin were found to be reversible on washing away the ligand. Viability of parabactin-treated cells, taking cell samples every 5 h for 35 h after washing away of the ligand, was verified by dye exclusion and Rh-123 uptake methods. At 10 h after washing, the viability decreased to a minimum of 88% by the dye exclusion methods and only 85% by Rh-123, the most sensitive of the methods used. These results were in agreement with the cloning assay which indicated 91% of colonies were cloned or single cell after short-term exposure (5 h) to the chelator compared to single control cells. The number of cells per colony from the parabactin-treated cells was consistently less than from the control cells.

Cells having been treated for 5 h with 10 μM vibriobactin showed similar reversibility of inhibitory effects on washing away of the ligand and reseeding the cells in fresh medium. A ^{51}Cr release assay performed on vibriobactin treated cells at 15 h after removal of the ligand showed no increase in ^{51}Cr release relative to control cells,
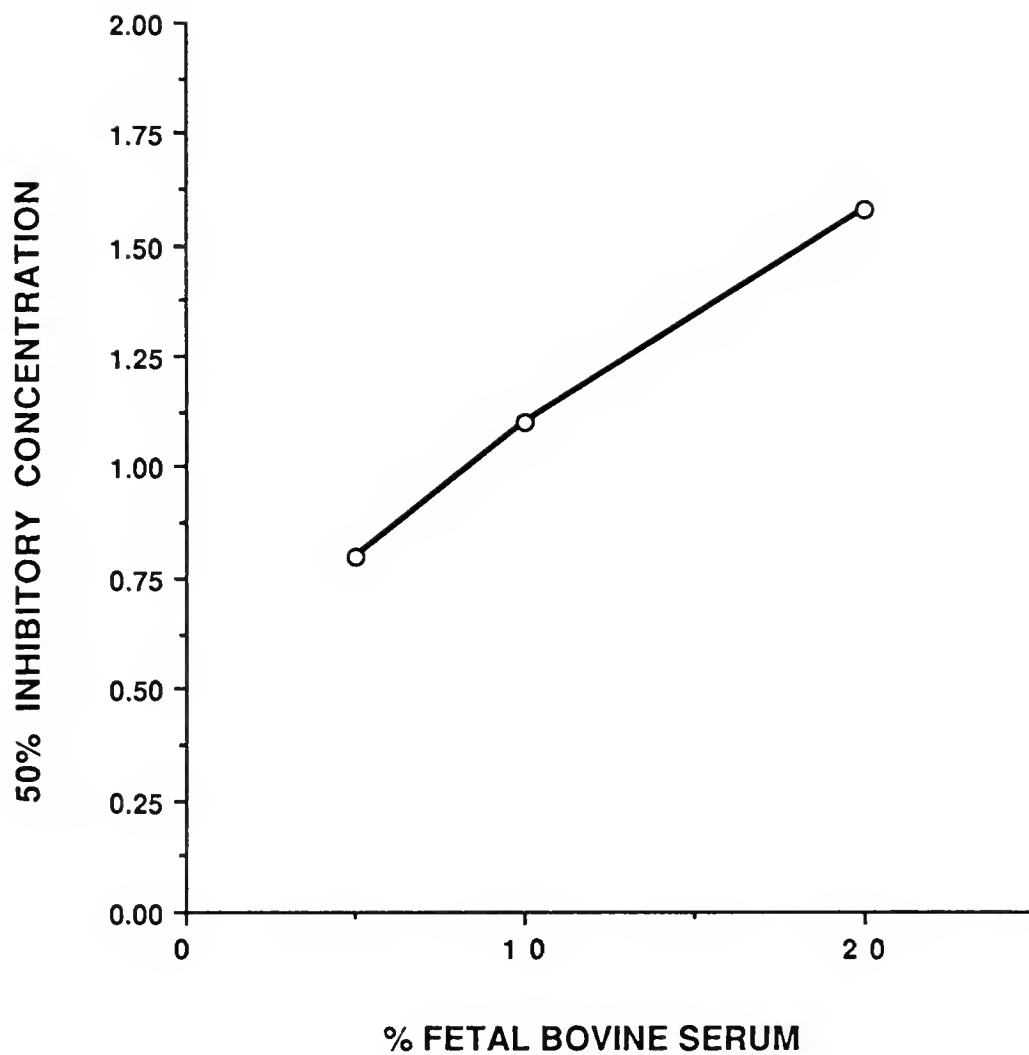
Figure 2-4.   The effect of varying amounts of fetal bovine serum in the L1210 growth medium on the 50% inhibitory concentration of parabactin.

establishing little, if any, cytotoxicity due to short term (less than 5 h) 10 μM vibriobactin.

However, when cells were treated for an extended period of time with 5 μM parabactin, cytocidal activity was observed (Table 2-2). For example, at 60 h, only 30% of the cells were viable as determined by trypan blue exclusion. Dye exclusion of cells treated with 10 μM vibriobactin for 48 h indicated only 10% viability, and only 20% viability of cells exposed to 100 μM desferrioxamine for 60 h. Surprisingly, 300 μM hydroxyurea was the least toxic of the compounds tested with only 25% cytotoxicity after 60 h of treatment. Although in dividing HFF cells, growth was inhibited by parabactin (IC_{50} value of 2 μM at 96 h), treatment of a confluent, nondividing, monolayer of HFF cells with 20 μM parabactin for 24 h appeared to be nontoxic by light microscopy. Also, the treated confluent cells diluted and regrown in drug-free medium grew at the same rate as control cells.

Effects of the Catecholamide Chelators on Cell Cycle Kinetics

Flow cytometric analysis was employed as the method to follow the effects of the chelators on the cell cycle progression. The time course for the effect of 10 μM vibriobactin on the DNA content of L1210 cells is seen in Figure 2-5. Flow cytometric analysis of untreated L1210 cells reveals high S (50%) and G_2-M (15%) phase components of the cell population with about 35% of the cells having G_1 phase DNA content. After only 2 h alterations in the DNA content of the vibriobactin treated cells were observed. There was a substantial effect on the cell cycle kinetics with a clear block at the G_1-S border after 3

TABLE 2-2
CYTOCIDAL ACTIVITY OF CHELATORS

Ligand	Percent of Activity[a]				
	0	12 h	24 h	48 h	60 h
Parabactin (5 µM)	<2	5	15	49	70
Vibriobactin (10 µM)	<2	4	36	90	-
Desferrioxamine (100 µm)	<2	5	20	60	80
Hydroxyurea (300 µM)	<2	-	15	-	25

[a]The percentage of L1210 cell kill in cells treated with parabactin, vibriobactin, desferrioxamine and hydroxyurea with treatment time. Cell viability determined by trypan blue exclusion.
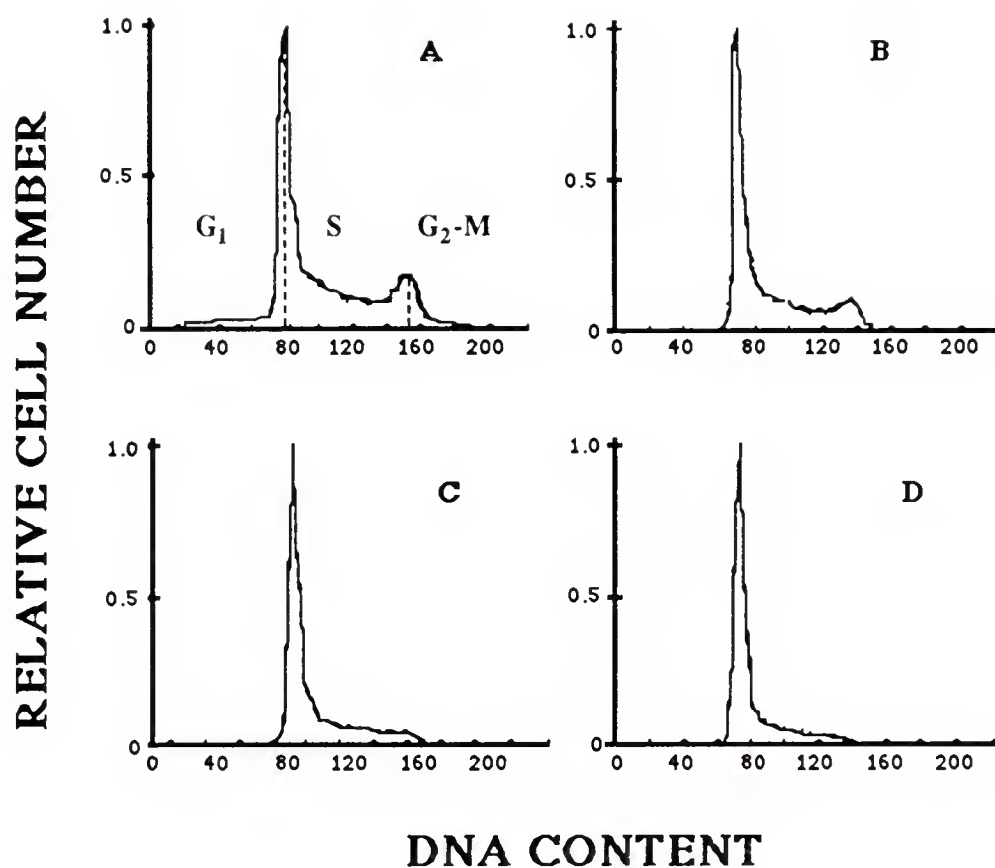
Figure 2-5. Flow cytometric analysis of L1210 cells.

A. Control cells.
B. Cells treated with 10 μM vibriobactin for 3 h.
C. Cells treated with 10 μM vibriobactin for 4 h.
D. Cells treated with 10 μM vibriobactin for 5 h.

h. Within 5 h, cells with G_2-M phase content were eliminated, and cells with S phase content were reduced to 30%. The cells were prevented from entering S phase and 70% of the cells have G_1 phase content. A comparable cell cycle block in DNA synthesis was observed in the DNA histograms of cells treated with 5 µM parabactin for 5 h (Fig. 2-6). Cells treated for up to 24 h with 5 µM parabactin, however, showed no greater block in cell cycle kinetics than cells treated for 5 h, and cells treated with less than 4 µM parabactin did not appear to reduce S phase to the extent that the 5 µM treatment did. For further studies it was therefore indicated that the minimum concentration and time for parabactin to effectively eliminate DNA synthesis in L1210 cells was 5 µM for 5 h.

In a study to determine the ability of 5 µM parabactin to cause a cell cycle block in L1210 cells grown in culture mediums with various percentages of fetal bovine serum (5%, 10%, 15% and 20%), it was found that there was no significant alteration in time to reach complete cell cycle block (5 h) for the cells in any of the different culture mediums.

In a comparative study, parabactin was shown to be a far more effective cell cycle blocking agent than either hydroxyurea or desferrioxamine (Fig. 2-6). For example, to generate cell cycle blocks similar to that produced by 5µM parabactin (IC_{50}, 1.5 µM) at 5 h, L1210 cells required 100 µM desferrioxamine (IC_{50}, 7.5 µM) for 5 h or 300 µM hydroxyurea (IC_{50}, 50 µM) for 5 h. When comparing the IC_{50} value of each of the ligands, it is clear that the compounds with the higher IC_{50} values are also the poorer cycle blocking agents.
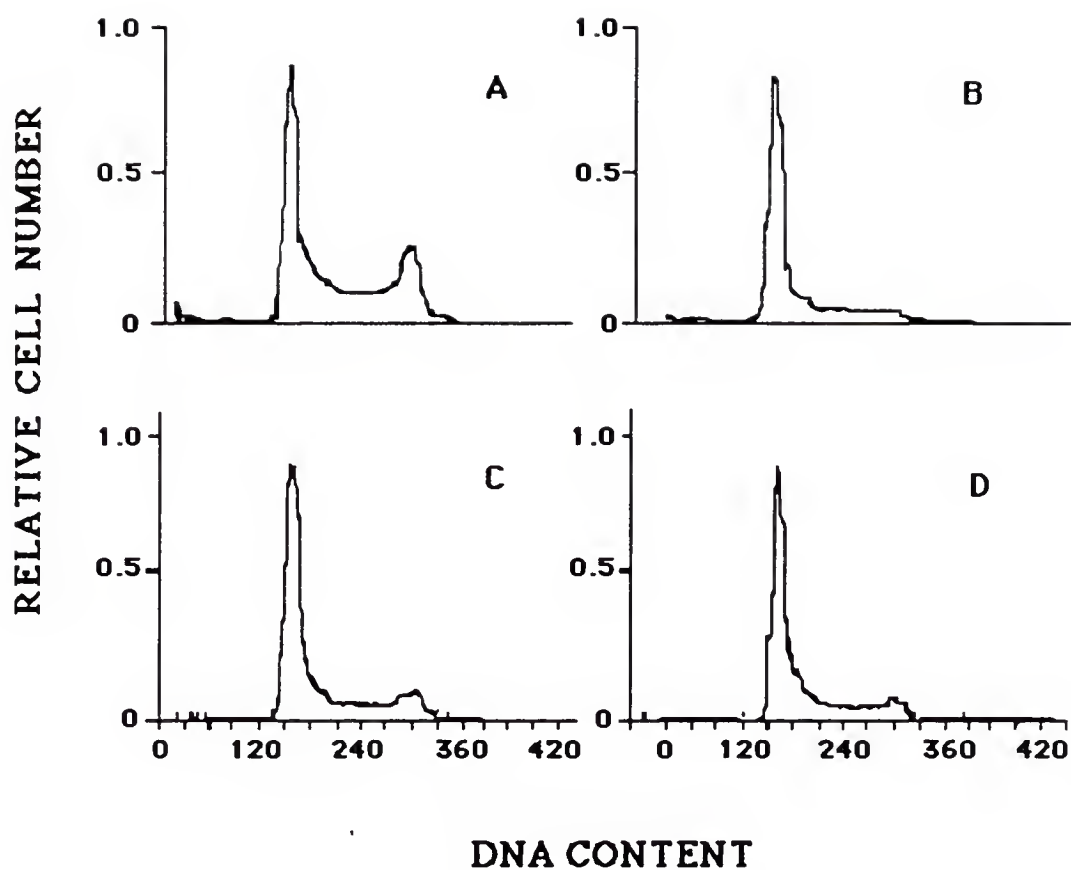
Figure 2-6. Flow cytometric analysis of L1210 cells.

A. Control cells.
B. Cells treated with 5 μM parabactin for 5 h.
C. Cells treated with 100 μM desferrioxamine for 5 h.
D. Cells treated with 300 μM hydroxyurea for 5 h.

Synchronization Effects

Flow cytometry analysis of the cell cycle kinetics of cells treated with 10 μM vibriobactin for 5 h indicated a clear block at the G_1-S border of the cell cycle. Washing and reseeding the treated cells in fresh complete medium caused pronounced changes in the cell cycle phases with time (Fig. 2-7). The block in DNA synthesis is released and at 5 h after removal of the drug the majority of cells have S phase DNA content. The progression through the cell cycle phases continued for up to 20 h. Cell cycling was further substantiated by BrdUrd incorporation into DNA (Table 2-3). The percent BrdUrd incorporation at various times after removal of the chelator was roughly consistant with changes in S phase DNA content as determined by flow cytometry.

Cells incubated with 5 μM parabactin for 5 h exhibited a block in DNA synthesis at the G_1-S border (by flow cytometry) with a greatly decreased S and G_2 phase (Figs. 2-6 and 2-8). Concentrations of 100 μM desferrioxamine and 300 μM hydroxyurea for 5 h were required to produce similar blocks. On removal of the chelators by simple washing and reseeding the cells in drug-free culture medium, the block in DNA synthesis was removed and the cells cascaded into S phase. Parabactin-treated cells maintained a synchronous population of cells for 3 cell cycles. (Figure 2-8 only includes cells moving into the third cycle.) However, desferrioxamine- and hydroxyurea-treated cells showed normalized DNA histograms after 12 h.

Radiolabeled Thymidine Incorporation.--Incorporation of [^{3}H]thymidine into L1210 cells after the cells were treated with 5 μM
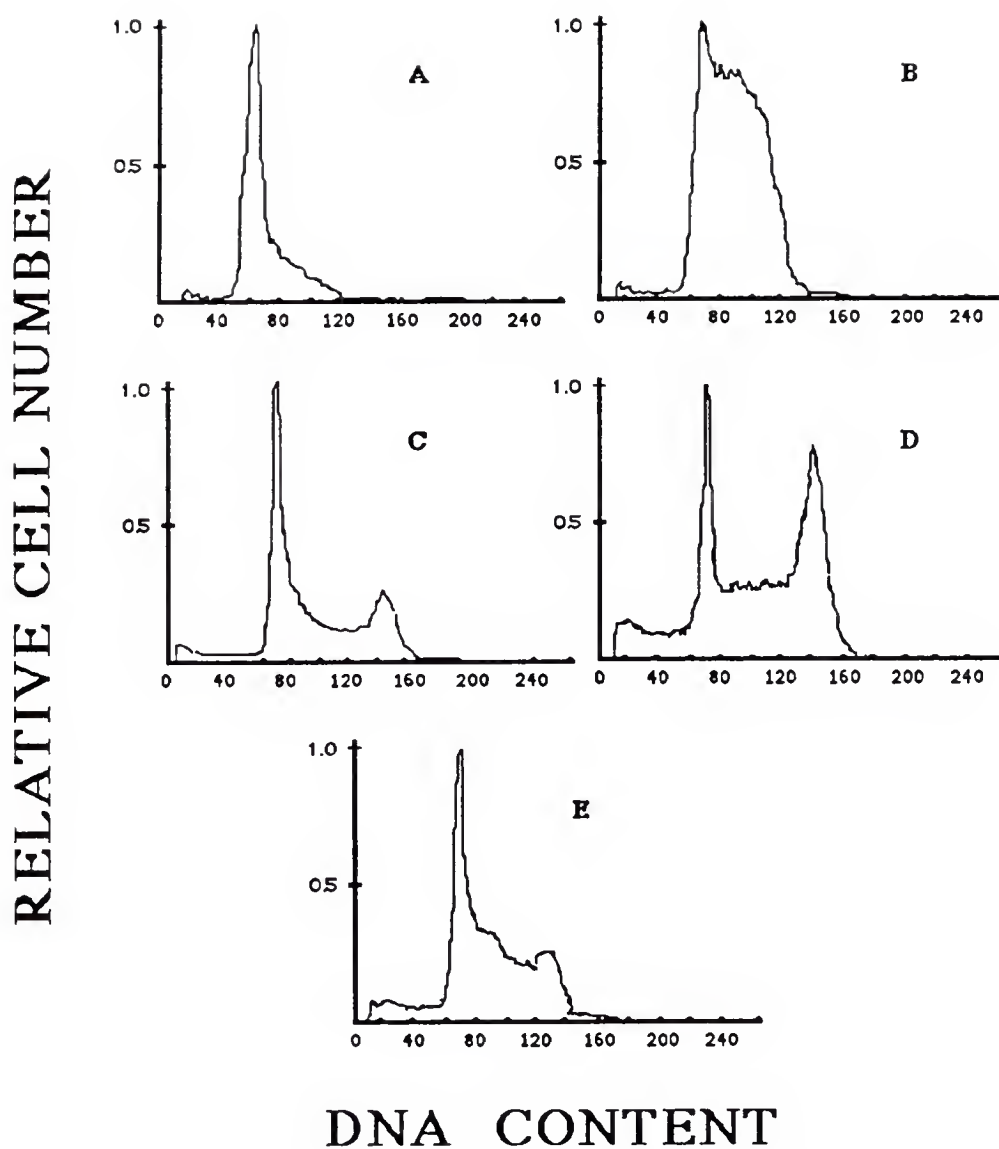
Figure 2-7. Flow cytometric DNA content analysis of L1210 cells washed and regrown in fresh medium after a 5-h treatment with 10 μM vibriobactin.

Analysis performed after removal of ligand.

A. 0 h
B. 5 h
C. 10 h
D. 15 h
E. 20 h

TABLE 2-3

PERCENT BROMODEOXYURIDINE INCORPORATION INTO L1210
CELLS TREATED WITH 10 μM VIBRIOBACTIN FOR 5 H THEN
WASHED AND RESEEDED IN FRESH MEDIUM

| Time after Wash	Percent BrdUrd Incorporation	
	Control	Treated
0	44	16
5	50	47
10	53	45
15	47	16
20	49	32

Figure 2-8. Cell synchronization of L1210 cells by 5 µM parabactin. DNA content determined by flow cytometric analysis.

A. Control cells.
B. Cells treated with 5 µM parabactin for 5 h.

Cells were then washed, resuspended in drug-free medium, and samples removed at the following times.

C. 4 h.
D. 6 h.
E. 10 h.
F. 12 h.
G. 14 h.
H. 16 h.
I. 18 h.
J. 22 h.
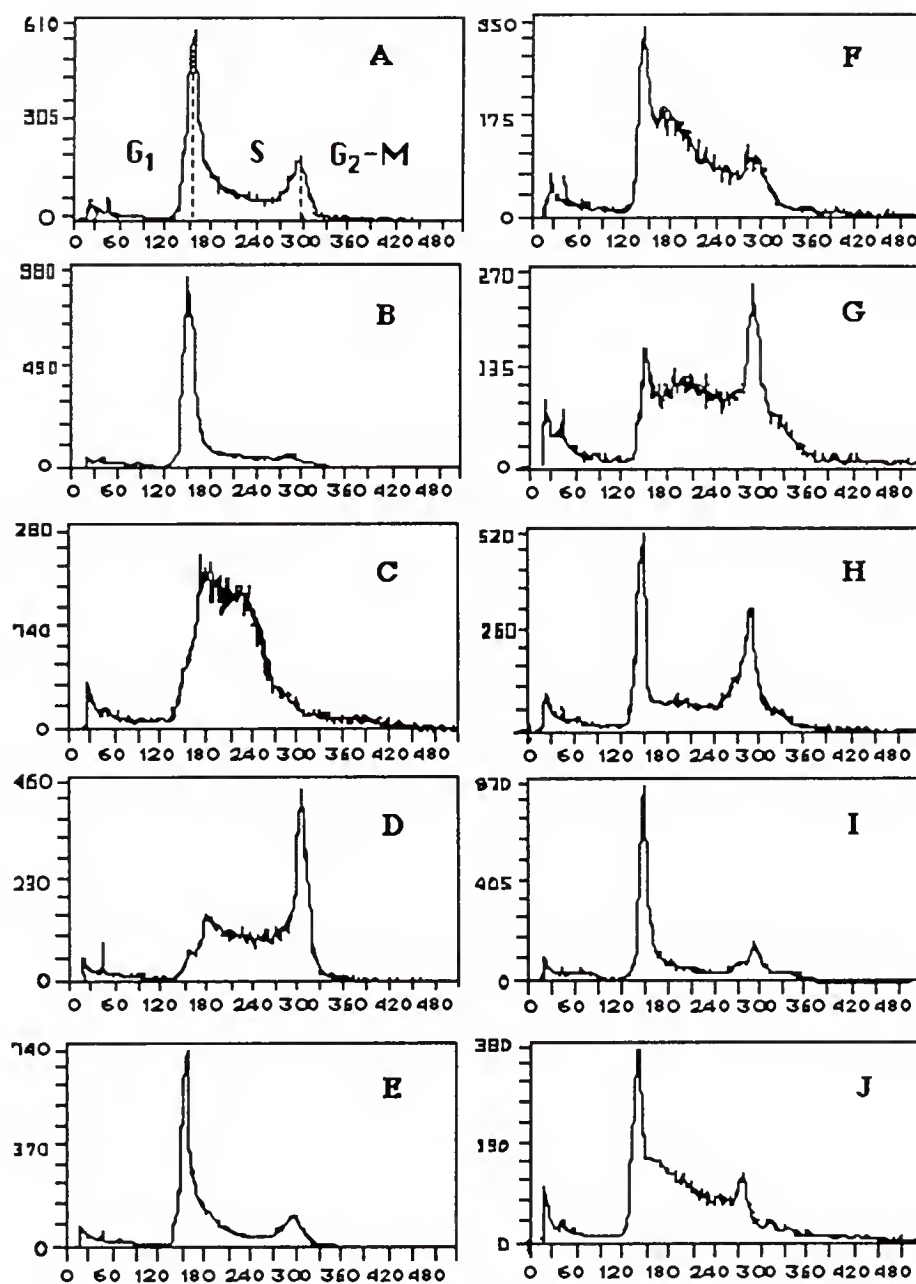
parabactin for 5 h and washed (Fig. 2-9) revealed cycling of incorporation in a time frame consistent with the normal 10 h to 12 h doubling time of L1210 cells, and with the cycling of DNA content as seen in the flow cytometric studies (Fig. 2-8).

Drug Combination Studies

Adriamycin-treated Cells.--The Adriamycin IC_{50} under our experimental conditions was 0.027 μM at 48 h, while the parabactin IC_{50} was 1.34 μM at 48 h. However, when L1210 cells were treated with parabactin and Adriamycin in simultaneous combination, the results indicated that the combination was "anatagonistic" (Fig. 2-10). Following the method of analysis of Chou and Talalay, the cells were exposed to a constant molar ratio of parabactin to Adriamycin of 100:1. The micromolar concentrations at this constant ratio were 2:0.02, 1.75:0.0175, 1.5:0.015, 1.25:0.0125, 1.0:0.01, and 0.5:0.005. The IC_{50} of the combination was 1.42 μM (CI = 1.57). Chou and Talalay's analysis of the data (see Materials and Methods) clearly revealed the combination to be "antagonistic" at the 100:1 ratio.

In a second experiment, cells were treated with 5 μM parabactin for 5 h, washed free of the ligand, placed in fresh medium to allow the cells to cascade into the S phase of the cell cycle, and grown with 0.02 μM or 0.03 μM Adriamycin (Fig. 2-11). In this experiment the parabactin clearly potentiated the activity of Adriamycin (see Discussion). Finally, in a third experiment cells were treated with 5 μM parabactin for 4 h and then Adriamycin 0.2 μM was added for an additional 2 h. Cells were washed, reseeded and grown in fresh drug-free
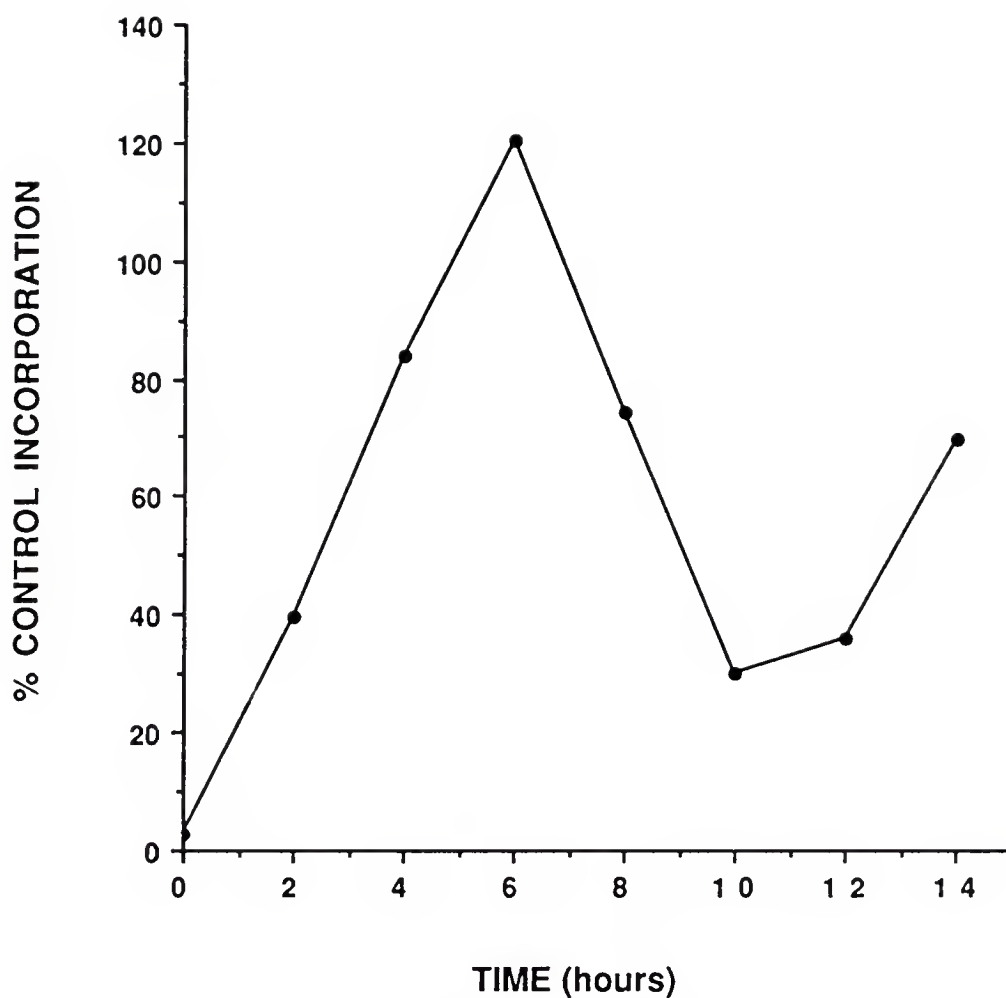
Figure 2-9. Time course for the incorporation of [³H]thy-
midine into the acid-precipitable fraction of L1210 cells grown in
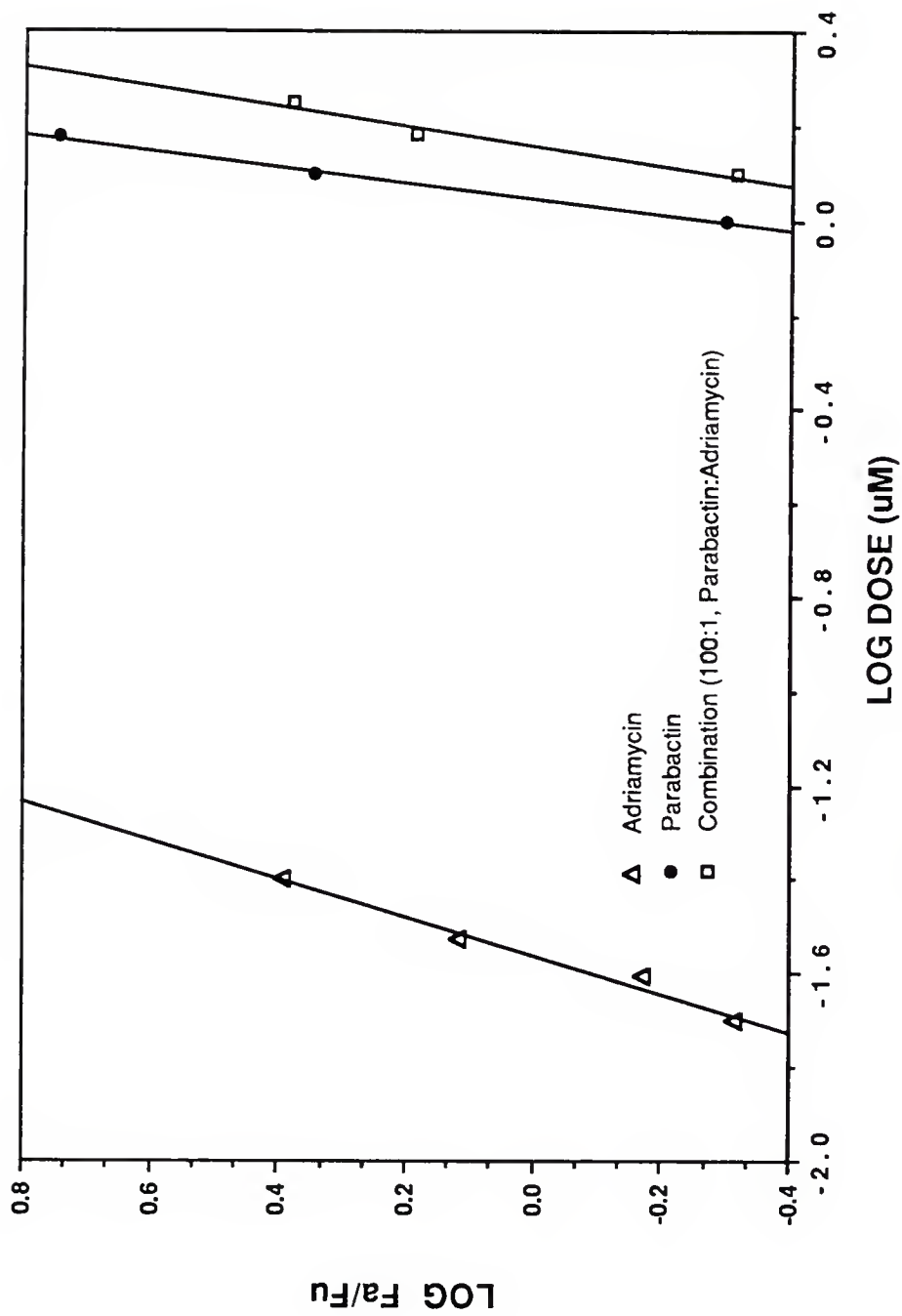fresh medium after treatment with 5 μM parabactin for 5 h.

Figure 2-10. Median effect plots for L1210 cells exposured for 48 h to Adriamycin, parabactin, and the simultaneous combination of parabactin:Adriamycin at a molar ratio of 100:1.
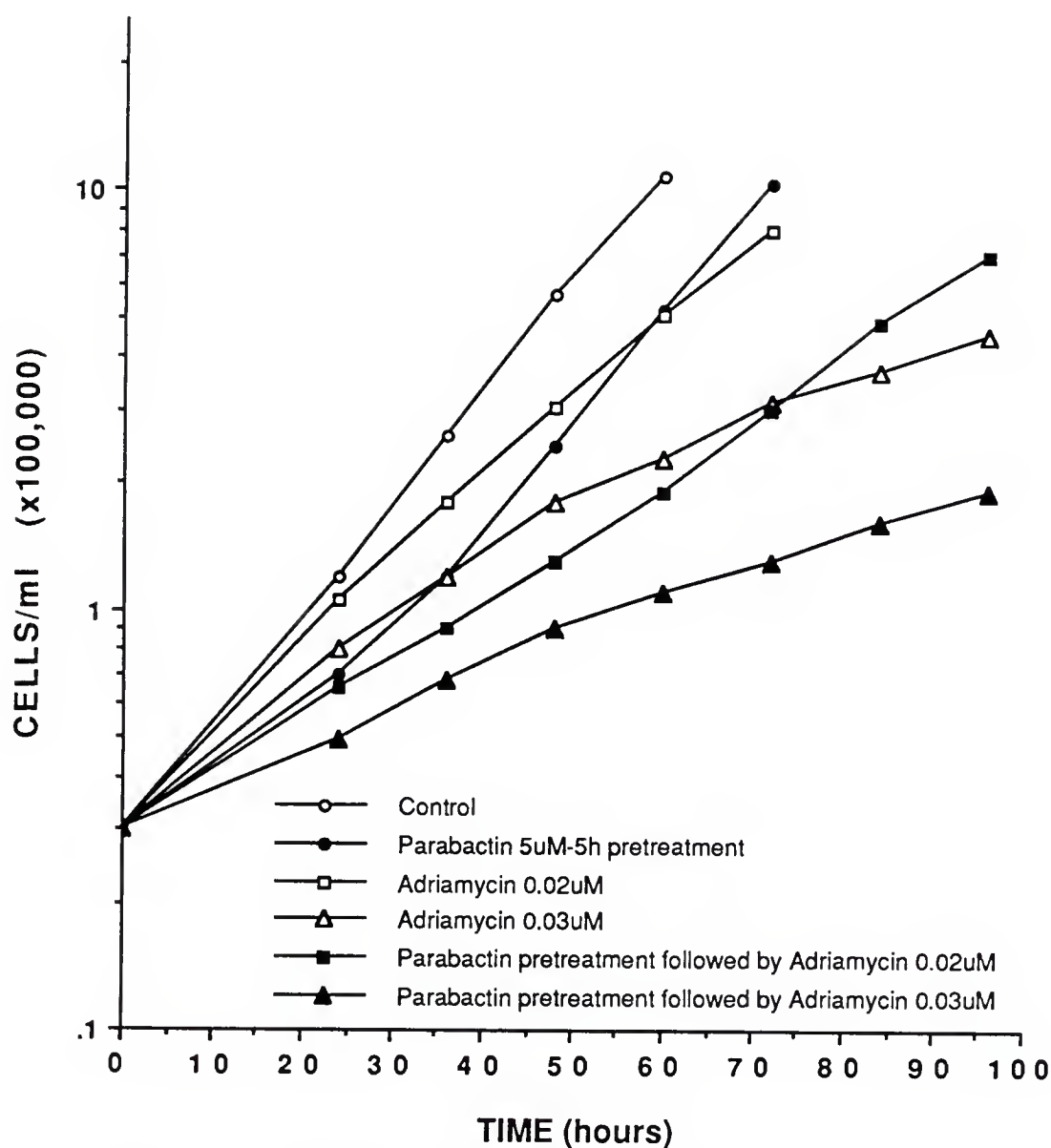
Figure 2-11. The effects of Adriamycin on the growth of L1210 cells, and Adriamycin on the growth of cells which have been pretreated with 5 µM parabactin for 5 h then washed to remove the block in DNA synthesis. The growth of control cells and cells exposed to 5 µM parabactin for 5 h and resuspended in drug-free medium is shown for comparison.

medium (Fig. 2-12). The results indicated additivity of the two drug effects.

Ara-C-treated Cells.--The IC_{50} of ara-C in our L1210 cell assay system was 0.033 μM, L1210 cells were treated with parabactin and ara-C simultaneously at a constant molar ratio of 100:1. The concentrations at a constant ratio of parabactin to ara-C were 1.75:0.0175, 1.5:0.015, 1.25:0.0125, 1.0:0.01, 0.75:0.0075, and 0.5:0.005. The IC_{50} of the combination was 1.39 μM (CI = 1.33). Again, Chou and Talalay analysis of the growth data indicated "antagonism" (Fig. 2-13).

However, when cells were first treated with 5 μM parabactin for 5 h, washed with fresh medium, and followed by treatment with ara-C, as with the Adriamycin:parabactin combination, the parabactin potentiated the activity of the ara-C (Fig. 2-14).

When cells were simultaneously treated with 5 μM parabactin and 1 μM or 2 μM ara-C for 5 h (Fig. 2-15), or first treated with 2 μM parabactin for 4 h then 1 μM or 2 μM ara-C for an additional 12 h, then washed, reseeded and grown in fresh drug-free medium (Fig. 2-16), the results indicated additivity of the two drug effects for both combinations.

BCNU-treated Cells.--The IC_{50} for BCNU in our system was 4.13 μM. When cells were treated simultaneously with parabactin and BCNU at a molar ratio of 1:1, the IC_{50} of the combination was 2.28 μM (CI = 1.1), indicating additivity (Fig. 2-17). The absolute micromolar drug concentrations to which cells were exposed were 3:3, 2:2, 1:1, 0.5:0.5, and 0.25:0.25.

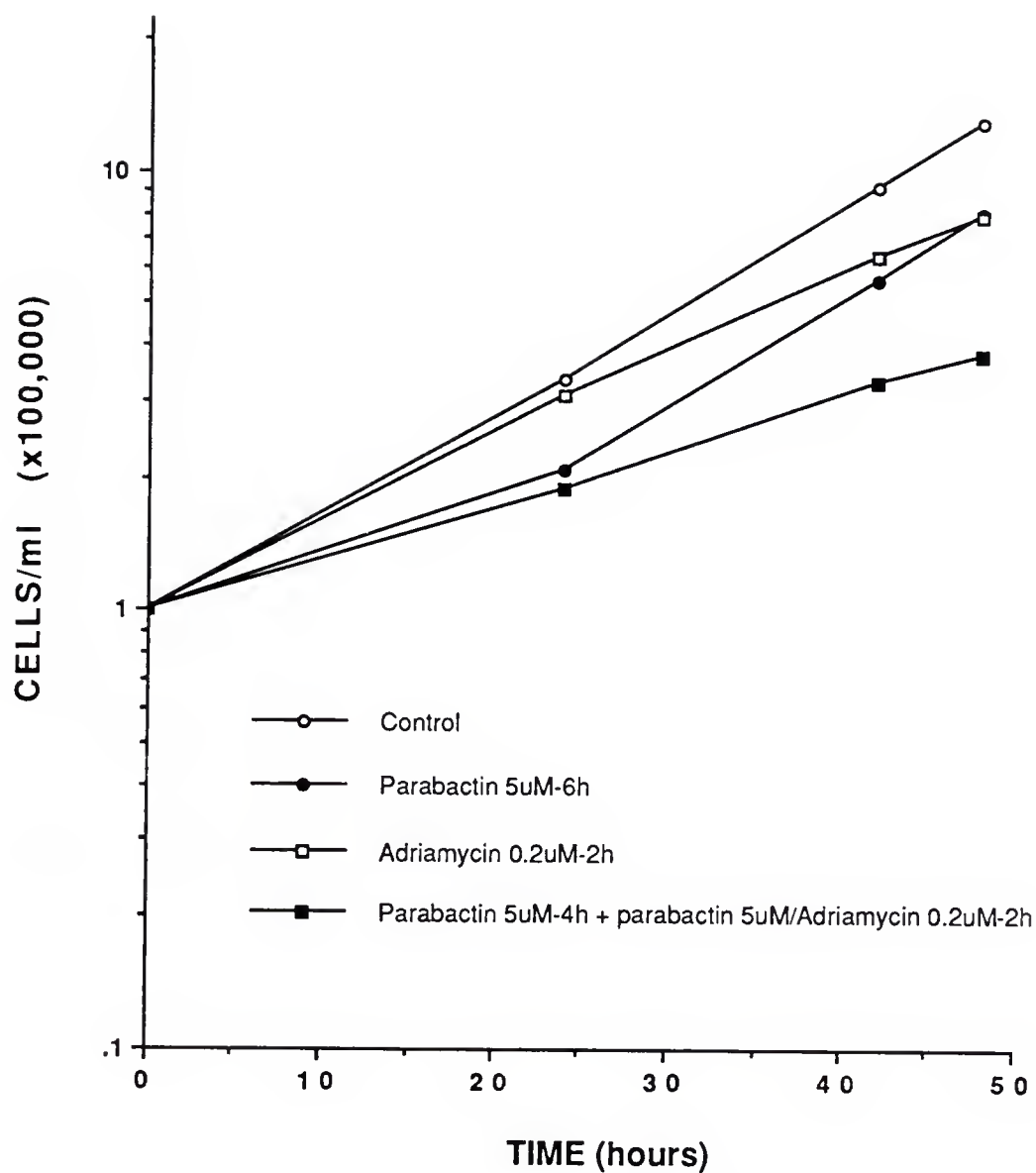Figure 2-12. The effects of 0.2 μM Adriamycin exposure for 2 h, parabactin 5 μM treatment for 6 h, and 5 μM parabactin for 4 h plus the simultaneous exposure of 0.2 μM Adriamycin for an additional 2 h on the growth of L1210 cells. Treated cells were washed and resuspended in drug-free medium at time = 0 h.
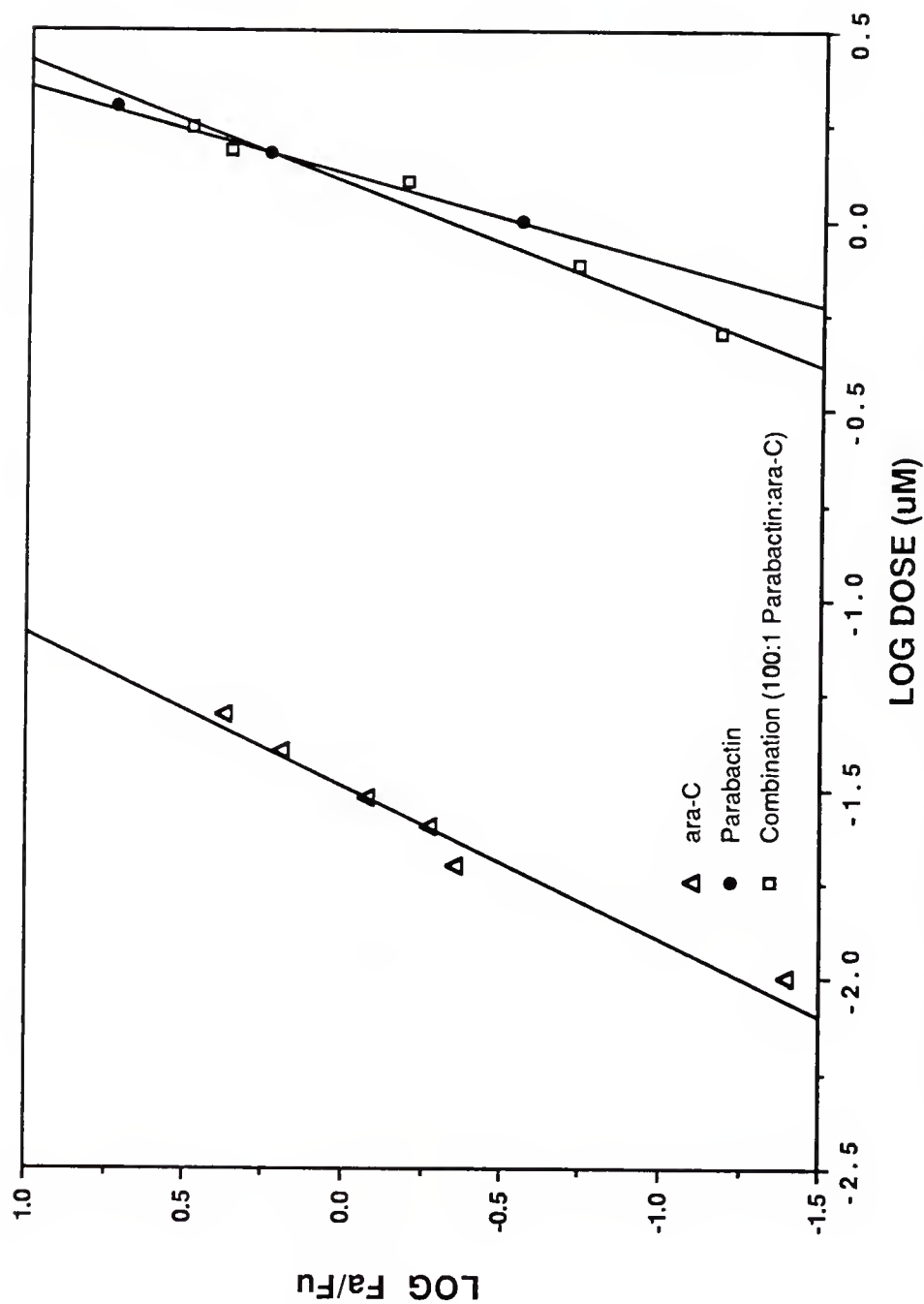
Figure 2-13. Median effect plots for L1210 cells exposed for 48 h to ara-C, parabactin and the simultaneous combination of parabactin:ara-C at a molar ratio of 100:1.
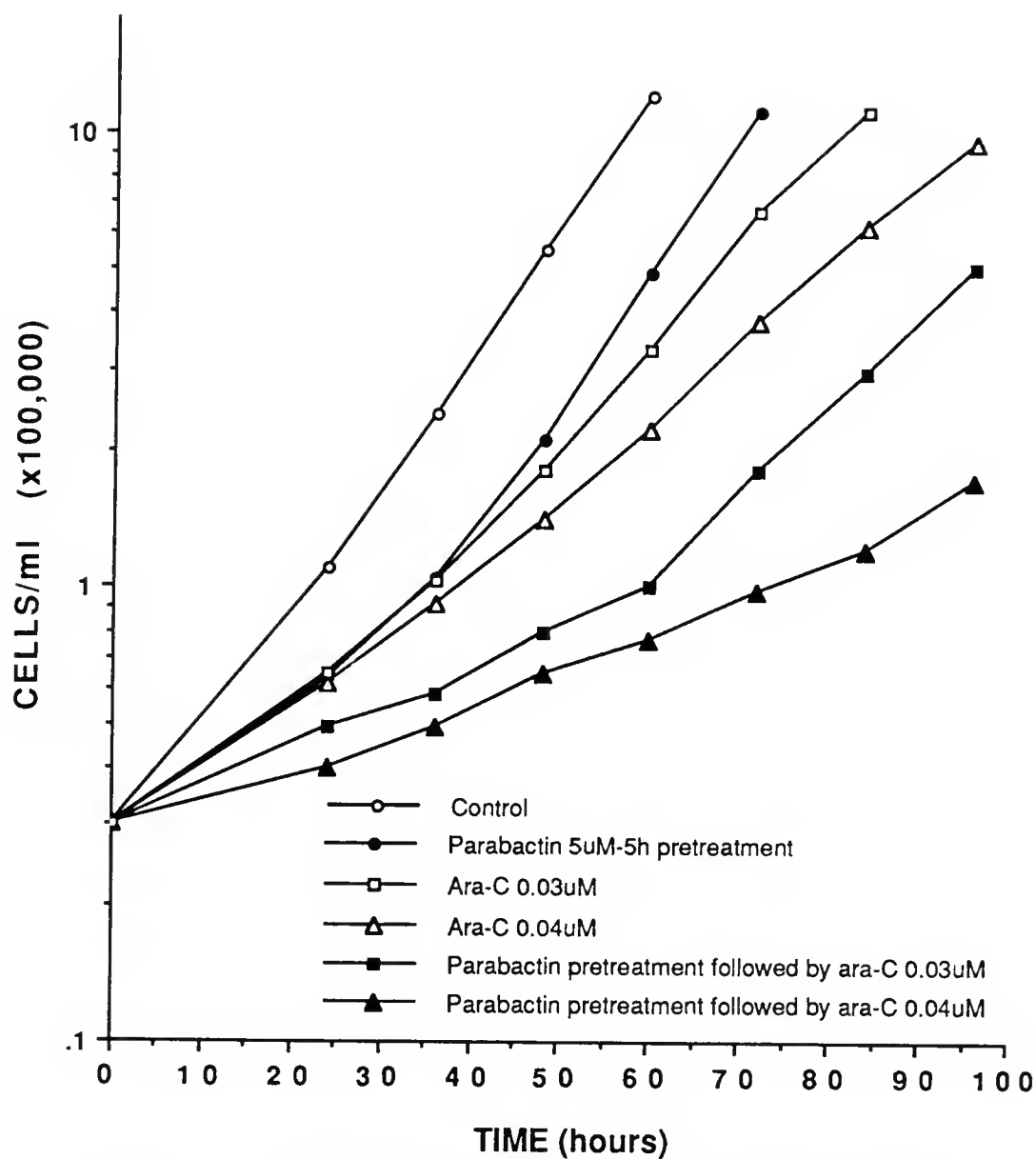
Figure 2-14. The effects of ara-C on the growth of L1210 cells, and ara-C on the growth of cells which have been pretreated with 5 µM parabactin for 5 h then washed to remove the block in DNA synthesis. The growth of control cells and cells exposed to 5 µM parabactin for 5 h and resuspended in drug-free medium is shown for comparison.

Figure 2-15. The effects of ara-C exposure for 5 h, parabactin 5 µM treatment for 5 h, and the simultaneous exposure of 5 µM parabactin plus ara-C for 5 h on the growth of L1210 cells. Treated cells were washed and resuspended in drug-free medium at time-0 h.
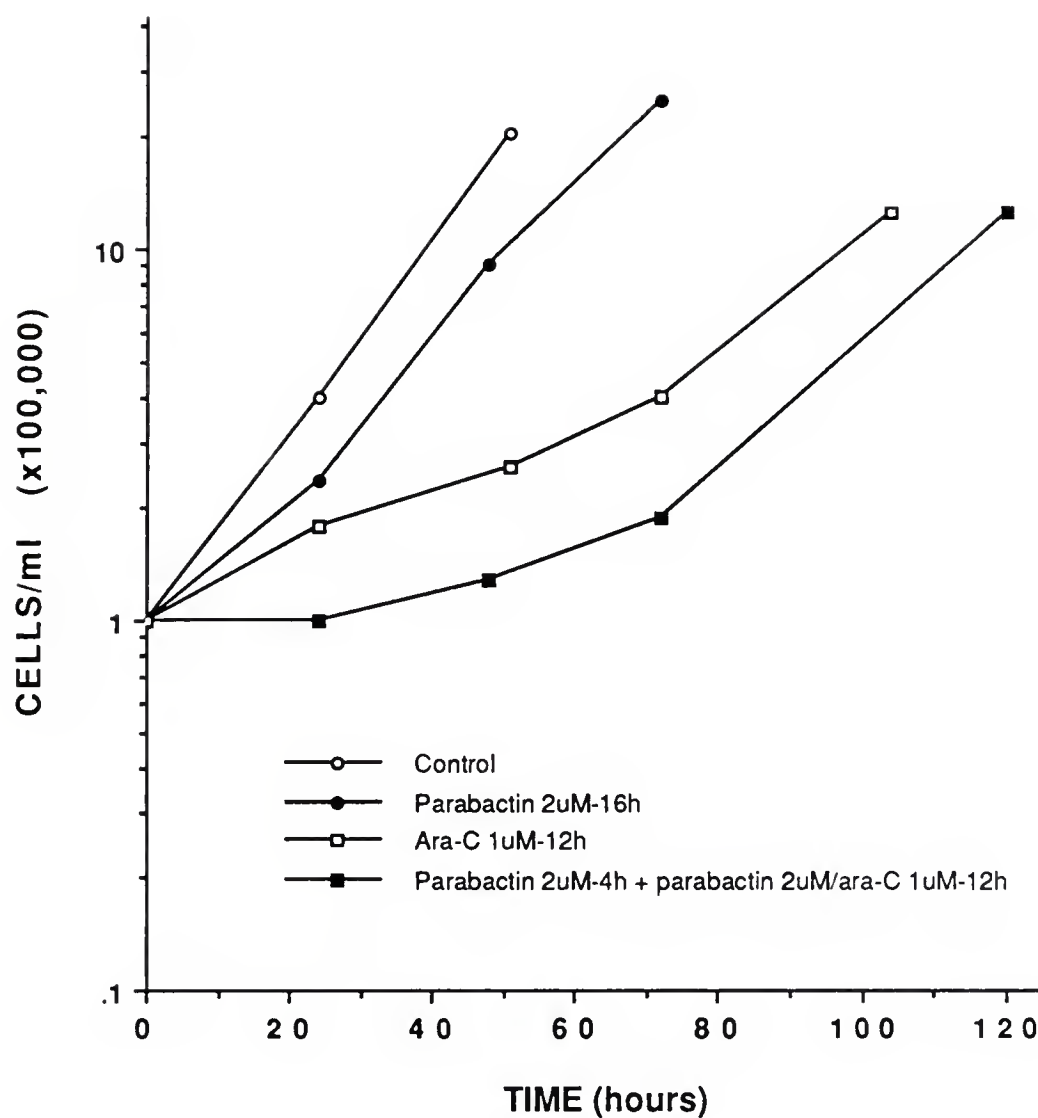
Figure 2-16. The effects of ara-C exposure for 12 h on the growth of L12110 cells, and 2 μM parabactin treatment for 4 h plus exposure to ara-C and parabactin for an additional 12 h on the growth of L1210 cells. The growth of control (untreated) cells and cells exposed to 2 μM parabactin for 16 h is shown for comparison. Treated cells were washed and resuspended in drug-free medium at time-0 h.
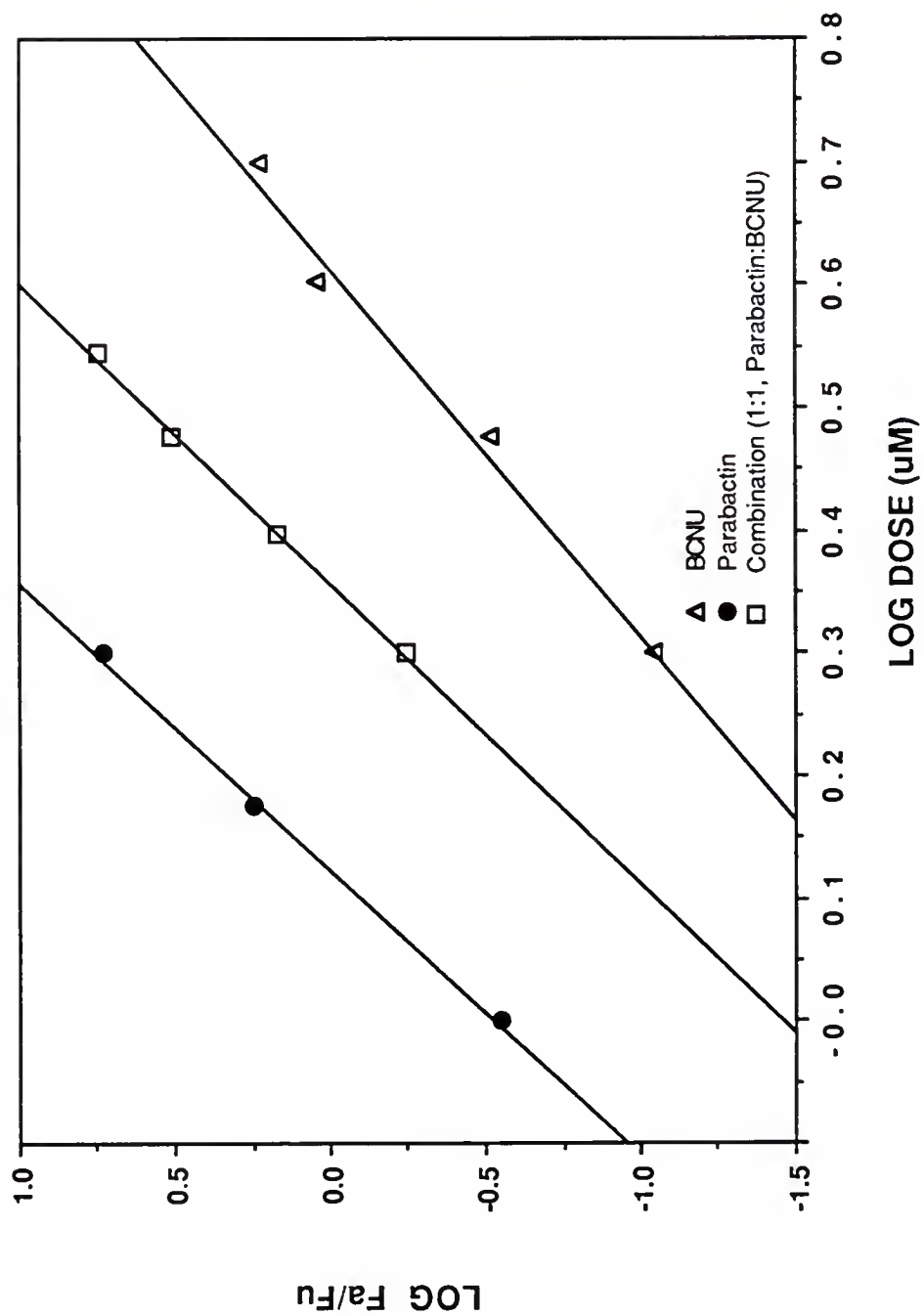
Figure 2-17. Median effect plots for L1210 cells exposed for 48 h to BCNU, parabactin and the simultaneous combination of parabactin:BCNU at a molar ratio of 1:1.

When cells were first treated with 5 µM parabactin for 5 h, washed with fresh medium, and treated with BCNU immediately, an additive effect was again observed (Fig. 2-18).

However, when cells were first exposed to 5 µM parabactin for 3 h, then presented with varying concentrations of BCNU for an additional 5 h, washed, and resuspended in fresh medium, cell growth indicated parabactin potentiation of BCNU activity (Fig. 2-19).

Animal Studies.--Ascites L1210 tumor cells in DBA/2 mice were blocked and synchronized by a single i.p. injection of parabactin 100 mg/kg (Fig. 2-20). The DNA histogram of the untreated ascites tumor shows a DNA content distribution similar to that of the cultured cells. At seven hours after the parabactin treatment a block in DNA synthesis at the G_1-S border of the cells is evident by the reduction in G_2 phase content and the broadening of the G_1-S content peak. At 8 h cells which were blocked at the G_1-S border begin to enter S phase, and by 9 h after the injection a large majority of the ascites cells have S phase DNA content indicating a synchronous population of cells.

There was no significant increased life span in mice given 1×10^5 L1210 cells i.p. and then treated with a daily (OD) injection of parabactin 100 mg/kg on days 1-6 compared to untreated mice or mice treated with only the 10% Cremophore drug vehicle. However, there was an 80% reduction in the ascites tumor burden of mice treated with parabactin 100 mg/kg every 8 h (98 h) for 5 injections beginning on day 5, compared to untreated mice. This dosage schedule could not be
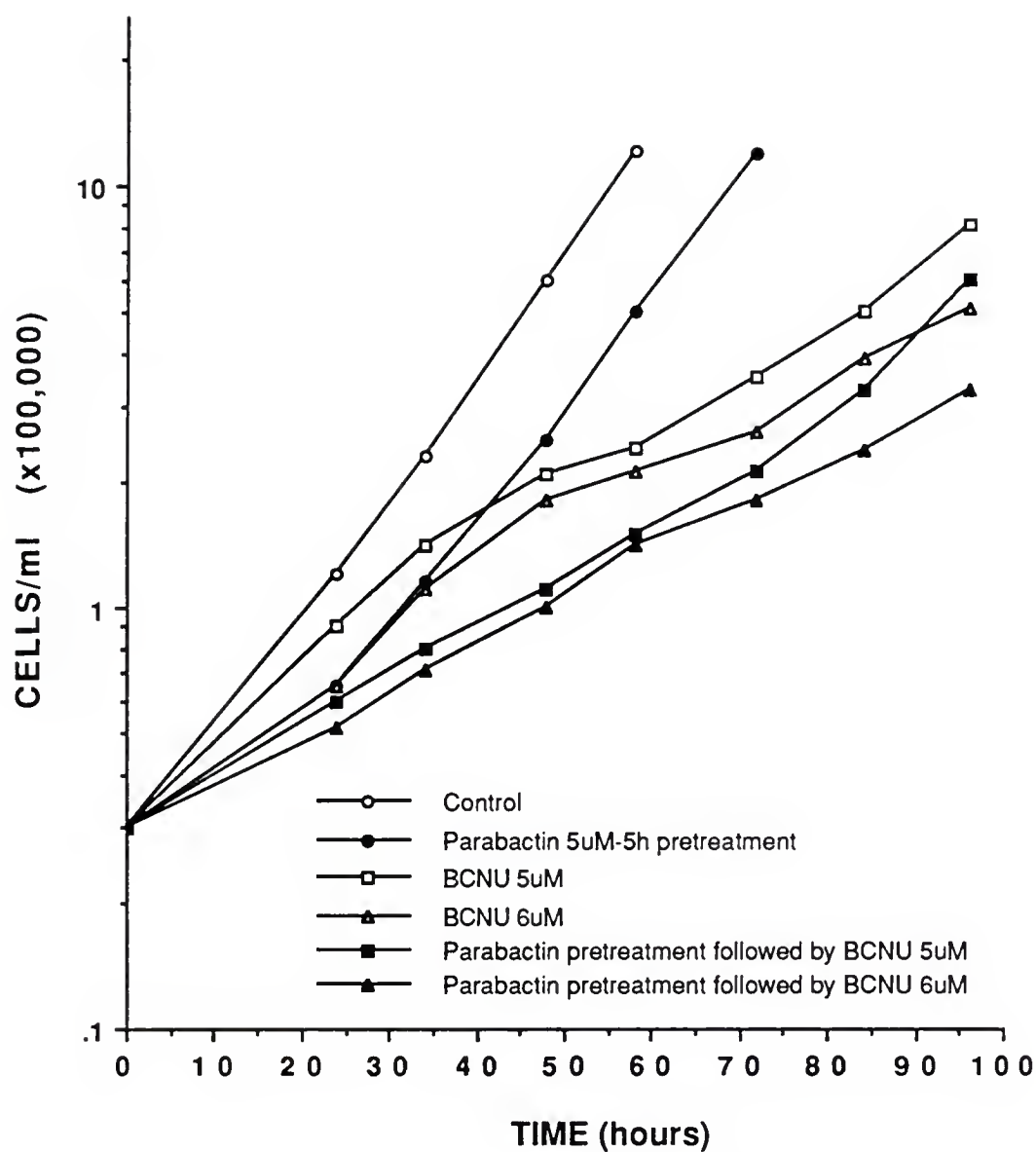
Figure 2-18. The effects of BCNU on the growth of L1210
cells, and BCNU on the growth of cells which have been pretreated
with 5 μM parabactin for 5 h then washed to remove the block in DNA
synthesis. The growth of cells exposed to 5 μM parabactin for 5 h
and resuspended in drug-free medium is shown for comparison.
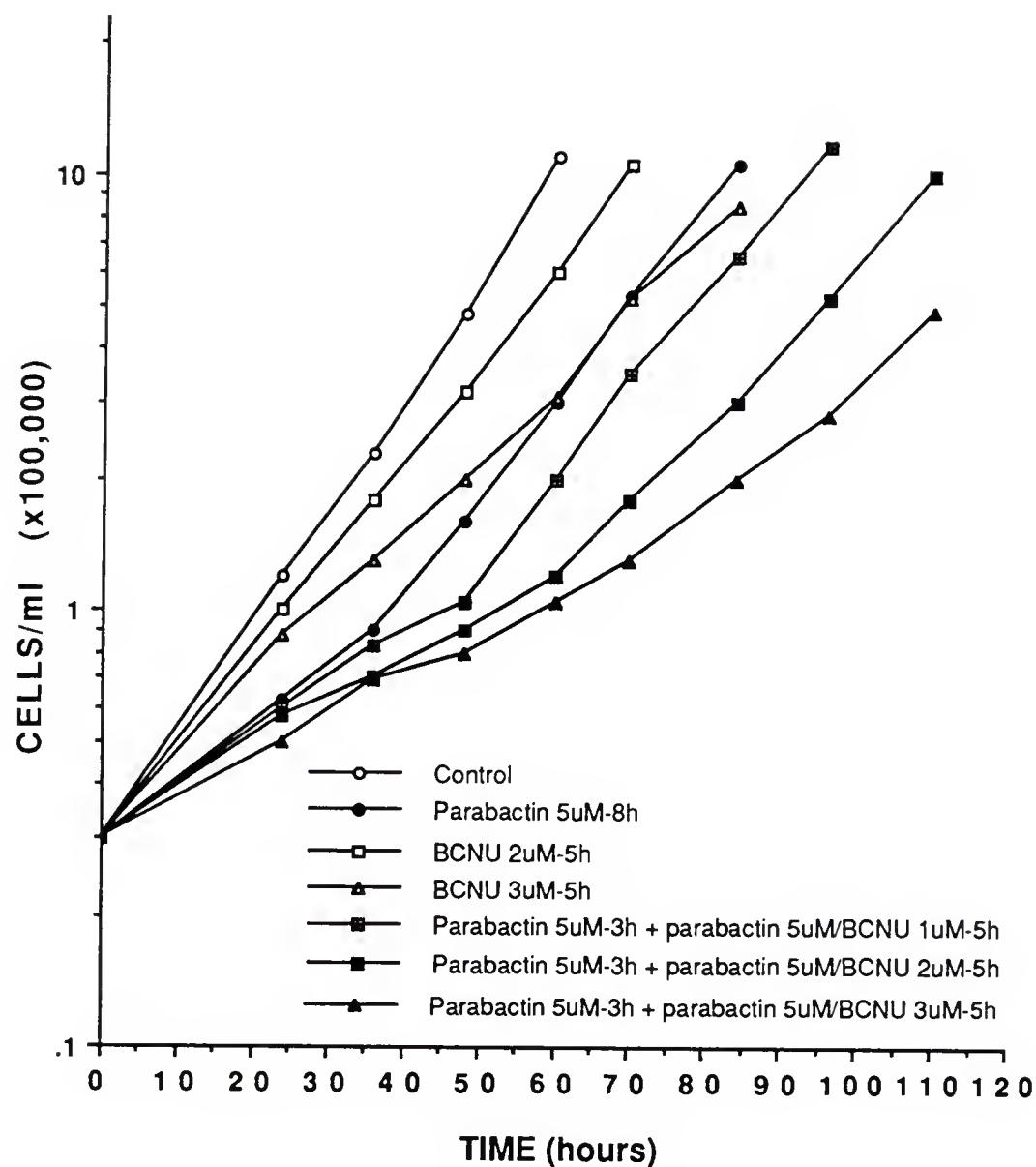
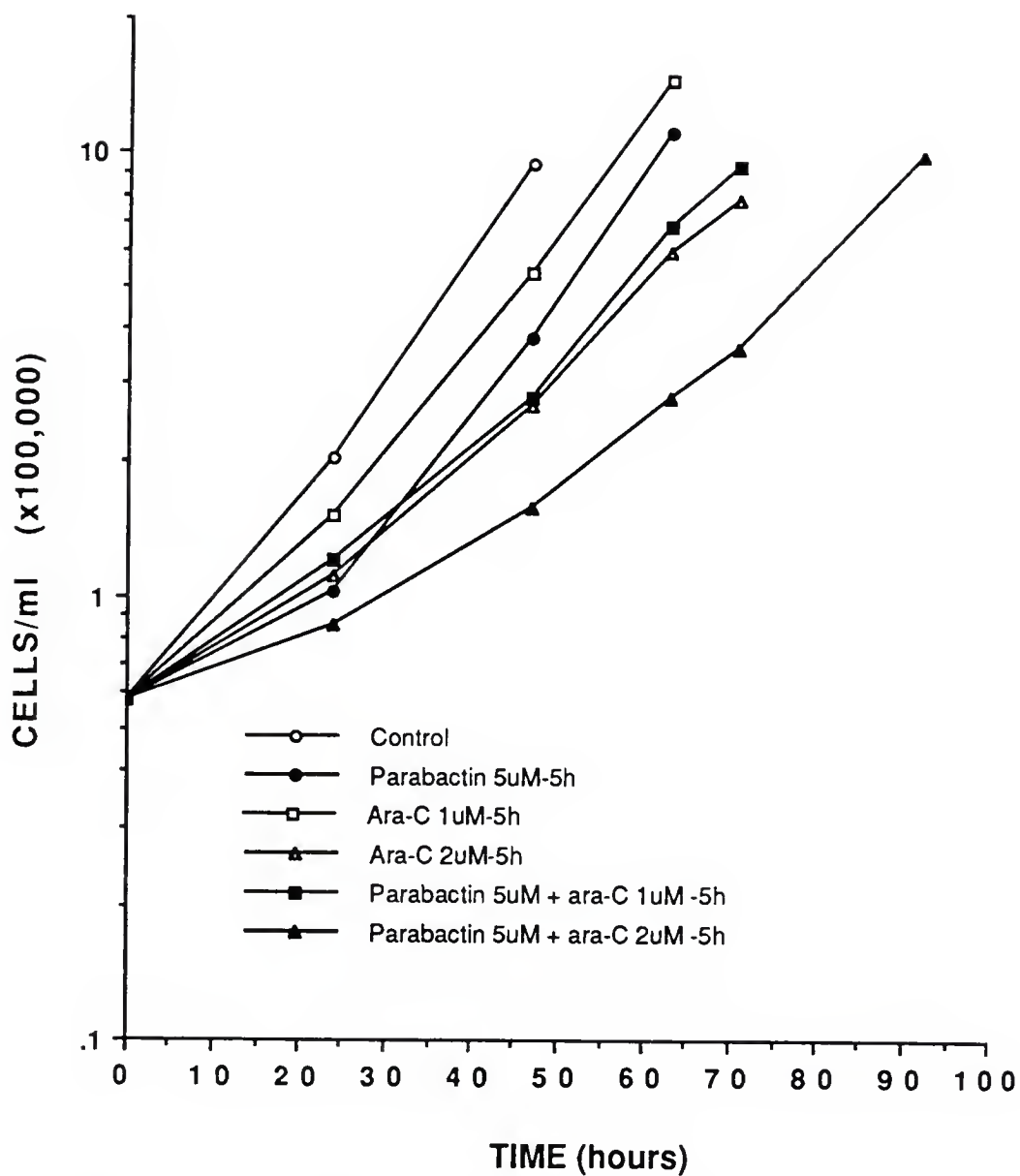Figure 2-19. The effects of BCNU exposure for 5 h, parabactin 5 µM treatment for 8 h, and 5 µM parabactin for 3h plus the simultaneous exposure to BCNU for an additional 5 h on the growth of L1210 cells. Treated cells were washed and resuspended in drug-free medium at time-0 h.
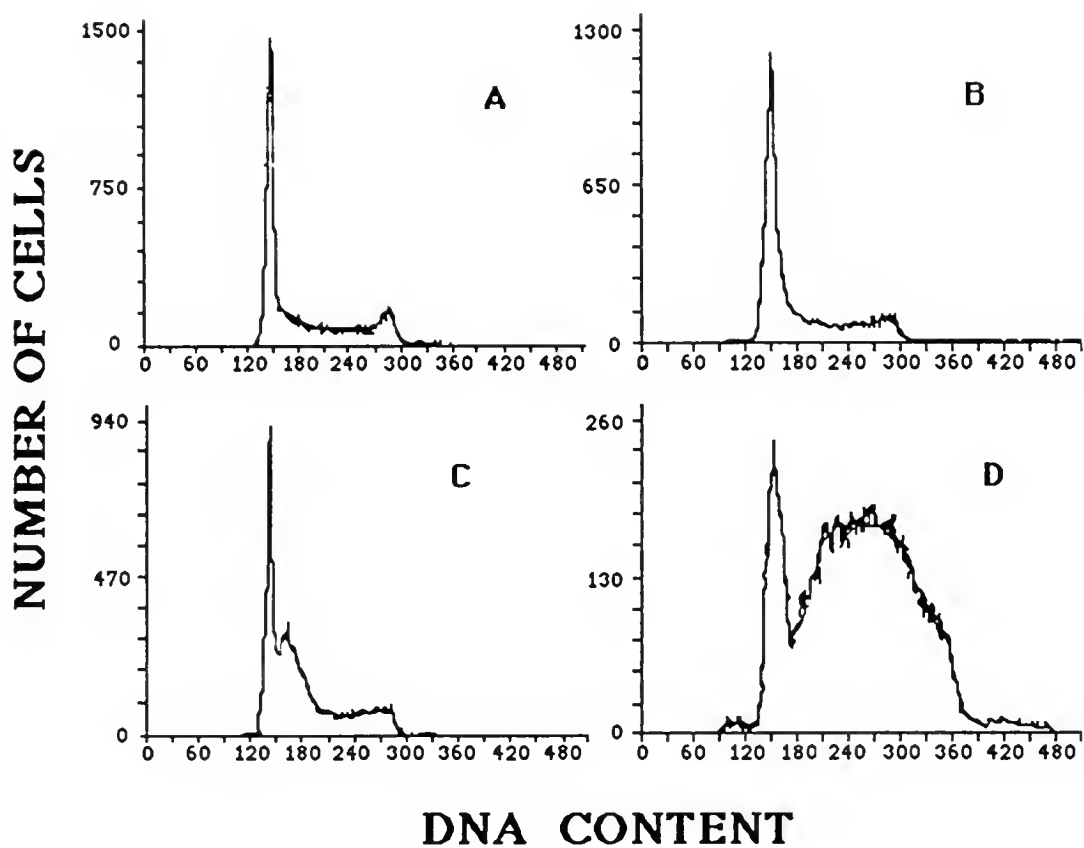
Figure 2-20.   Flow cytometric analysis of ascites L1210 cells from DBA/2 mice after a single i.p. injection of parabactin 100 mg/kg.

     A.   0 h
     B.   7 h
     C.   8 h
     D.   9 h

continued for more than the 5 doses in the mice due to the observed toxic effects (constipation and death) of the Cremophore vehicle when administered alone at concentrations necessary to solubilize this dose of parabactin.

Various combinations of parabactin with ara-C or Adriamycin in mice with L1210 tumors (Table 2-4) did not disclose any significant increases in life span beyond the additive effects of the individual treatments.

Discussion

Iron chelators have been shown to have profound effects on the growth properties of various tumor cell lines (37,41-43). The antiproliferative activity of the siderophores against L1210 cells as assessed by their IC_{50} values indicated that, when ranked according to their ability to sequester iron, the compounds with the higher iron binding constants generally demonstrated better antileukemic activity (37). The most active of the compounds tested here (the hexacoordinate catecholamide chelators, vibriobactin and parabactin) have an enormous affinity for iron and exhibited the most potent antiproliferative activity with IC_{50} values against L1210 cells of 2 μM and 1.5 μM, respectively. Both compounds were able to cause nearly complete cessation of cell growth in 24 h at concentrations above 5 μM while below 1 μM little growth inhibition was seen.

In an effort to ascertain the broadness of activity of the catecholamide chelators, they were tested against various other cultured cell lines. Parabactin and vibriobactin were found to be potent growth inhibitors of various animal and human tumor cells with 48 h IC_{50}

TABLE 2-4
ACTIVITY OF PARABACTIN, ARA-C AND ADRIAMYCIN, EITHER ALONE OR IN COMBINATION, AGAINST L1210 MURINE LEUKEMIA IN DBA/2 MICE

Experi-ment Number	Drug	Treatment	Dosage Schedule	Mean Survival (days) ± S.D.	% ILS
1.	Parabactin	100 mg/kg	OD day 1	9.5 ± 1.0	3
	Ara-C	120 mg/kg	Day 1	12.0 ± 1.9	23
	Ara-C/Parabactin[a]		OD day 1	12.6 ± 1.8	29
	NONE		OD	9.7 ± 0.8	0
2.	Parabactin	100 mg/kg	q12h days 1-2 and 6-7	11.0 ± 2.2	13
	Ara-C	40 kg/mg	q12 h days 1-2 and 6-7	19.5 ± 2.7	100
	Ara-C/Parabactin[b]		Days 1-2 and 6-7	15.7 ± 5.9	62
	NONE			9.8 ± 0.8	0
3.	Parabactin	100 mg/kg	OD day 1	10.0 ± 1.0	5
	Adriamycin	2 mg/kg	OD day 1	10.5	11
	Adriamycin/Parabactin[c]		OD day 1	11.5 ± 1.2	21
	NONE			9.5 ± 0.7	0
4.	Parabactin	100 mg/kg	OD days 2 and 4	10.0 ± 1.0	11
	Adriamycin	3 mg/kg	OD days 2 and 4	14.1 ± 5.2	57
	Adriamycin/Parabactin[d]		OD days 2 and 4	15.1 ± 3.3	68
	NONE			9.0 ± 0.4	0

[a]Ara-C given 7 h after parabactin.
[b]Ara-C alternated q12 h after parabactin.
[c]Adriamycin given 7 h after parabactin
[d]Adriamycin given 7 h after parabactin.

NOTE: DBA/2J mice given 10^5 L1210 cells i.p. on day 0.
All treatments given by i.p. injection.
OD = Once daily.
q12h = every 12 h.

values of approximately 2 µM for all cell lines tested. Parabactin was
also found to be a potent inhibitor of actively-dividing normal HFF
cell growth with a 96 h IC_{50} value of 2 µM.

That growth inhibition is due to iron chelation seems apparent
from studies in which iron, added at the same time as the chelators,
prevents the effects. This is consistent with previous findings (37)
in which the antileukemic and antiviral viral activities of compound II
could similarly be prevented. Also, methylation of the ligand's cate-
chol groups essentially blocking the siderophore's chelating function-
alities (Fig. 1-3) eliminated the antileukemic activity of vibriobactin
and greatly reduced the activity of parabactin (Figs. 2-2 and 2-3).
The residual activity of tetramethyl parabactin is likely due to the
remaining central oxazoline nitrogen and phenolic hydroxyl group's
ability to chelate iron. It has also been shown that parabactin was
able to suppress the growth of a variety of bacteria, while the addi-
tion of the tetramethylated parabactin analogue or the preformed
ferric-parabactin chelate was unable to inhibit microbial prolifer-
ation (72).

Cytostasis (apparent by dye exclusion, Rh-123 mitochondrial stain-
ing, ^{51}Cr release and clonagenic assays) is observed on a short-term
exposure (5 h) of L1210 cells to 5 µM parabactin or 10 µM vibriobactin,
and cidal activity when the cells are exposed for longer periods of
time (Table 2-2). The stasis is reversible by simply washing the lig-
and away from the cells within the first 5 h. However, a nondividing
confluent monolayer of HFF cells exposed to 20 µM parabactin (10 times
its IC_{50} value) for 24 h exhibited no apparent toxic effects.

The effects of vibriobactin and parabactin on L1210 cell growth are even more apparent after examining their impact on cell cycle kinetics. Both ligands hold the cells at the G_1-S border until they are released by washing the chelator away, at which point cells cascade into S phase (Figs. 2-7 and 2-8). This synchronous population of cells can be followed through the cell cycle with time, and in the case of parabactin a portion of the cells remained synchronized for 3 cell cycles. When parabactin treated cells are reseeded in fresh medium there is approximately a 14 h lag in growth relative to untreated controls. At this point cells appear to grow normally with a doubling time of 12 h (Figs. 2-11, 2-14, 2-18.)

Cycling of [^{3}H]thymidine incorporation into DNA (Fig. 2-9) during the first 12 h after washing parabactin from treated cells, or cycling of BrdUrd incorporation into DNA after vibriobactin pretreatment (Table 2-3) was consistant with the time frame of changes in S-phase followed by flow cytometry. However, the percentage of control incorporation during certain phases in the cell cycle reveals an actual DNA synthetic rate which does not correspond to the levels expected from the percentages of cells with S-phase DNA content by flow cytometry (Fig. 2-8). For example, flow cytometry indicated that at 8 h after washing the percentage of cells having S-phase DNA content is approximately twice that (200%) of control; however, [^{3}H]thymidine incorporation corresponds to a DNA synthetic rate of only 120% of control. From these studies it seems that while a sizeable fraction of the cells moves synchronously through the cell cycle in 10 to 12 h, there is also a fraction of cells which are moving more slowly through the cell cycle. Together, the fraction of cells moving more slowly through the cell

cycle along with the decrease in viability of cells after short-term parabactin treatment may account for the 14 h delay in cell growth relative to controls.

The phase specificity of the effects of the catecholamides is similar to that seen with hydroxyurea (80-81) which is believed to inhibit cell growth through interference with the enzyme ribonucleotide reductase by a free radical scavaging mechanism (26). The hydroxamate iron chelator desferrioxamine has also been shown to inhibit DNA synthesis through interference with the same enzyme. Interfering with this enzyme's activity blocks DNA synthesis, and cells accumulate at the G_1-S boundary of the cell cycle (81). It has been demonstrated that parabactin is a potent inhibitor of ribonucleotide reductase (38).

It is highly unlikely that the growth inhibition and cell cycle effects of the catecholamides are a consequence of extracellular iron chelation. It has been shown that the removal of iron from transferrin by siderophores occurs at a rate greater than 10% per hour only at high ligand to transferrin ratios (82), and removal is impeded in the presence of serum proteins (83). Transferrin is supplied to the cell growth medium along with other growth factors as a 10% serum supplement. Unless the removal of iron from the extracellular medium by the chelator occurred at a rate far in excess of 10% per hour it would not account for the early onset of inhibitory effects of the siderophores on DNA synthesis (3 h) (Fig. 2-5) or cell growth (12 h) (Fig. 2-3) since L1210 cells grown in medium with 5% or 10% serum proliferate at essentially the same rate. Also, there was not a proportional increase in IC_{50} values or significant change in the time to obtain a complete

cell cycle block when parabactin treated cells are grown in 5%, 10% or 20% fetal calf serum. If cell growth inhibition required an established concentration of chelator to limit extracellular iron, there should be a proportional response of IC_{50} values in relation to changes in serum concentration in the medium. Hence, if deprivation of iron to the cells caused by chelator-induced deferration of transferrin in the medium was the mechanism by which the catecholamides inhibit DNA synthesis, the times necessary to see a reduction in cell growth (5 μM parabactin for 12 h) and DNA content (5 μM parabactin for 3 h) would be expected to be much greater. Finally, there exists a good correlation between the antiproliferative activity and lipophilicity of various catecholamide chelators examined (37). This correlation would not be expected if extracellular chelation were taking place.

The effects of the parabactin on the cell cycle kinetics of L1210 cells were compared with the effects of desferrioxamine and hydroxyurea (Fig. 2-6). Cells exposed to 5 μM parabactin experienced a block at the G_1-S border in 5 h, while desferrioxamine was required to be in excess of 100 μM for a 5 h exposure. Finally, hydroxyurea needed to be in excess of 300 μM concentration for the same 5 h exposure time. It is interesting that the concentration of desferrioxamine required to block cells at the G_1-S border is in excess of 13 times the 48 h IC_{50} value of desferrioxamine and 7.5 times the 48 h IC_{50} value of hydroxyurea. The cell cycle blocking ability of parabactin at a concentration of 3.5 times its IC_{50} value was therefore far superior to that

of hydroxyurea or desferrioxamine. The release of the desferrioxamine (84) and hydroxyurea (85) blocks results in less effective cell cycle synchronizations, as the DNA histograms are normalized following one passage through the cell cycle.

As mentioned above, the reversibility of the effects of parabactin is dependent on how long the cells are exposed to the ligand. For example, when the cells are exposed to 5 μM parabactin for 48 h 59% of the cells die and 10 μM desferrioxamine kills 60% (Table 2-2).

The potent cell cycle blocking ability of parabactin and its reversibility suggested its application in combination with other phase-specific antineoplastic drugs.

Parabactin-treated cells offer two opportunities for potentiation of growth inhibition.

a. Agents acting at the G_1-S border should be more effective since the cells are held at this phase.

b. Agents acting during S phase should have improved activity since a larger percentage of the cell population will be synchronized into the S phase when the parabactin block is released.

When utilized in combination with ara-C, Adriamycin, or BCNU, parabactin can produce "antagonistic," "additive," or "synergistic" (potentiation) effects depending on the time frame during which the drugs are applied.

Two basic experiments were run in the combination chemotherapy studies.

a. Parabactin was used in simultaneous combination for 48 h with BCNU, ara-C, or Adriamycin.

b. Cells were first blocked with parabactin and held at the G_1-S border, then the parabactin was washed away allowing cells to cascade into S phase. The cells were then exposed to BCNU, ara-C, or Adriamycin.

The latter experiments relied heavily on cell cytometry techniques to evaluate the fraction of cells in each phase of the cell cycle after treatment with the catecholamide chelator.

A third experiment was performed with BCNU. The cells were treated with parabactin for 3 h and then with BCNU for 5 h. Then, after both drugs were washed away, cells were resuspended and regrown.

When cells are exposed to parabactin and ara-C simultaneously for 48 h, the effect of the combination is an "antagonistic" one (Fig. 2-13). This is in keeping with the previous observations that ara-C, an inhibitor of DNA polymerase (86), kills cells best in S phase (87) and that parabactin holds cells at the G_1-S border. This parabactin block thus diminishes the S-phase component of the cell population reducing the number of cells most susceptible to ara-C. Finally, the "antagonism" is apparent from the analysis of drug-induced growth inhibition. The IC_{50} value for the ara-C direct combination with parabactin at a 100:1 ratio was 1.33 µM with a CI>1 indicating an "antagonistic" effect.

However, when cells were first exposed to 5 µM parabactin for 5 h, washed free of the ligand releasing the block, and then treated with ara-C, the parabactin potentiates the activity of ara-C particularly at 0.04 µM ara-C (Fig. 2-14). Inspection of Figure 2-14 reveals that the growth of parabactin-treated cells is approximately 14 h behind the

growth of the control cells. Consequently, when comparing the effects

of the parabactin:ara-C-treated cells with ara-C treated cells, the 14

h lag for the parabactin-treated cells must be considered. Therefore,

in evaluating the combination curve relative to the ara-C curve, one

must look at a point on the combination line 14 h ahead of the ara-C

line. Even at this, it is clear that parabactin potentiates the activ-

ity of ara-C.

The same experiments were carried out with Adriamycin. The sim-

ultaneous drug combination experiment with 100:1 ratio of parabactin to

Adriamycin indicated "antagonism." Applying Equation A to the data

from Figure 2-10 resulted in a CI value of 1.57 indicating antagonism.

However, again when the cells were treated first with parabactin to

initiate a block at G_1-S and then washed free of the ligand and treated

with Adriamycin, the effect of Adriamycin was potentiated particularly

at 0.03 μM (Fig. 2-11). Again, one must consider the 14-h lag time in

growth generated by the parabactin. However, even after accounting for

this, reduction in growth rate is about twice that observed for the

Adriamycin itself. In view of the toxicity of Adriamycin, this may be

of some practical significance. As both Adriamycin (88) and ara-C are

proposed to operate best on cells in the S phase, the observed results

are as expected.

The final drug studied in this evaluation was BCNU. When cells

were exposed to parabactin and BCNU simultaneously for 48 h the results

indicated the combination to be additive with a CI approximately equal

to 1 (Fig. 2-17).

When the cells were first treated with 5 μM parabactin for 5 h,

and then released and immediately treated with BCNU (Fig. 2-18), the

effects were still additive. However, when the cells were treated with 5 μM parabactin for 3 h, then exposed to BCNU for an additional 5 h, and then washed and resuspended in culture, there is clearly a potentiation of the combined drug effects (Fig. 2-19). After accounting for the parabactin-induced lag the effect of the BCNU was two times as great as it was in the absence of parabactin. It was interesting to note that 1 μM BCNU in combination with parabactin was more active than 3 μM BCNU alone. In fact, cells treated with 1 μM BCNU (not shown) grew at the same rate as controls. The literature suggests that BCNU operates best at the G_1-S border and in G_2 of the cell cycle, while cells in S phase are more resistant (89). The BCNU potentiation effects of the drug combination were consistent with the observation that cells treated with parabactin were held at the G_1-S border. It remains somewhat unclear, however, why we did not observe synergistic effects when the drugs were used in direct simultaneous combination without washing.

The above observations also suggest that proper pretreatment of cells with parabactin could result in a decrease of the cytoxic effects of phase-specific antineoplastics by reducing the population of cells in the phase where the chemotherapeutic exerts its greatest cytotoxic action. In an attempt to demonstrate the possible "protective" effects of parabactin treatment against phase-specific toxicity, several experiments were devised. Cells were first treated with parabactin to reduce the S-phase population of cells. Adriamycin (Fig. 2-12) or ara-C (Fig. 2-16) was then added for an additional amount of time, and the

cells were washed and regrown in drug free medium. Additionally, cells were treated simultaneously with both parabactin and ara-C for 5 h and the cells were washed and regrown (Fig. 2-15). The results revealed additive effects of the combinations in all cases, thus failing to indicate any protection afforded cells out of synchronization with the phase specificity of ara-C or Adriamycin by parabactin treatment. The implications of these results may demonstrate, that while ara-C and Adriamycin are reported to exert their greatest cytotoxic effects on cells in S phase, they may enter the cell during any phase of the cell cycle. These results further imply that studies of simultaneous combinations for these types of drugs deserve further consideration. Analysis of the median effect plots by the method of Chou and Talalay (73) is only a mathematical manipulation of the 48-h IC_{50} values of the drugs at one specific molar ratio. The CI may not be a true reflection of the activity of the simultaneous combination of two compounds with such different mechanisms of action and the results must be interpreted with care.

The ability of parabactin to enhance the chemotherapeutic effects of various antineoplastic drugs was highly dependent on its ability to block cell cycle kinetics and to effectively reverse this block releasing the cells into a synchronized cell cycle. A consideration of the IC_{50} values of the drugs is probably relevant when considering the effectiveness of these compounds as cell cycle blocking agents. At 3.5 times its IC_{50} parabactin was an excellent cell blocking agent; it was better than desferrioxamine at greater than 13 times its IC_{50} and the hydroxyurea at 7.5 times its IC_{50} (Fig. 2-6). Furthermore, one of the most critical issues was the fact that parabactin-treated cells maintained partial synchronization for at least three cell cycles while

cell synchronization disappeared after one cell cycle in desferrioxamine- and hydroxyurea-treated cells.

The antiproliferative effects of parabactin were also studied in vivo. The L1210 cell tumor model has been used as a useful preclinical screening system for potential antineoplastics (90). The murine L1210 leukemia is a convenient and very reproducible in vivo model system. The tumor is very aggressive having an in vivo doubling time of about 10-12 h. Mean survival time of animals injected with 10^5 cells is approximately 9.5 days. It has been determined that one viable cell will kill an animal in about 18 days with a tumor burden of approximately 10^{10} cells (91). Therefore, it would require a one log reduction in cell number (90% cell kill) to see a one day increase in life span (ILS), and a two-log reduction in cell number (99% cell kill) to see a 2-3 day ILS, while even with a 99.99% cell kill the animals would still die in less than 20 days.

It is, therefore, not very surprising that leukemic mice treated with parabactin, which requires constant exposure of cells for significant periods of time to exhibit cytotoxic activity, on a single daily injection schedule for 6 days, showed no increased life span over untreated mice. However, leukemic mice treated with parabactin every 6 h for 5 injections did exhibit a reduction in tumor burden of 80% over controls. Considering the doubling time of this tumor, even this reduction in cell number would not extend the life of the mice to a significant degree. A drug having an ILS of greater than 35% in this system is considered to have significant activity by the National

Cancer Institute (92). Extended dosing on this schedule, while exhib-
iting promising activity, is prevented by the low solubility of the
catecholamides in most vehicles suitable for parental administration
(the solubility of parabactin in phosphate buffered saline being on the
order of 1.25×10^{-5} M) (37), and the toxicity of the vehicle alone on
frequent administration.

The ability of parabactin to block and synchronize cells has also
been demonstrated in vivo. Ascites L1210 cells were synchronized by a
single i.p. injection of parabactin (Fig. 2-20) in a manner similar to
that seen in culture. Attempts to demonstrate enhanced cytotoxic
effects of ara-C and Adriamycin on a parabactin synchronized in vivo
cell population resulted in no significant increase in life span of
L1210 mice over the additive effects of the individual treatments
(Table 2-4). Considering the optimum conditions studied with cultured
cells, which exhibited a maximum 2-3 fold potentiation of the cytotoxic
effects of the antineoplastics tested, very little increase in life
span would be expected in vivo by a reduction in tumor burden of
50-75%. Further refinements in the drug dosage and multiple dosing
schedules are currently under investigation.

CHAPTER III
POLYAMINE ANALOGUES

Materials and Methods

The polyamine analogues were synthesized by methods previously described (30,31). Stock solutions (10 mM) of analogues and dilutions were made in sterile water, and passed through a 0.2 μm filter prior to use. RPMI 1640, fetal bovine serum, HEPES, and MOPS were obtained from Gibco (Grand Island, NY). Cell culture flasks, 25 and 75 cm^2, were purchased from Corning (Corning, NY). Diamidino-phenylindole (DAPI), propidium iodide (PI), actinomycin-D and proteinase K were obtained from Sigma (St. Louis, MO). Rhodamine-123 (Rh-123) was purchased from Eastman Kodak Company (Rochester, NY). RNase T1 was obtained from BRL Scientific (Gaithersburg, MD). DBA/2J and C57B1/6J mice were obtained from Jackson Laboratories (Bar Harbor, ME). Albino CD-1 mice were obtained from Harlan Sprague-Dawley (Indianapolis, IN). Sprague-Dawley rats were obtained from Charles River (Wilmington, MA).

Cell Culture

All cell culture lines were grown as previously described in Chapter II. Several additional cell lines utilized in these studies were maintained in complete medium as before except where noted. Chinese hamster lung (DC3F) cells were grown as monolayers in 25 cm^2 flasks, seeded at 2×10^5 total cells and grown to confluency in in approximately 96 h. Actinomycin-D resistant Chinese hamster lung

(DC3F/ADX) cells were similarly maintained with actinomycin-D 10 μg/mL present in the medium. The Chinese Hamster Lung cell lines, DC3F and DC3F/ADX, were kindly donated by Dr. June Biedler of Memorial Sloan-Kettering Cancer Center, NY.

Resistant L1210 cell Lines

L1210 cell lines resistant to DESPM (L1210/DES-10) and DEHSPM (L1210/HDES-1) were selected out by maintaining the cells in increasing concentrations of polyamine analogues over an extended period of time. Initially, L1210 cells were exposed to either 1 μM DESPM or 0.1 μM DEHSPM for seven days and maintained between 1×10^5 and 1×10^6 cells/mL. Cells were then washed free of the drug and incubated in fresh medium until cell doubling time returned to normal (12 h). These cloned cells were then again exposed to a higher concentration of the analogue until normal cell doubling time resumed. Analogue concentrations were gradually increased over a period of approximately one month until cells could be maintained at a concentration of 10 μM DESPM and 1 μM DEHSPM. Resistant cells maintained at these concentrations of analogue for over six months had normal L1210 morphology and doubling time.

An Adriamycin resistant L1210 cell line (L1210/DOX-0.6) was similarly selected out by initially exposing cells to 0.01 μM Adriamycin. When approximate normal doubling time resumed, the Adriamycin concentration was increased until over a period of three months the cells could be maintained in the presence of 0.6 μM Adriamycin. The L1210/DOX-0.6 cells maintained for over six months differed from the normal L1210 cells in that they had irregular shapes and longer doubling times of 14-16 h.

IC$_{50}$ Determinations

The cells were treated while in logarithmic growth (L1210 cells, 3×10^4 cells/mL; Daudi and HL-60, 1×10^5 cells/mL) with the polyamine derivatives diluted in sterile water and filtered through a 0.2 µM filter immediately prior to use. Following a 48 h incubation with L1210 cells and a 72 h incubation with Daudi or HL-60 cells, cells were reseeded (L1210 cells, 3×10^4 cells/mL; Daudi and HL-60 cells, 1×10^5 cells/mL) and incubated in the presence of the polyamine derivative for an additional 48 h or 72 h, respectively.

Determination of IC$_{50}$ values for the most active compounds (IC$_{50}$ <5 µm at 96 h) was also performed in the presence of 1 mM aminoguanidine, a serum diamine oxidase inhibitor (93).

Chinese hamster ovary (CHO) cells and murine B-16 melanoma cells were seeded at 2×10^5 cells/25 cm^2 flask and allowed to attach for 4 h. At this time the cells were exposed to the polyamine analogue for 48 h. Monolayer cells were not reseeded for additional exposure times due to problems in plating efficiency after the initial 48 h treatment.

Cell samples were removed at the indicated time periods for counting. Cell number was determined by electronic particle analysis (Coulter Counter, Model ZB1, Coulter Electronics, Hialeah, FL) and confirmed periodically with hemocytometer measurements.

The percentage of control growth was determined as follows:

$$\% \text{ of control growth} = 100 \times [\text{Final treated cell no.} - \text{initial inoculum}]/[\text{Final untreated cell no.} - \text{initial inoculum}]$$

The IC_{50} is defined as the concentration of compound necessary to reduce cell growth to 50% of control growth after defined intervals of exposure.

Analysis of Drug Effects on Mitochondrial DNA

The L1210 cells (in complete media at 1×10^5 cells/mL) were incubated at 37°C in the presence of the compound to be tested. Every 24 h, for 144 h, cell samples were removed for counting, and the cells were reseeded in fresh medium and drug at 1×10^5 cells/mL. Cells were assayed daily for mitochondrial DNA (mtDNA) content. Mitochondrial DNA assays were performed by R. Bortell and L. Raynor of Dr. A. Neims' laboratory, Department of Pharmacology and Therapeutics, College of Medicine, University of Florida.

Because recovery of the organelles might vary with drug treatment, a dot blot procedure for assay of mtDNA was developed which involves analysis of cell lysates rather than preparations of mitochondria (94). Cells (5×10^4 to 2×10^5/mL) were lysed in 2% SDS in the presence of proteinase K (5 mg) and RNase T1 (100 units). The total cell lysate was applied to nitrocellulose paper with use of a 96-well, vacuum operated dot-blot apparatus. The blots were hybridized to a ^{35}S-labeled dATP nick translated probe made by inserting full-length mouse mtDNA into pSP64 vector at the Sac1 site. Dot blots were visualized by autoradiography and cut out, and radioactivity was determined by scintillation counting.

Flow Cytometric Analysis

Flow cytometric analysis of nuclear DNA (nDNA) content was performed with the RATCOM flow cytometer (RATCOM Inc., Miami, FL) interfaced with a microcomputer (IBM-XT). Cultured L1210 cells in log-phase growth were incubated at 37°C with various polyamine analogues and samples removed at 0 h, 48 h, 96 h and 144 h were analyzed for nDNA content distributions after staining with diamidinophenylindole in a nuclear isolation media (NIM-DAPI) (75).

Alternately, cell analysis was performed with a FACS II flow cytometer (Becton Dickinson FACS Systems, Sunnyvale, CA) interfaced with a microcomputer (Hewlett Packard 45B, Fort Collins, CO). Samples of 10^6 cells were removed and stained with propidium iodide (PI) (Calbiochem, San Diego, CA) and then exposed to RNase. DNA distributions were obtained from analysis of the red fluorescence from the PI-stained DNA (76).

Cloning Assay

L1210 cells maintained between 10^5 and 10^6 cells/mL were incubated with 10 µM DESPM for 96 h. At 24 h intervals treated cells were washed (2 x 10 mL) and diluted in fresh complete media and plated in triplicate 96-well microtiter plates at 0.4 cells/well with each well containing 100 µL of sample. The plates were incubated at 37°C in a humidified incubator in an atmosphere of 5% CO_2 and 95% air. The plates were examined with an inverse phase microscope at 100X magnification. The final number of colonies per plate was quantitated seven days after plating. Groups of 50 or more cells/well were identified as having been cloned from a single viable cell.

Regrowth Studies

L1210 cells maintained between 10^5 and 10^6 cells/mL were incubated with 10 µM DESPM, 30 µM DENSPM or DEHSPM 0.6 µM for 96 h. At each 24 h interval, treated cell samples were washed and the cells resuspended in fresh media at 1 x 10^5 cells/mL in duplicate 10 mL flasks. The regrowth of the treated cells was followed for up to 144 h.

Cell Size

Cell size was determined directly by the method of Schwartz, et al. (95). In brief, uniform polymeric microspheres ranging from 4.72-10.2 µM in diameter (Polysciences, Warrington, PA) were diluted in Hematall (Fisher Scientific Co.). Electronic size was measured on the FACS Analyzer (Becton Dickinson, Sunnyvale, CA) with the amplifier in the log mode. The peak channel number for each size microbead was plotted against the corresponding calibrated diameter and calculated volume to obtain a calibration curve. L1210 cells were treated with 10 µM DESPM, 30 µM DENSPM or DEHSPM 0.6 µM for 0-144 h and samples of 10^6 cells were removed at 24 h intervals and pelleted. The cells were resuspended in 0.5 mL of Hematall and analyzed. The peak channel number of the treated cells was plotted on the calibration curve to obtain the approximate cell size directly.

Viability Assay

The viability of cells which had been treated with 10 µM DESPM or 0.3 µM DEHSPM and or 30 µM DENSPM maintained between 5 x 10^4 and

1.2×10^6 cells/mL was assayed at appropriate times using two different methods: trypan blue dye exclusion and Rh-123 mitochondrial staining (74).

Briefly, 1×10^6 cells were pelleted by centrifugation and resuspended in 1 mL of complete medium containing Rh-123 10 µg/mL, incubated at 37°C for 10 min, and washed once with medium. Trypan blue was added prior to counting to give a final concentration of 0.2 µg/mL. Rh-123 and trypan blue stained cultures were observed in a hemocytometer using a Zeiss epifluorescence Axioscop microscope at 630X magnification. The excitation wavelength was 485 nm. Viable cells show mitochondrial specific uptake of the Rh-123 dye while dying cells showed diffuse cytoplasmic staining and dead cells did not fluoresce at all. Cells which did not fluoresce did not exclude trypan blue. Both methods gave comparable results as to cell death, however, trypan blue exclusion does not reflect dying cells.

Animal Studies

The polyamine analogue was diluted in sterile 0.9% saline within 24 h of use and the unused portion stored at 5°C. Concentrations of the spermine analogue tetrahydrochlorides, at each dose were adjusted so that the mice were injected with a volume of 1 mL/100 g (i.e. a 25 g mouse was injected with 0.25 mL of drug solution). Untreated mice served as controls.

The compounds were administered by i.p. injection according to the appropriate dosing schedule. The murine L1210 leukemia cells were maintained in DBA/2J mice. Cells from a single mouse which was injected i.p. with 1.25×10^4 cells seven days earlier were

harvested and diluted with cold saline so that an inoculum of 10^5 or 10^6 cells could be administered by a 0.25 mL i.p. injection. In each study mice were injected i.p. with the appropriate number of L1210 cells on day 0.

Alternately, Alzet mini-osmotic pumps, model 2001 (Alza, Palo Alto, CA) designed to deliver 1 μL/h for 7 days, were filled with DEHSPM so that the pump would deliver 20 mg/kg/day. The filled pumps were placed in sterile saline 0.9% and incubated at 37°C for 8 h prior to placement in the mice. The pumps were implanted, on day 1, subcutaneously (s.q.) in the dorsal side of the mice through an incision behind the right flank, and the incision closed with a wound clip. After 6 days the pumps were removed and the wound closed. The parameter used for treatment evaluation of activity against L1210 leukemia was mean survival time (percent increased life span, % ILS).

%ILS = 100 x [mean survival time treated animals-
mean survival time controls]/[mean survival time controls]

The murine B-16 melanoma was maintained in C57Bl/6J mice. The solid tumor was excised from a single mouse, which was injected sub-cutaneously (s.q.) 14 days earlier, and minced with 9 volumes of Hanks' balanced salt solution (10:1 brei). The brei (0.1 mL) was administered by s.q. injection in the right flank of the animal on day 0.

The murine Lewis lung carcinoma was maintained in C57Bl/6J mice. The solid tumor was excised from a single mouse which was injected s.q. 14 days earlier, and the tumor divided into equal

fragments 2-4 mm in size. Each mouse was injected s.q. with a frag-
ment in the sternum region using a 14 g trochar needle on day 0.

The parameter measured for treatment evaluation was median
tumor weight change based on length and width measurements in milli-
meters (92). The tumor weights (mg) were calculated from tumor
dimensions (mm x mm) following the formula for volume of a prolate
ellipsoid:

$$\frac{L \times W^2}{2}$$
where L is the longer of the two
measurements recorded

Median tumor weights were calculated for test (T) and control (C)
groups on days 10, 14 and 17 after inoculation of the tumor.

The activity of the analogue was reported as T/C% on the
measurement day giving the lowest value.

Rates of Uptake of Polyamine Analogues in L1210 Cells

L1210 cells maintained in mid-log phase growth were exposed to
the polyamine analogues for 0, 2, 6, 12 and 24 h, and samples of 10^6
cells were removed. The cells were washed with fresh medium (2 x 10
mL) and centrifuged to pellet the cells. The supernatant was care-
fully removed and the cells resuspended in 0.6 N perchloric acid
(10^7 cells/mL). Cells were freeze-fractured by four successive
freeze-thawings using liquid nitrogen. Cell lysates were stored at
-20°C until HPLC analysis. For HPLC analysis an aliquot of the solu-
bilized polyamine perchlorates was reacted with dansyl chloride, sod-
ium carbonate and diaminohexane as an internal standard. After con-
centration of the reaction products on a C18 chromatographic plug,
the dansylated polyamines were analyzed on reversed phase analytical

C18 column and quantitated using fluorescence detection and electronic integration. Analysis of HPLC samples were performed by J.R.T. Vinson, B. Jennings, and V. Andaloro of Dr. R.J. Bergeron's laboratory, Department of Medicinal Chemistry, College of Pharmacy, University of Florida.

Pharmacokinetic Studies

Preliminary pharmacokinetic studies to determine half-life of the analogues in the serum were studied in mice. Blood samples were collected by exsanguination of CD-1 mice into nonheparinized tubes at appropriate times after a single i.p. injection of DESPM (25 mg/kg). The serum was separated from the cells by centrifugation and diluted with an equal volume of 1.2 N perchloric acid. Analogue levels in the serum were determined by HPLC analysis by the above method.

The excretion of DEHSPM (25 mg/kg) after a single i.p. injection was followed in the urine and bile of Sprague-Dawley rats utilizing bile duct cannulation model. Rat bile duct cannulations were performed by K. Crist and E. LaGraves of Dr. R.J. Bergeron's laboratory, Department of Medicinal Chemistry, College of Pharmacy, University of Florida. The bile duct was cannulated with a segment of 22 ga polyethylene tubing and the bile directed from the rat to fraction collector by a fluid swivel mounted above a metabolic cage. Normal urine flow was also diverted with a segment of 5 mm tubing from the bottom of the metabolic cage to the fraction collector. This system allows the animal to move freely in the cage while continuous bile and urine samples were being collected in 3 h fractions for 24 h. Sample volumes were measured and diluted with an

equal volume of 1.2 N perchloric acid. Analogue levels in each fraction were determined by HPLC analysis by the above method.

Toxicity Studies

Both single dose and five-day daily-dose toxicity in CD-1 white mice were determined for DESPM and DEHSPM. Initially, small groups of 2-3 mice were used to determine the approximate range of toxicity for the compound. More accurate determinations of toxicity were made using groups of greater than 6 mice at each dose of analogue. Dosages ranged so that at the lowest dosage 10% or less of the animals die and at the highest dosage >90% of the animals die. At least 3 toxicity dosages between these two extremes were determined.

The polyamine analogue was diluted in sterile 0.9% saline within 24 h of use and the unused portion stored at 5°C. Concentrations of the spermine analogue tetrahydrochlorides at each dose were adjusted so that the mice were injected i.p. with a volume of 1 mL/100 g.

For the single dose toxicity studies each group of mice received a single i.p. injection of the analogue at an appropriate dosage. For the 5-day daily-dose toxicity studies each group of mice received a single i.p. injection of the analogue at an appropriate dosage daily for 5 days. Animal deaths were checked daily for 30 days. The number of deaths was expressed as percent lethality [100 x (number of deaths per group in 30 days/number of mice per group)].

Results

In Vitro Activity

The polyamines which were evaluated for their antiproliferative activity include the spermidine analogues (Fig. 3-1);

a. N,N'-bis(ethyl)-1,8-diaminooctane (BEDAO),

b. N^1,N^8-bis(propyl)spermidine (BPSPD),

c. N^1,N^8-bis(ethyl)-N^4-(p-nitrophenyl)spermidine (BEPNPSPD),

d. N^1,N^7-bis(ethyl)norspermidine (BENSPD),

e. N^1,N^8-bis(ethyl)spermidine (BESPD),

and the spermine analogues (Fig. 3-2);

f. N,N'-diethyl-1,12-diaminododecane (DEDAD),

g. N^1,N^{12}-dibenzylspermine (DBSPM),

h. N^1,N^{12}-di(2,2,2-trifluoroethyl)spermine (FDESPM),

i. 1,4-bis-[3-(ethylamino)propyl]piperazine (DEPIP),

j. N^4,N^9-diethylspermine (IDESPM),

k. N^1,N^1,N^{12},N^{12}-tetraethylspermine (TESPM),

and (Fig. 3-3)

l. N^1,N^{11}-diethylnorspermine (DENSPM),

m. N^1,N^4,N^9,N^{12}-tetraethylspermine (NTESPM),

n. N^1,N^{12}-dimethylspermine (DMSPM),

o. 1,20-bis(N-ethylamino)-4,8,13,17-tetraazaeicosane (YANK),

p. N^1,N^{12}-dipropylspermine (DPSPM),

q. N^1,N^{12}-diethylspermine (DESPM),

r. N^1,N^{12}-diethylhomospermine (DEHSPM).

The compounds described in this study are all in some way related to the natural products spermidine and spermine. They were
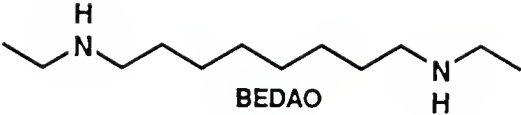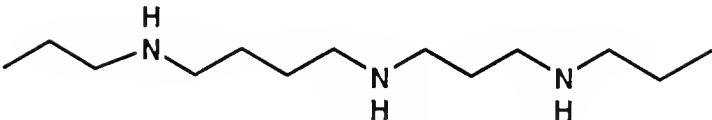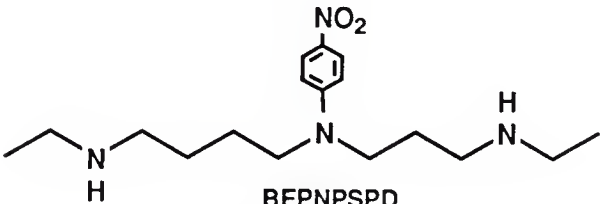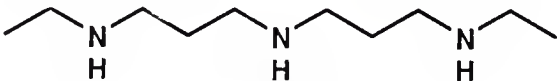
	48 h	96 h

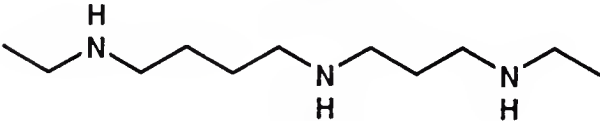BEDAO   >100 μM   >100 μM

BPSPD   > 30 μM   > 30 μM

BEPNPSPD   > 10 μM   > 10 μM

BENSPD   >100 μM   10 μM

BESPD   50 μM   10 μM

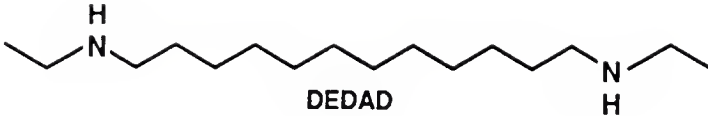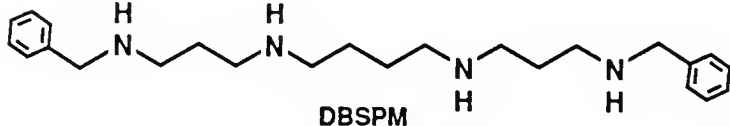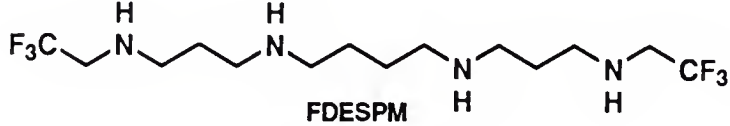Figure 3-1. Structure and IC_{50} values of the spermidine analogues.
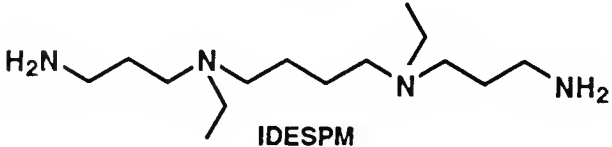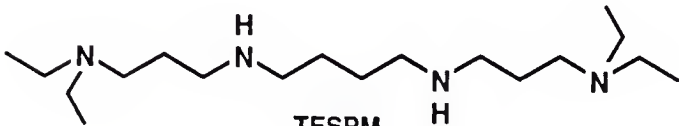
	48 h	96 h

DEDAD — Cytotoxic > 25 μM / No inhibition < 12.5 μM

DBSPM — Cytotoxic > 10 μM / No inhibition < 3 μM

FDESPM — >100 μM / >100 μM

DEPIP — > 50 μM / > 50 μM

IDESPM — > 25 μM / > 25 μM

TESPM — > 50 μM / 5 μM

Figure 3-2. Structure and IC_{50} values of the less active spermine analogues.
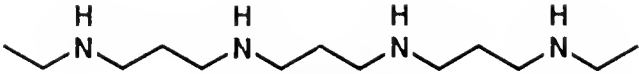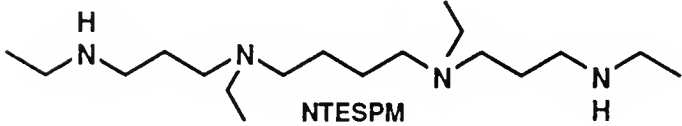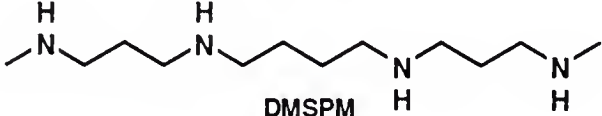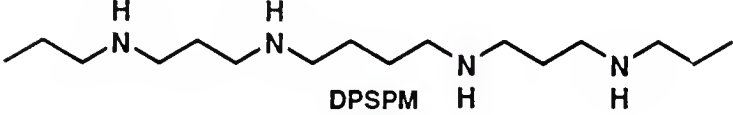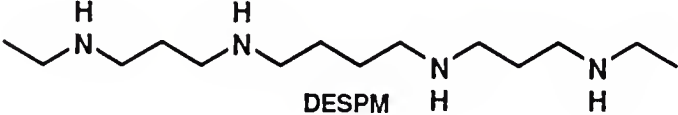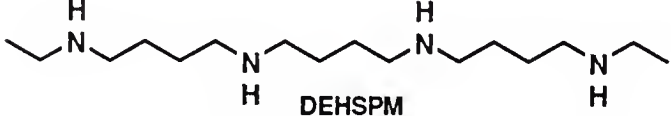
	48 h	96 h

DENSPM — >100 μM — 4 μM

NTESPM — 100 μM — 3 μM

DMSPM — >100 μM — 0.75 μM

YANK — 50 μM — 0.5 μM

DPSPM — 3 μM — 0.2 μM

DESPM — 10 μM — 0.1 μM

DEHSPM — 0.5 μM — 0.05 μM

Figure 3-3. Structure and IC_{50} values of the most active spermine analogues.
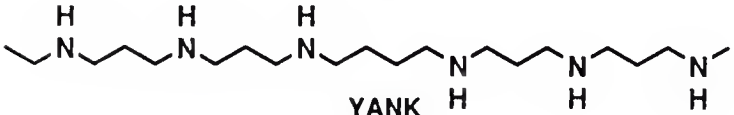
designed to evaluate relationships which might exist between the
structure of various alkylated polaymines and their activity against
tumor cells in culture. The relative antiproliferative activities of
the analogues were assessed by determining their 48-h and 96-h IC_{50}
values. In comparing the spermine compounds with their spermidine
counterparts (Figs. 3-1 to 3-3), it is clear that the spermine com-
pounds are substantially more active against L1210 cells.

Of the spermine analogues tested, DESPM and DEHSPM were the
most effective inhibitors of growth of L1210 cells. DESPM had 48 h
and 96 h IC_{50} values of 10 µM and 0.1 µM, respectively. DEHSPM
demonstrated superior activity and had 48 h and 96 h IC_{50} values of
0.5 µM and 0.05 µM, respectively. The IC_{50} values for the most
active analogues (IC_{50} value <5 µM at 96 h) determined in the
presence of 100 µM aminoguanidine, an inhibitor of diamine oxidase,
remained the same.

The activity of DESPM against Daudi cells and HL-60 cells is
comparable to that against L1210 cells. Because of the differences
in doubling times between L1210 cells (ca. 10-12 h) and Daudi or
HL-60 (ca. 25 h), the IC_{50}s of DESPM at 48 h and 96 h against L1210
cells are best compared with the IC_{50}s at 72 h and 144 h against
HL-60 (10 µM and 0.3 µM) and Daudi cells (>40 µM and 0.5 µM). Addi-
tionally, DEHSPM was shown to be active against CHO and B-16 melanoma
cells (doubling time for both lines 14-16 h) with IC_{50} values of
about 0.1 µM at 48 h for both cell lines.

L1210 cells which were selected for their ability to grow
in the presence of Adriamycin (L1210/DOX-0.6 cells) demonstrated
an approximate 50-fold increase in resistance to Adriamycin over the
parental L1210 cell line. The L1210/DOX-0.6 cells were demonstrated
by immunoblotting to have a large increase in the membrane

glycoproteins (P150-170 glycoproteins) and considered to be multidrug resistant cells (96). Both the parental cell line, as well as the resistant cell line, were colaterally sensitive to DEHSPM with IC_{50} values of 0.5 µM and 0.05 µM at 48 h and 96 h respectively.

The antiproliferative activity of DEHSPM was tested against DC3F cells and a proven multidrug-resistant subline, DC3F/ADX cells (97-99). Both cell lines were determined to be equally sensitive to DEHSPM having identical 96-h IC_{50} values of 0.1 µM.

L1210 cells which were developed for their resistance to the polyamine analogues L1210/DES-10 and L1210/HDES-1 did not demonstrate an overproduction of the P150-170 glycoproteins (96), indicating that they had not developed multidrug resistance; both were sensitive to Adriamycin to the same extent (IC_{50} value of 0.02 µM at 48 h). Both cell lines did, however, exhibit cross-resistance to other polyamine analogues. Both of the resistant cell lines were not inhibited by treatment with 100 µM DENSPM, and were able to grow to 70% of control in the presence of either 100 µM DESPM or 100 µM DEHSPM.

The role of the methylene backbone in the biological activity of the polyamine analogues was studied by comparing DENSPM, DESPM and DEHSPM. Reduction in the length of the polyamine backbone, decreased the activity of the analogue. The activity of DENSPM against L1210 cells (IC_{50} value of >100 µM at 48 h, and 4 µM at 96 h) is relatively poor when compared to that of DESPM and DEHSPM (Figs. 3-4 and 3-5).
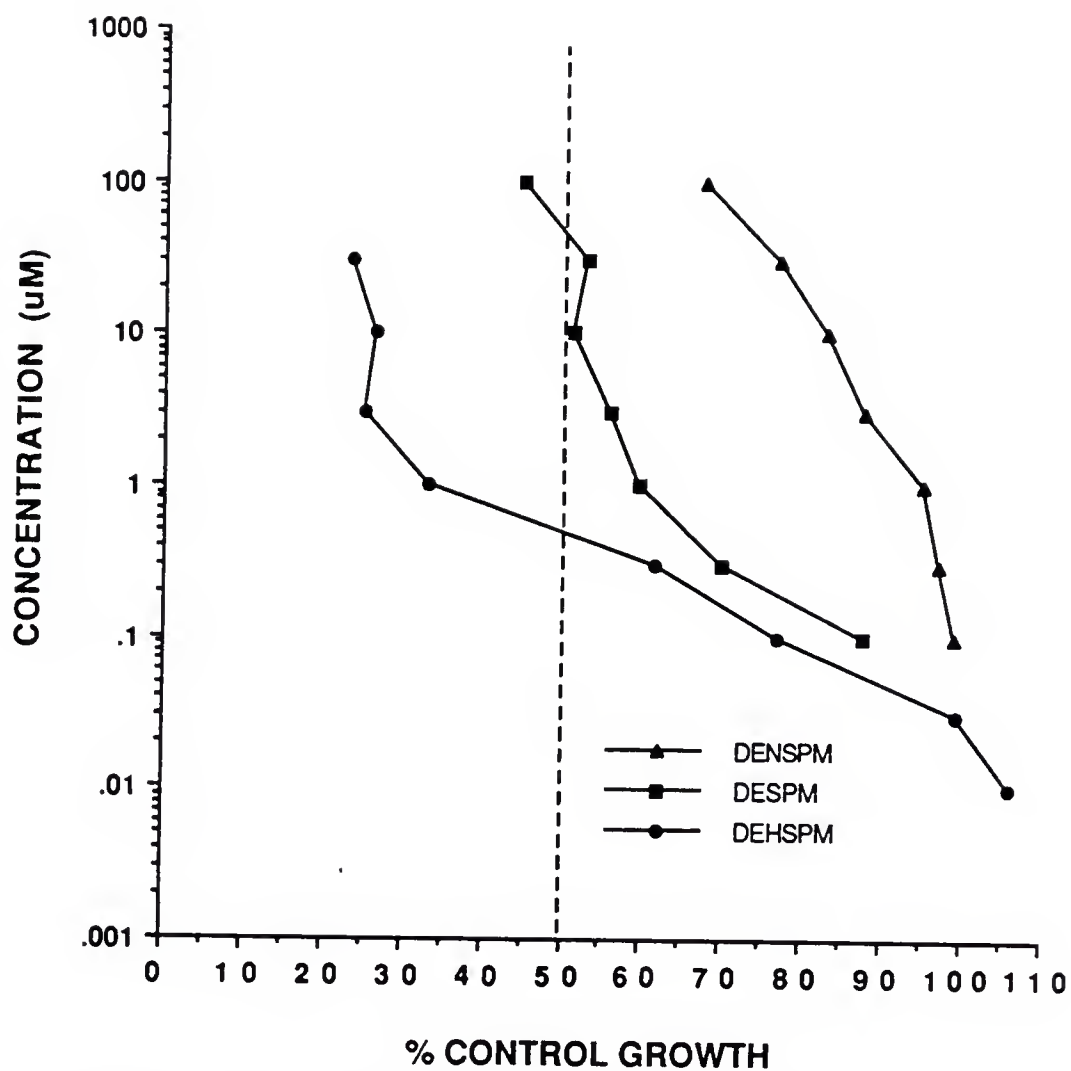
Figure 3-4. Concentration dependence of L1210 cell growth inhibition by DENSPM, DESPM and DEHSPM at 48 h.
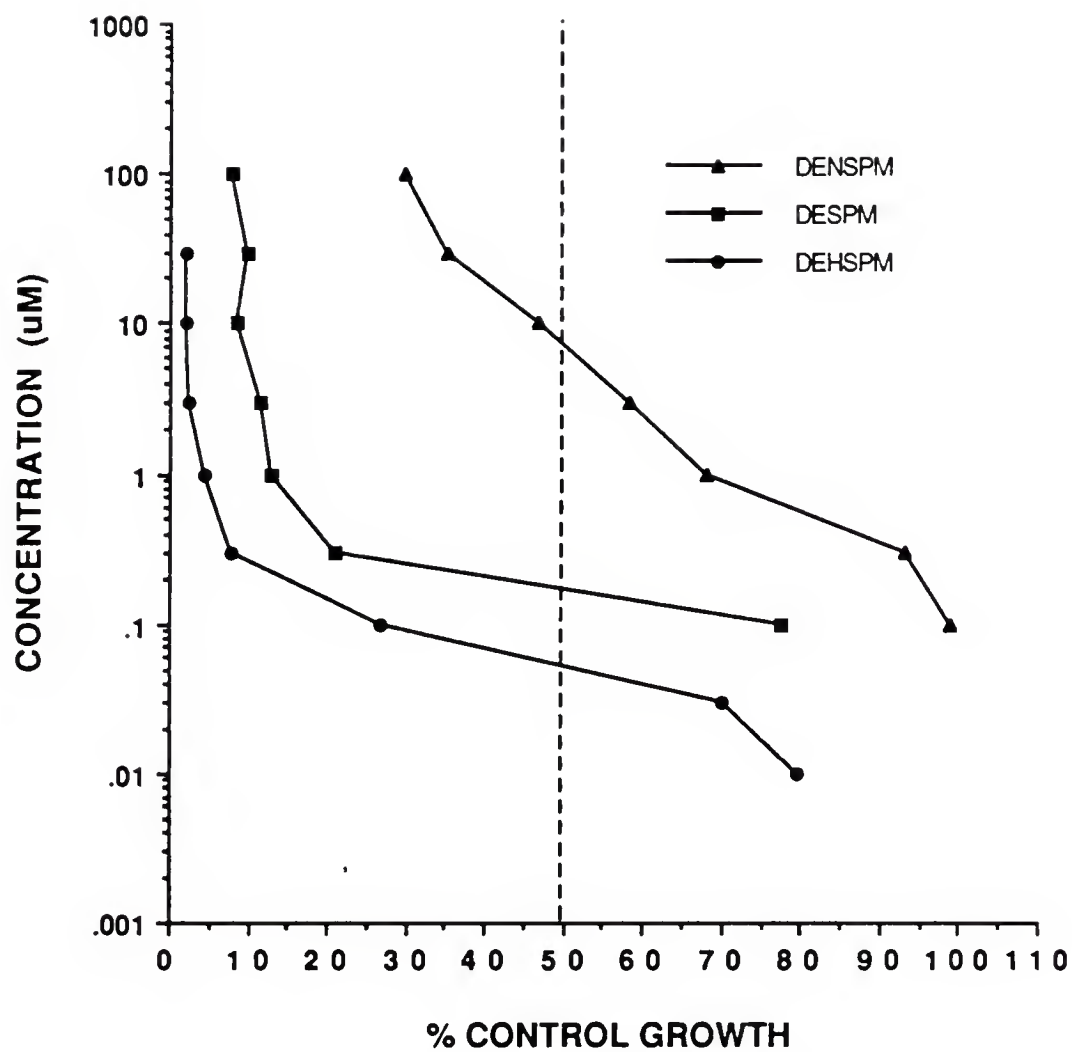
Figure 3-5. Concentration dependence of L1210 cell growth inhibition by DENSPM, DESPM and DEHSPM at 96 h.

The time course of growth inhibition of various concentrations of DENSPM (Fig. 3-6), DESPM (Fig. 3-7) or DEHSPM (Fig. 3-8) indicated that except at the lower concentrations studied (<0.1 μM), DEHSPM was a consistently and significantly more active antiproliferative. For example, 1 μM DEHSPM was 10 times as active as DESPM and at least 100 times more active than DENSPM at 144 h. The plot of the percent control growth vs. the log of drug concentration (IC_{50} determination) for DESPM (Fig. 3-4) exhibited a 48 h curve which approached the 50% control growth line asymptotically running almost parallel to the line from 1-100 μM and suggesting cytostasis and not cytotoxicity. The behavior of DENSPM is very similar to that of DESPM, however the curve never crosses the 50% control growth line. DEHSPM, however, does cross the 48 h-50% control growth line at 0.5 μM. A comparison of the growth curves reflects this behavior quite clearly (Figs. 3-6, 3-7, 3-8). For example, in comparing the growth curves of cells treated with DEHSPM and DESPM, the growth inhibitory behavior seen with 0.3 μM DEHSPM is similar to that seen with 1.0 μM, 10 μM or even 100 μM DESPM. In fact, DEHSPM at a concentration of 1.0 μM was more effective than DESPM at any concentration studied. The activity of DENSPM is not very impressive. For example, 30 μM DENSPM is comparable with 1 μM DESPM.

Cytocidal Activity

A comparison of the analogue's impact on cell viability vs. time (by trypan blue exclusion) further emphasizes their differences in behavior (Fig. 3-9). When comparing 0.3 μM DEHSPM with 10 μM

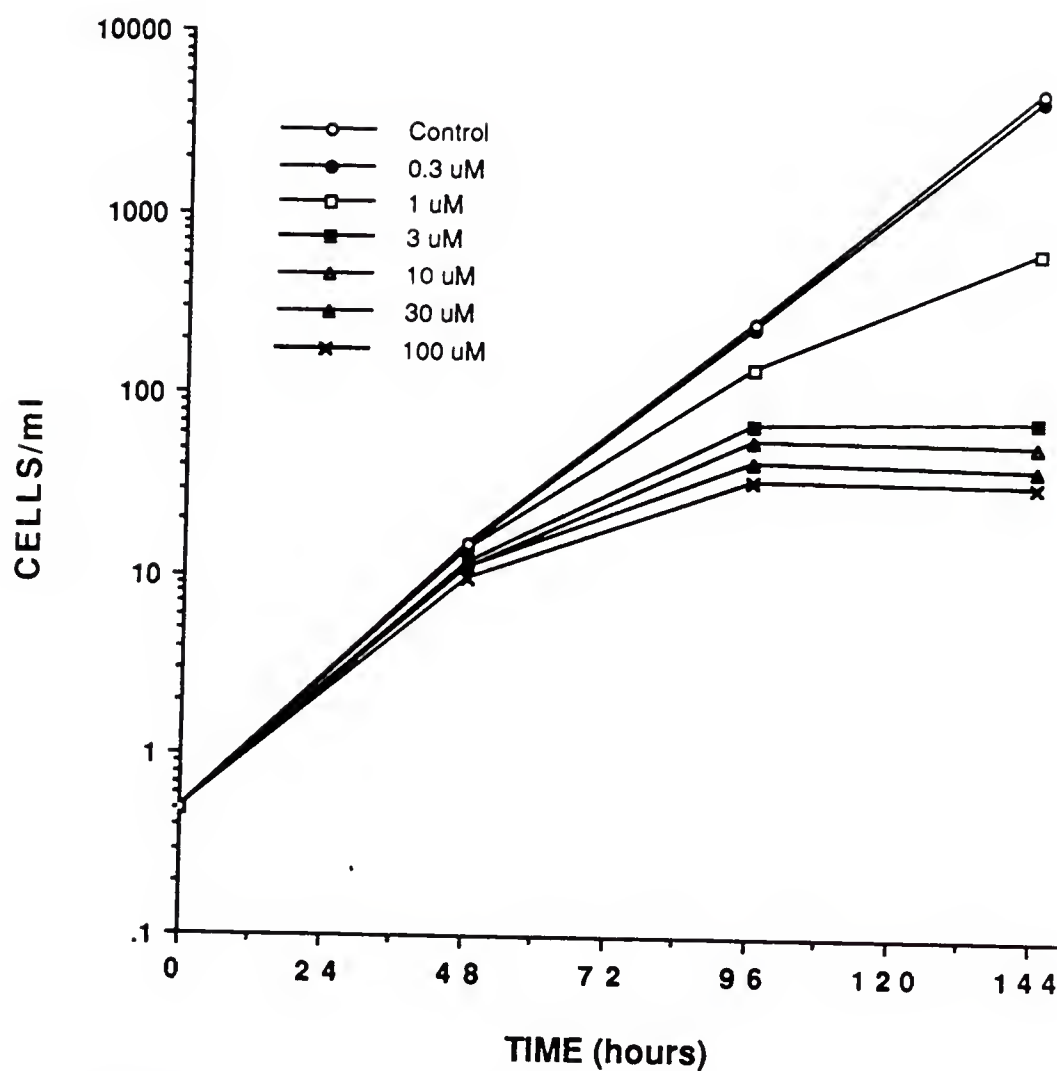Figure 3-6. Time dependence of L1210 cell growth inhibition by various concentrations of DENSPM.
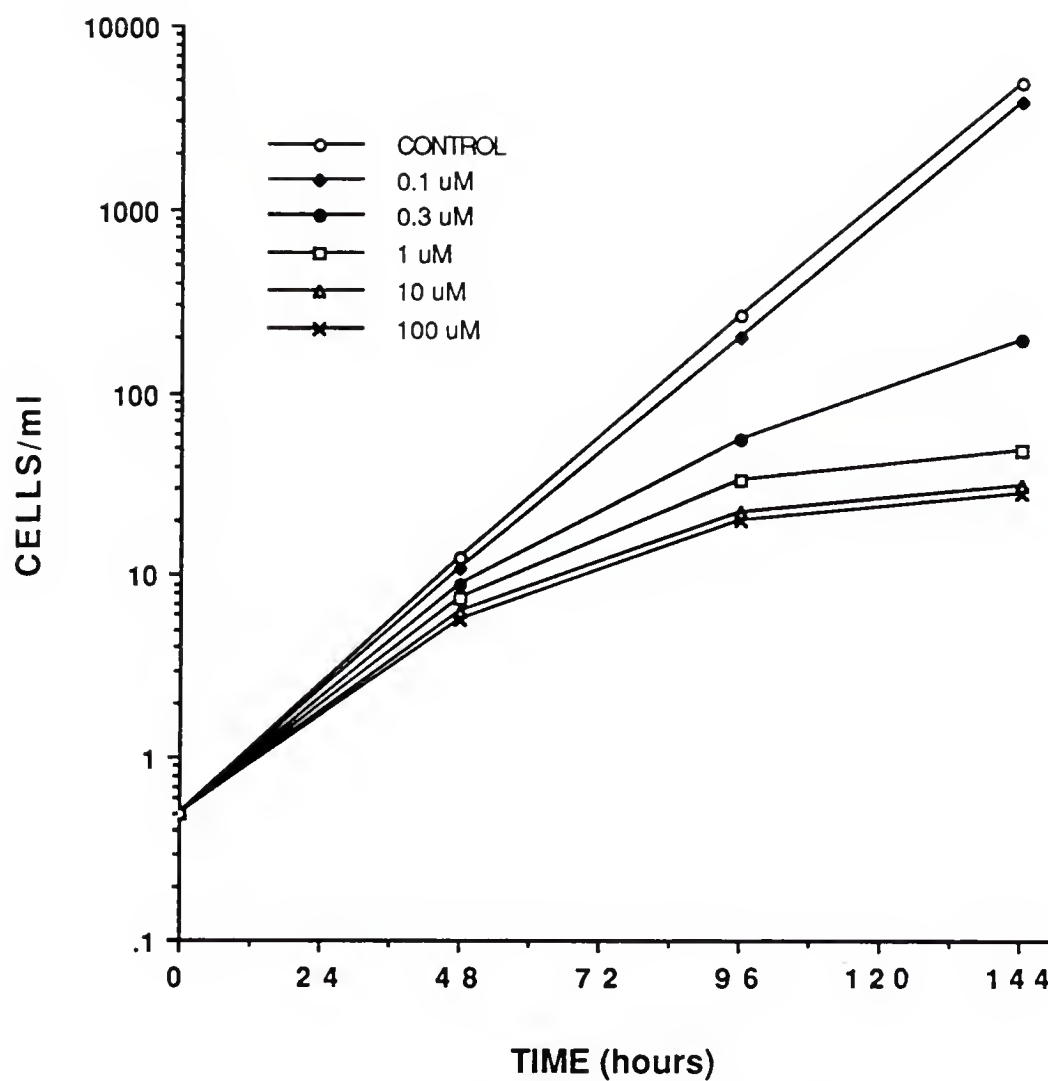
Figure 3-7. Time dependence of L1210 cell growth inhibition by various concentrations of DESPM.
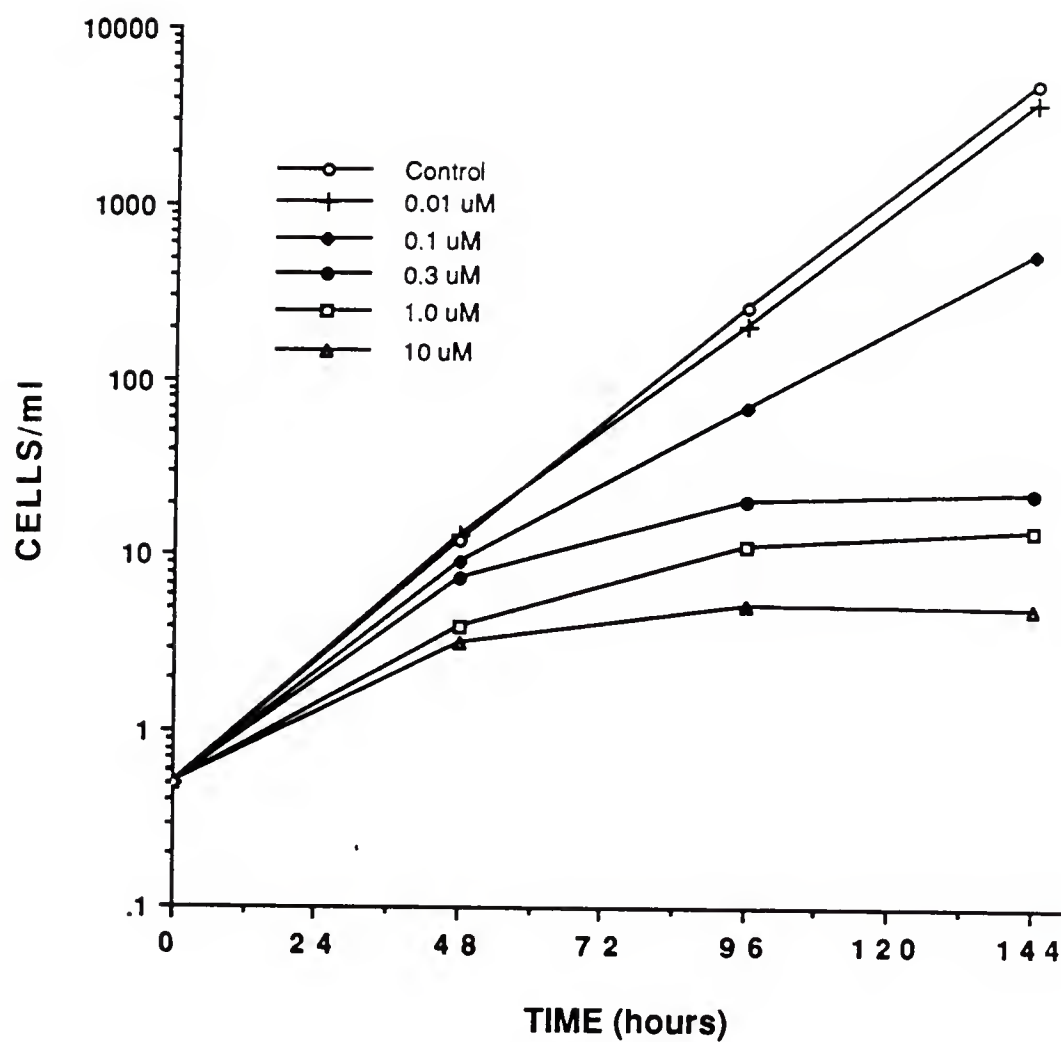
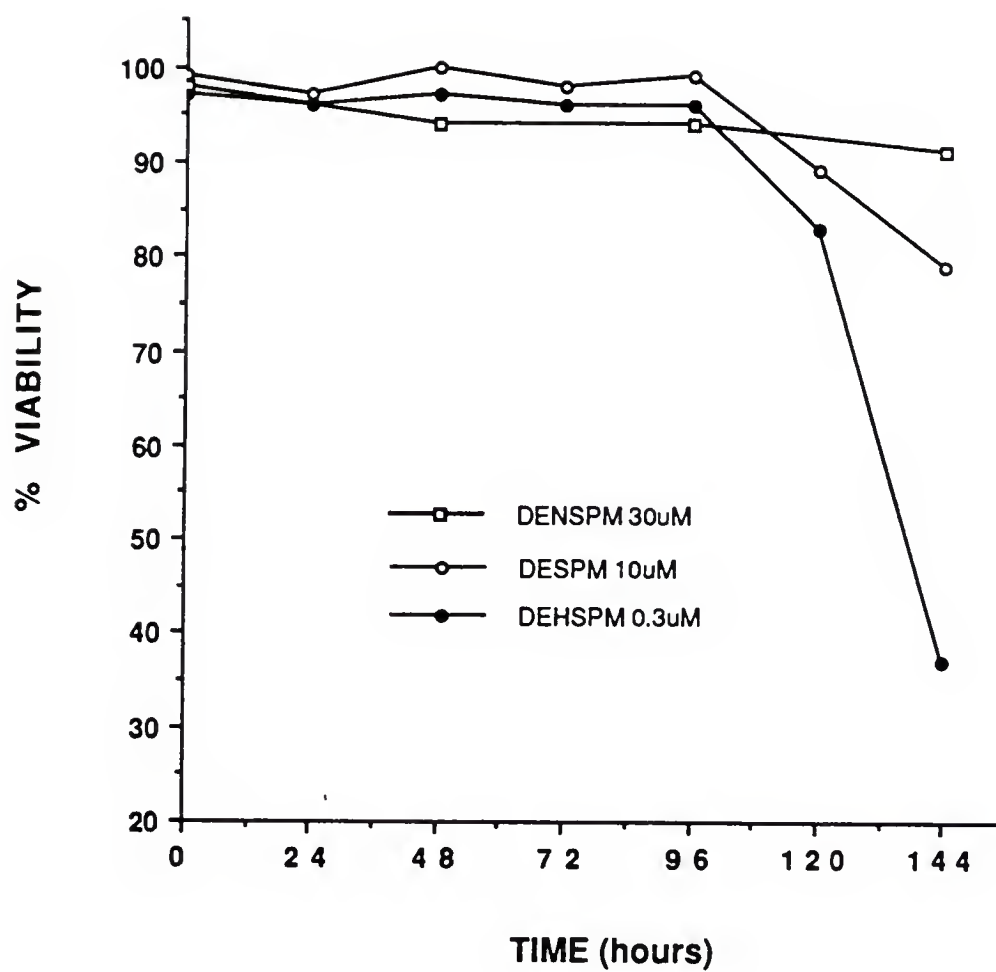Figure 3-8. Time dependence of L1210 cell growth inhibition by various concentrations of DEHSPM.

Figure 3-9. Trypan blue viability of L1210 cells treated with 30 μM DENSPM, 10 μM DESPM or 0.3 μM DEHSPM.

DESPM (their approximate 48 h IC_{50} values), cell death does not begin to occur until after 96 h of treatment. However, DEHSPM exhibited much greater cytotoxicity by 144 h than DESPM, while DENSPM wxhibited almost no cytotoxicity at this time. The difference in cytotoxicity between the compounds was further substantiated by measuring the ability of treated cells to incorporate Rh-123 into their mitochondria. This measurement provides information regarding the viability of the cells (74). Based on the nature of mitochondrial staining, cells can be separated into three populations: viable, dying and dead, each of which can be plotted as a function of time (Figs. 3-10, 3-11, 3-12). Although both measurements indicate the differences in cytotoxicity between the two drugs, the Rh-123 data are more informative.

The Rh-123 data clearly indicate that the events which impact on the cell's growth begin earlier in the process than the trypan blue exclusion data suggest. The data from the Rh-123 uptake method are known to be a more sensitive and earlier indicator of loss of cell viability with other antineoplastics (74). The effects of 30 μM DENSPM on cell viability as measured by both the methods suggests the compound has little activity relative to DESPM and DEHSPM. Trypan blue exclusion methods indicated 92% viability at 144 h while the RH-123 indicate 14% dead, 18% dying and 68% viable cells at 144 h.

Treatment Reversibility

The extent of treatment reversibility on cell growth upon removal of the drug depends on the duration of the treatment. The
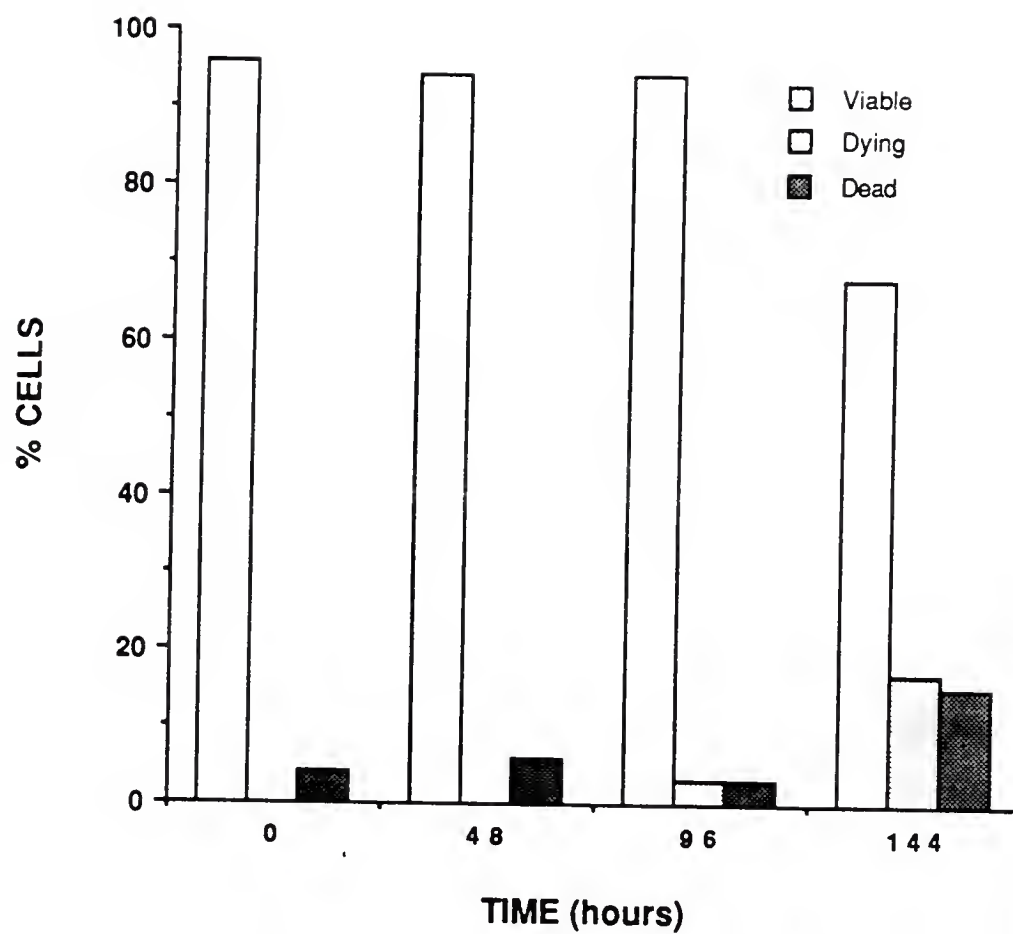
Figure 3-10.   Percentage of L1210 cells viable, dying and dead after treatment with 30 µM DENSPM as determined by Rh-123 staining.
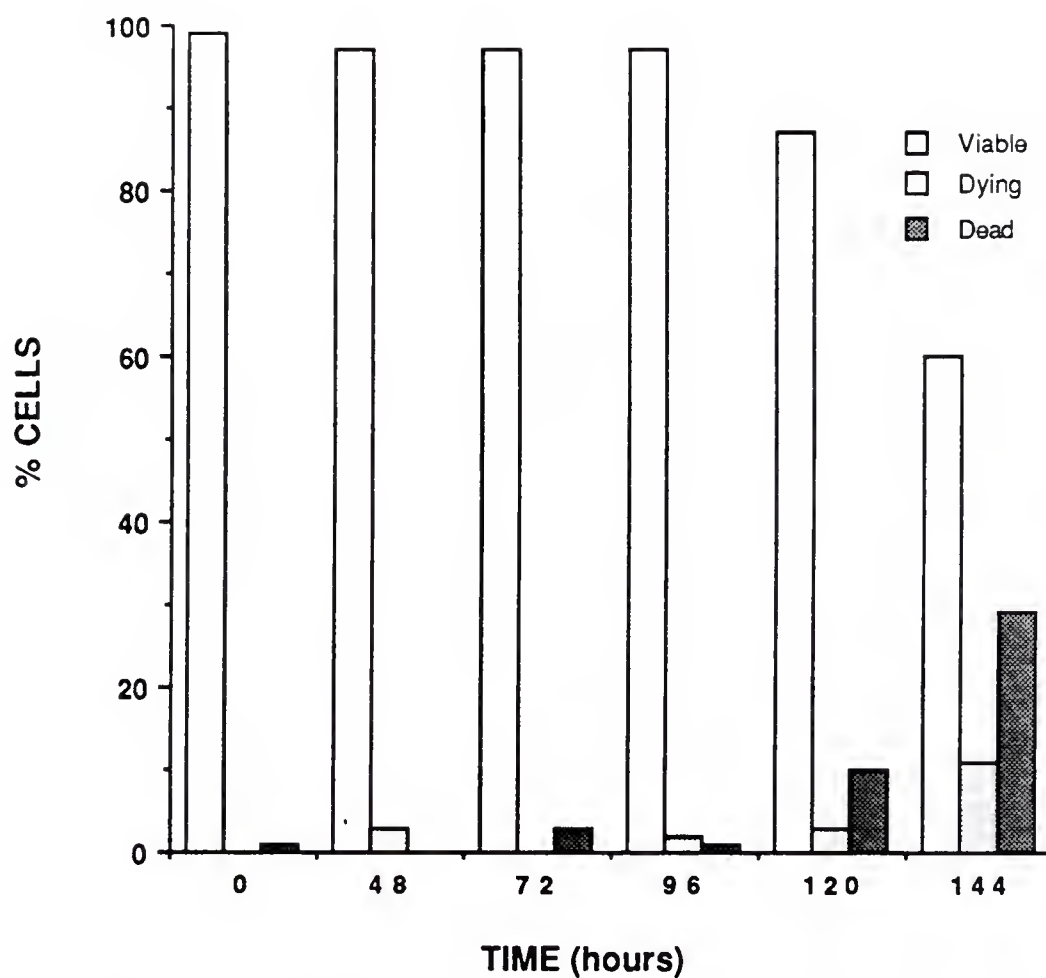
Figure 3-11. Percentage of L1210 cells viable, dying and dead after treatment with 10 μM DESPM as determined by Rh-123 staining.
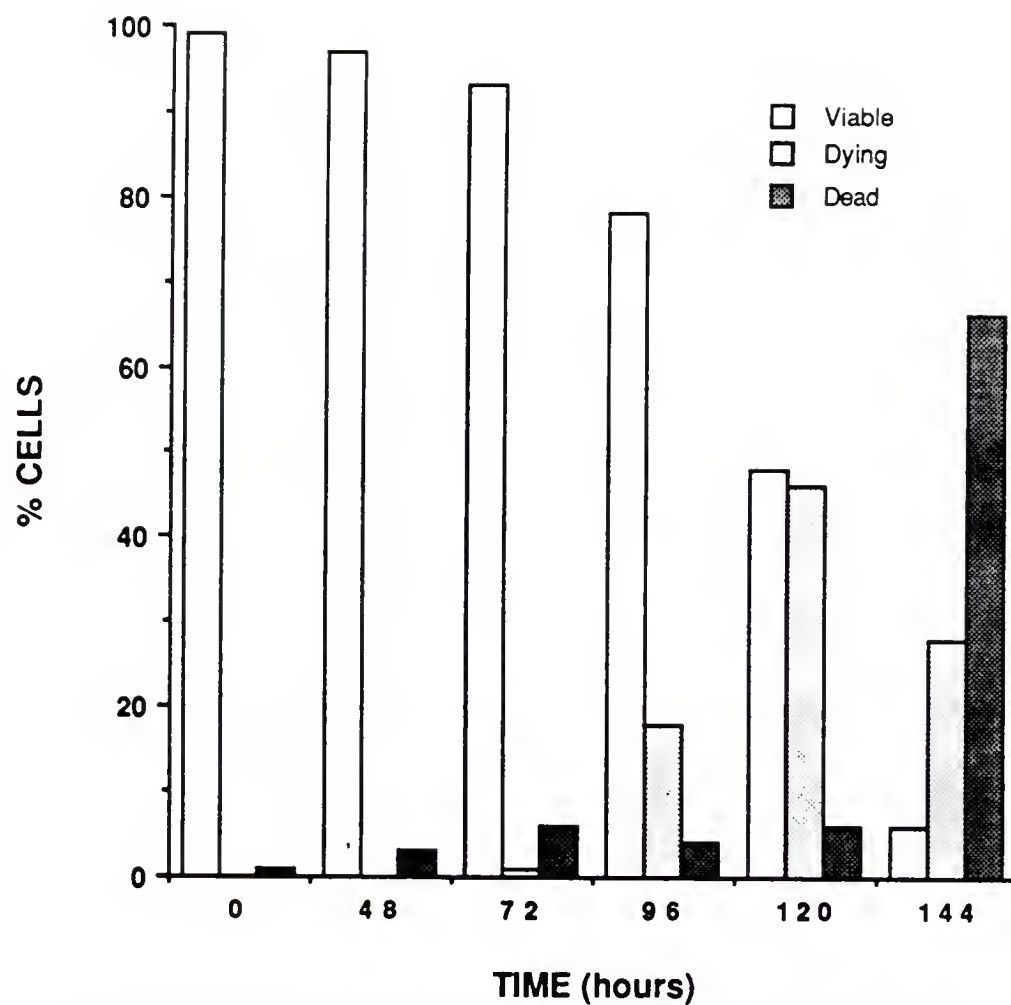
Figure 3-12.   Percentage of L1210 cells viable, dying and dead
after treatment with 0.3 μM DEHSPM as determined by Rh-123 staining.

longer the cells are exposed to the analogue, the slower they grew after transferring them into fresh media without the analogue. The growth inhibitory effects of 1 μM DESPM did not become apparent for approximately 48 h, and after 96 h there was little cell growth. Though cell division had nearly ceased by 144 h more than 90% of the cells remain viable by trypan blue exclusion. However, the fraction of clonogenic cells decreased significantly during the treatment (Table 3-1).

When cells were exposed to 0.6 μM DEHSPM, 10 μM DESPM or 30 μM DENSPM for 24, 48, 72 and 96 h, were washed and regrown in complete medium, the cytotoxicity of DEHSPM relative to DESPM and DENSPM became obvious (Fig. 3-13, 3-14, 3-15). A 72 h exposure of the cells to DEHSPM and DESPM essentially prevented cell regrowth. Growth inhibition of the cells treated with DENSPM, however, was reversible even after 144 h.

Cell Size

It was observed during these studies that cells substantially decreased in size while exposed to the analogues. Utilizing electronic particle sizing, exposure of L1210 cells to 10 μM DESPM, 0.6 μM DEHSPM or 30 μM DENSPM resulted in a progressive decrease in cell diameter from 12.5 μm for control L1210 cells to 9.5 μm for L1210 cells after exposure to the drug for 144 h. This corresponds to a decrease in cell volume of approximately 60% (1020 μm^3 to 450 μm^3). The time course of this phenomenon is presented in Figure 3-16.

TABLE 3-1
PERCENT OF CONTROL CLONAGENIC L1210 CELLS AFTER TREATMENT WITH
1 μM DESPM FOR UP TO 96 H

DESPM 1 μM Treatment	Percent of Clones Relative to Controls
24 h	89
48 h	75
72 h	21
96 h	2

Figure 3-13.   Growth of L1210 cells in fresh medium after
treatment with 30 μM DENSPM for 0 (control), 24, 48, 72 and 96 h.
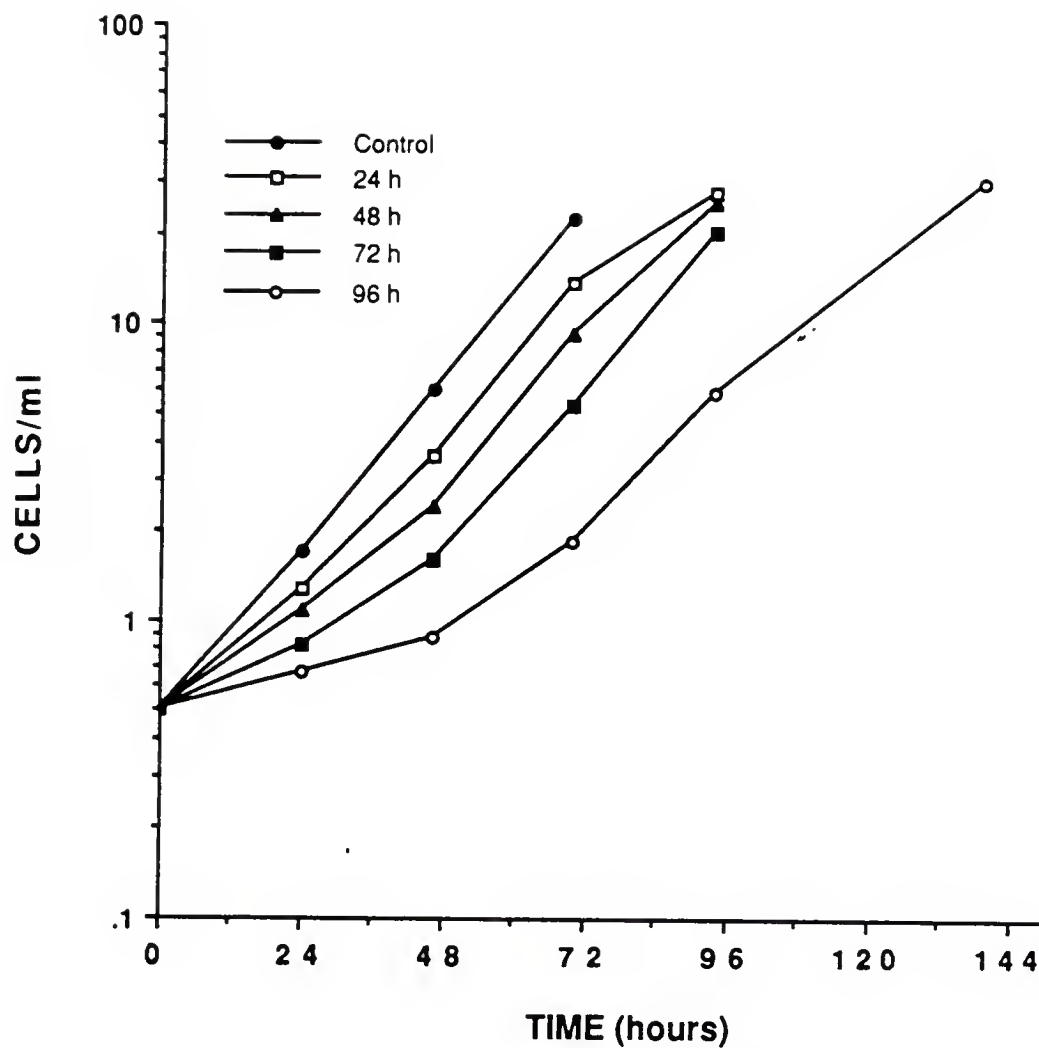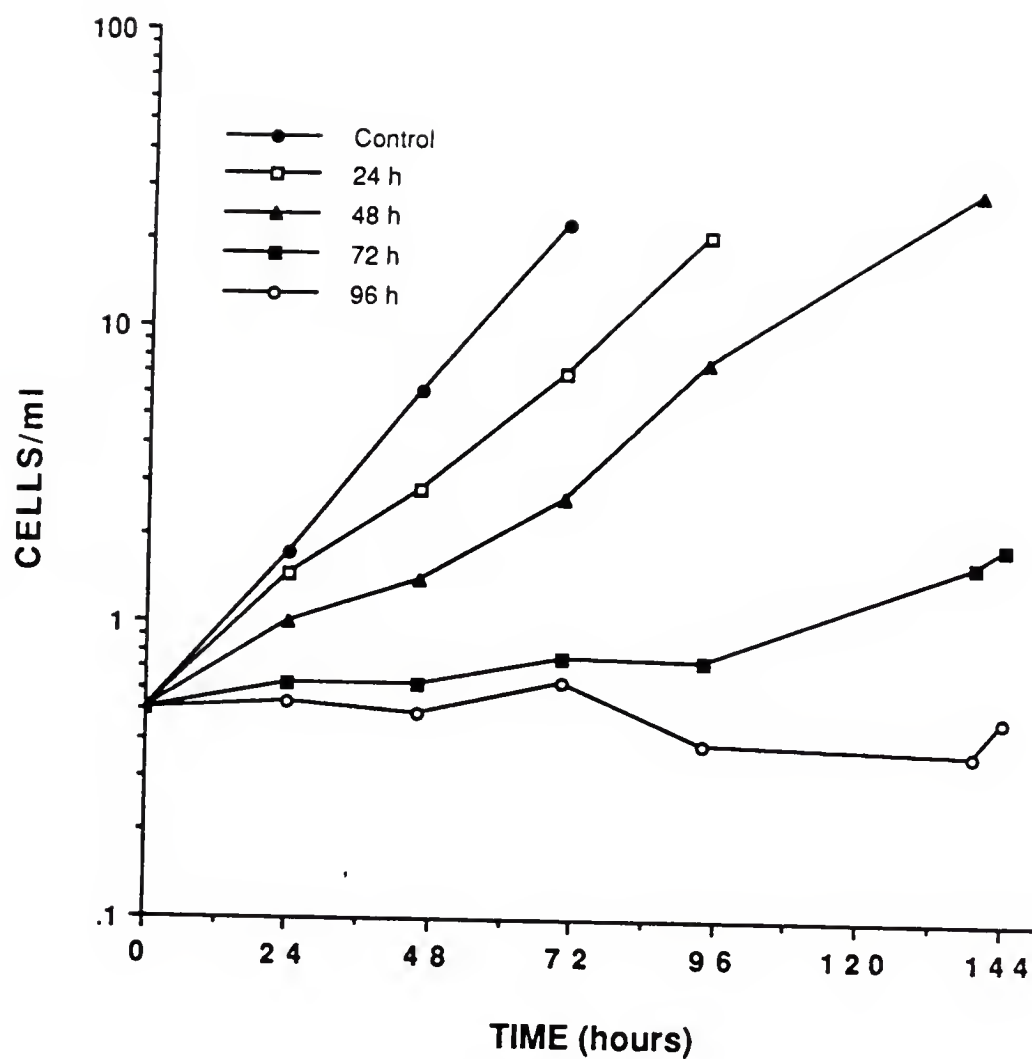
Figure 3-14. Growth of L1210 cells in fresh medium after treatment with 10 µM DESPM for 0 (control), 24, 48, 72 and 96 h.
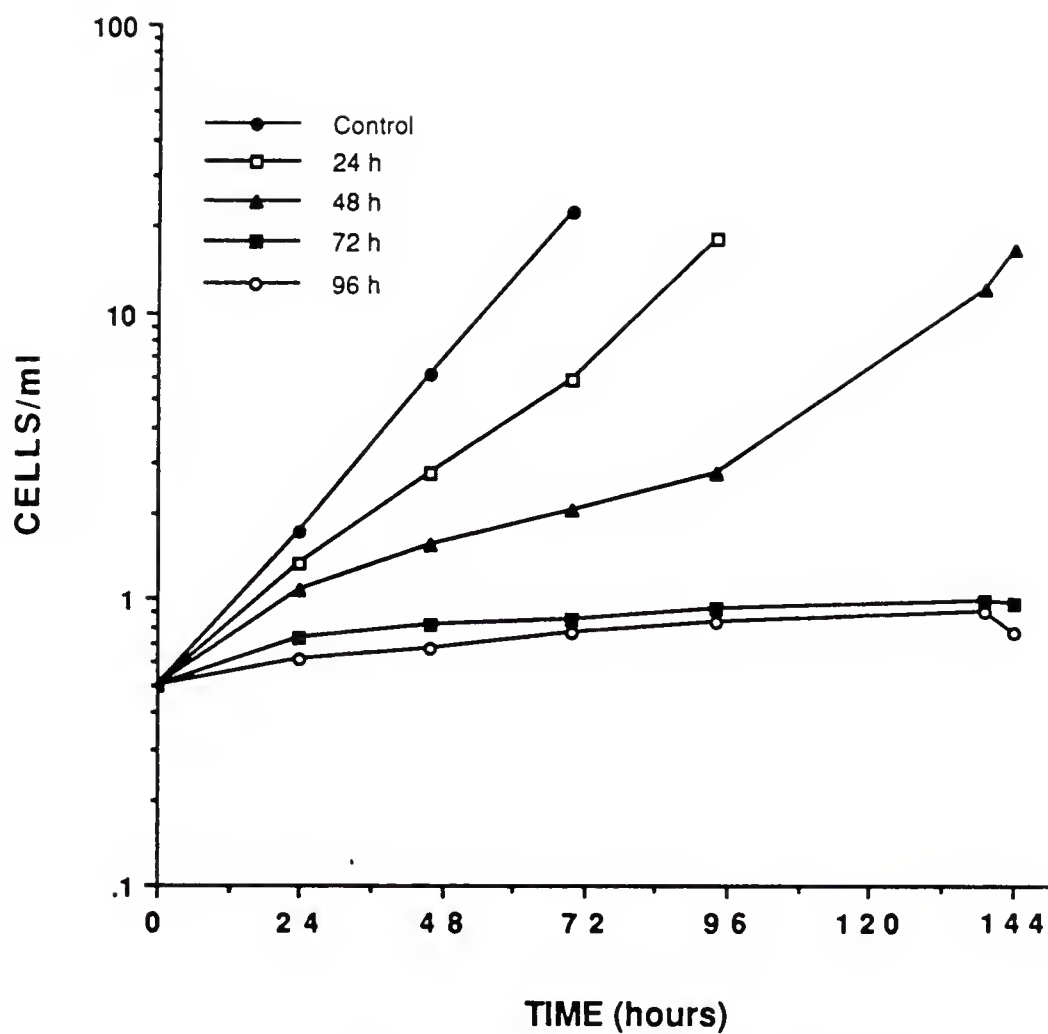
Figure 3-15.   Growth of L1210 cells in fresh medium after
treatment with 0.6 μM DEHSPM for 0 (control), 24, 48, 72 and 96 h.
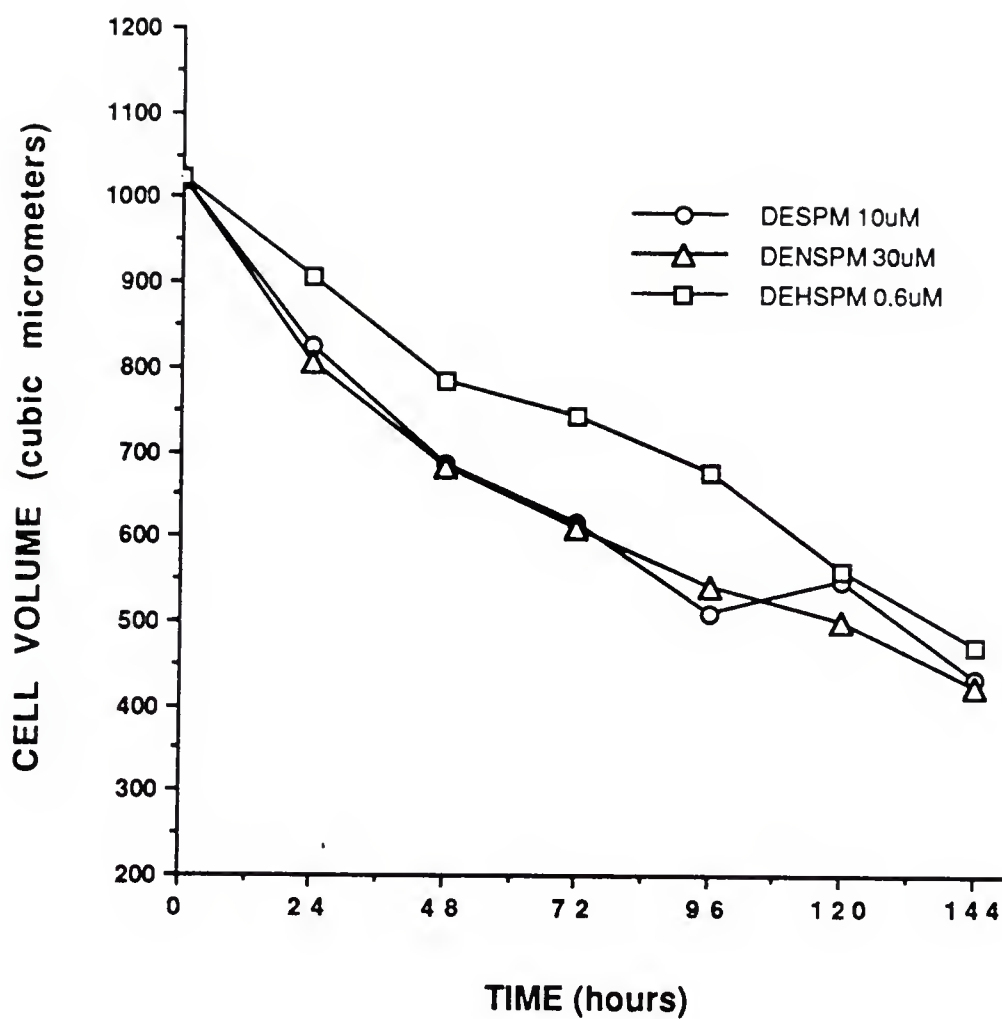
Figure 3-16. Time course of changes in L1210 cell volume after treatment with 30 μM DENSPM, 10 μM DESPM or 0.6 μM DEHSPM.

Impact on Nuclear DNA Content

Because of the unusual growth properties induced in the L1210 cells by DESPM, the nDNA histograms of the treated cells were evaluated (Fig. 3-17). Flow cytometric analysis of nDNA content of L1210 cells after treatment with 10 μM DESPM for 48 h and 96 h showed only a slightly decreased S-phase and G_2-phase cell populations compared with controls. This was not consistent with a decrease in cell growth caused by blocking progression of cells through any particular phase of the cell cycle. A significant number of cells accumulating at the G_1/S border was seen only after 144 h of treatment. L1210 cells were exposed to DEHSPM and DENSPM at approximately their 48 h IC_{50} concentrations. As with L1210 cells exposed to 10 μM DESPM there were no significant changes in nuclear DNA content (reduced S and G_2/M phase DNA content) of the L1210 cells until after more than 96 h of treatment with 0.6 μM DEHSPM or 30 μM DENSPM.

Impact on Mitochondrial DNA Content

There was a striking decrease in mtDNA content per L1210 cell after treatment with DESPM (Fig. 3-18). This decrease in mtDNA content is compatible with an almost immediate cessation of mtDNA synthesis coupled with dilution due to cell division for three or four doublings (Fig. 3-19). Control L1210 cells grew in log-linear fashion with a 10-12 h doubling time. Cells treated with DESPM showed no significant growth inhibition at 24 h. By 48 h, L1210 cells treated with DESPM contained about 20% of the normal amount mtDNA and the rate of cell doublings had just begun to decrease. The mtDNA content of treated cells had decreased to about 10% of control by 96 h at
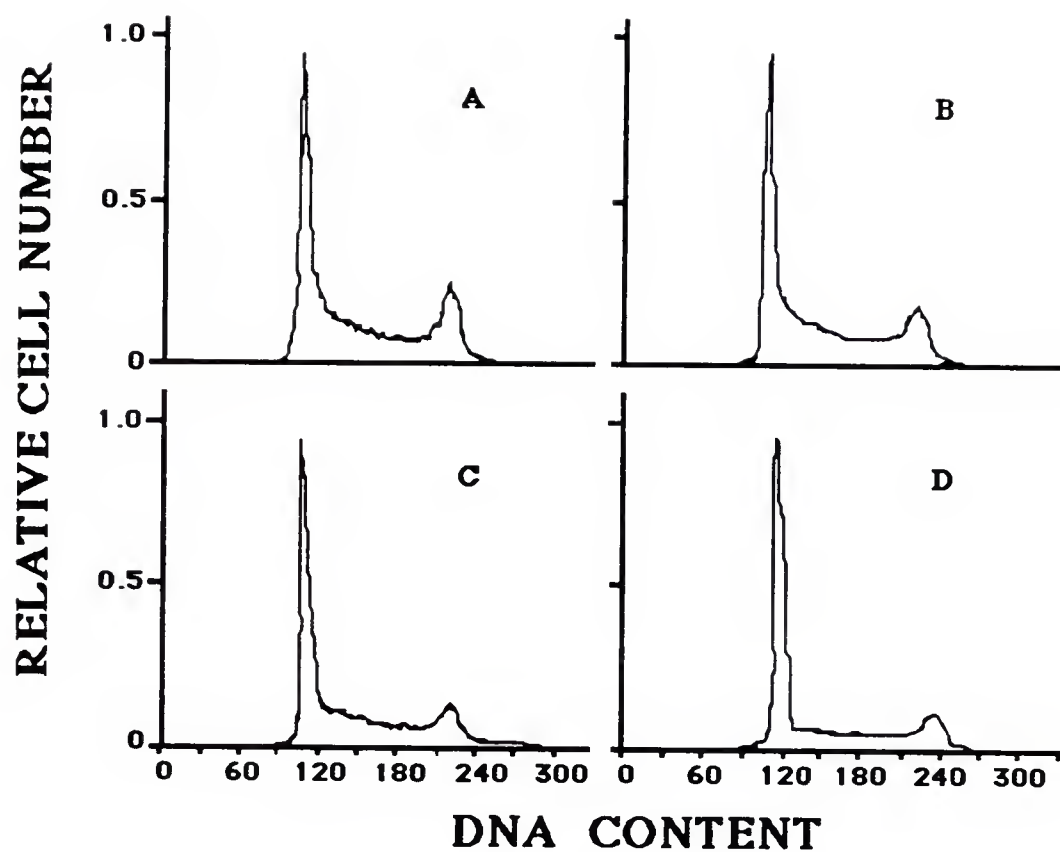
Figure 3-17. Flow cytometric analysis of nDNA content of L1210 cells after treatment with 10 μM DESPM.

A. 0 h
B. 48 h
C. 96 h
D. 144 h
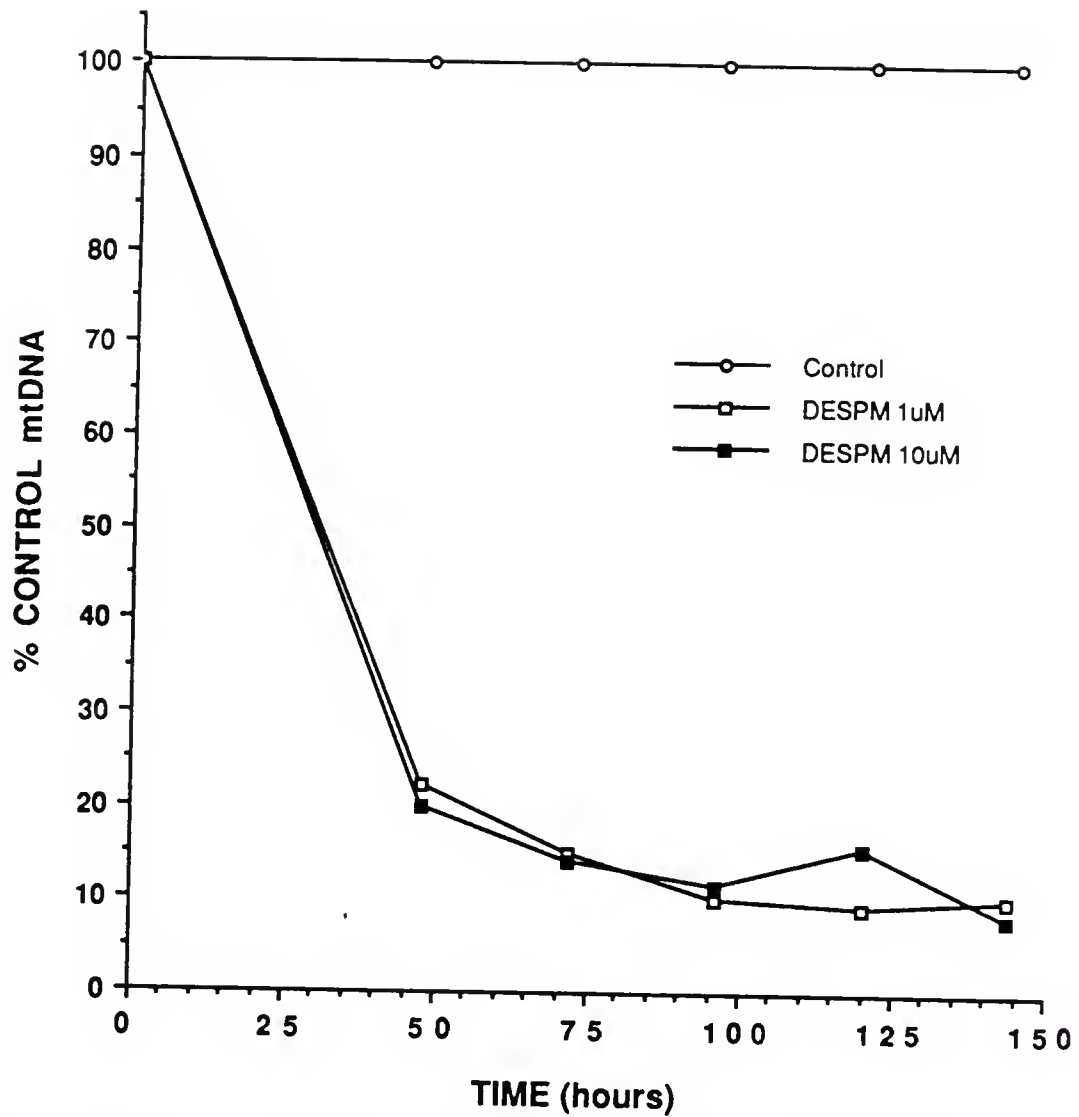
Figure 3-18. Time course for the effect of DESPM on the percent of control mtDNA in L1210 cells. The amount of mtDNA in untreated controls was assumed 100% at each time point.
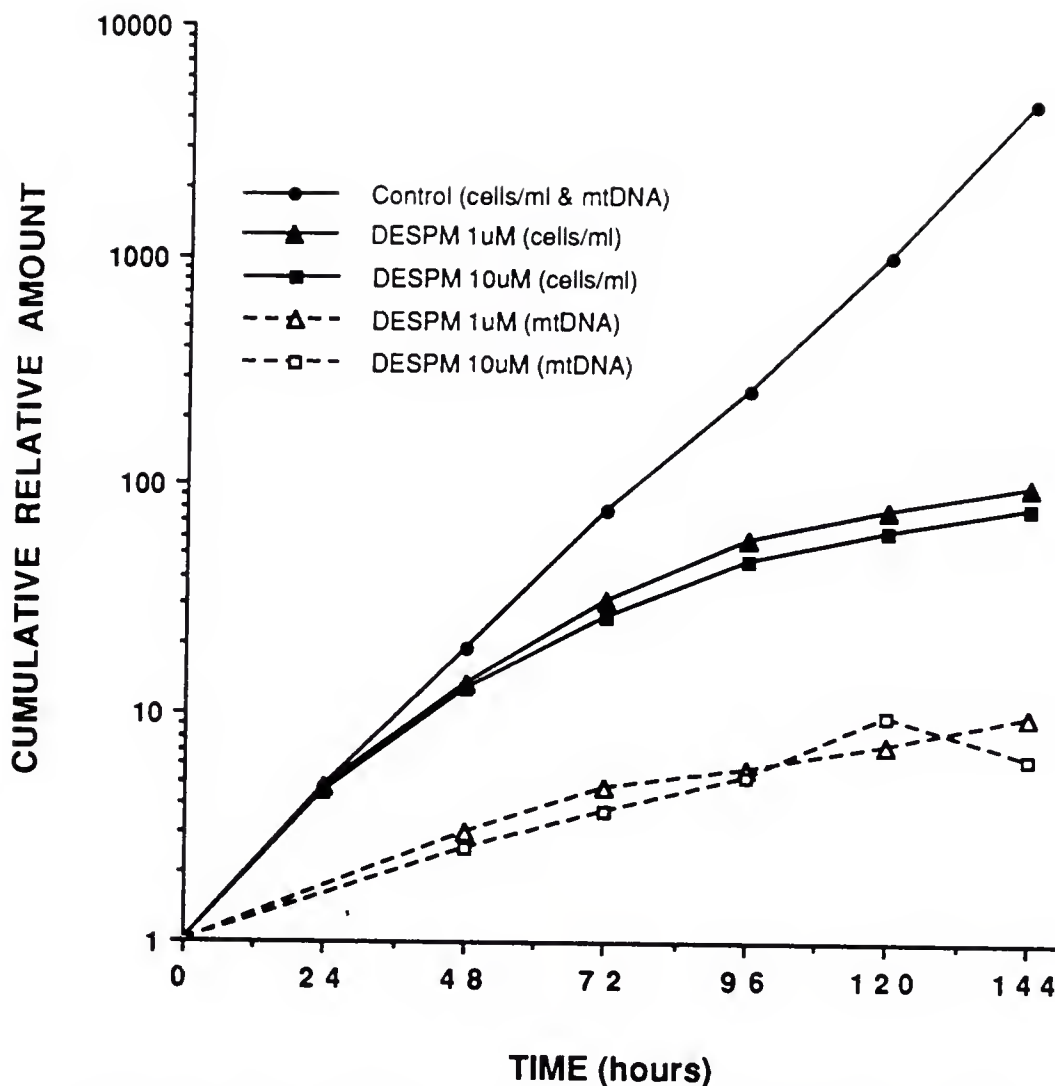
Figure 3-19. Kinetic study of accumulated L1210 cell growth (based on number of doublings) of untreated (control) L1210 cells and cells treated with DESPM. The time course of mtDNA accumulation (accumulated cell counts X percent control mtDNA/cell) for untreated cells follows the untreated cell growth curve, while mtDNA accumulation for cells treated with DESPM was consistent with lack of mtDNA synthesis coupled with cell division.

which point cell doubling time nearly tripled (30-35 h). Cells
treated with DESPM remained constant at 10% of control mtDNA content
up to 144 h at which time cell division had essentially ceased.
Exposure of L1210 cells to 10 μM DESPM rather than 1 μM DESPM had
little, if any, significant difference in effects on cell growth or
mtDNA content, a finding consistent with the almost complete inhibi-
tion of mtDNA accumulation caused by the lower concentration of
drug.

Exposure of L1210 cells to 30 μM or 100 μM BESPD for 72 h
decreased mtDNA content to 65% of control. It is clear that the less
active spermidine analogue, BESPD (IC $_{50}$value of 100 μM at 48 h, and
10 μM at 96 h), even at 10 times the concentration of DESPM, had less
of an impact on mtDNA content. In a comparative study, L1210 cells
were treated in log-phase growth with 0.1, 1.0 and 10 μM DMSPM, DESPM
or DPSPM for 72 h and analyzed for mtDNA content. The dose-effect
curves generated (Fig. 3-20) further demonstrated a positive correla-
tion between the antiproliferative and antimitochondrial activity of
the polyamine analogues.

Incubation of L1210 cells for 72 h with 100 μM or 400 μM DFMO
(IC_{50} value of 1 mM at 48 h, and 100 μM at 96 h), a known inhibitor
of polyamine biosynthesis, had no significant effect on mtDNA con-
tent.

Polyamine Analogue Uptake and Impact on Polyamine Pools

L1210 cells in complete medium exposed to 100 μM DESPM absorbed
the analogue to concentrations of 3150 pmole/million cells in 24 h
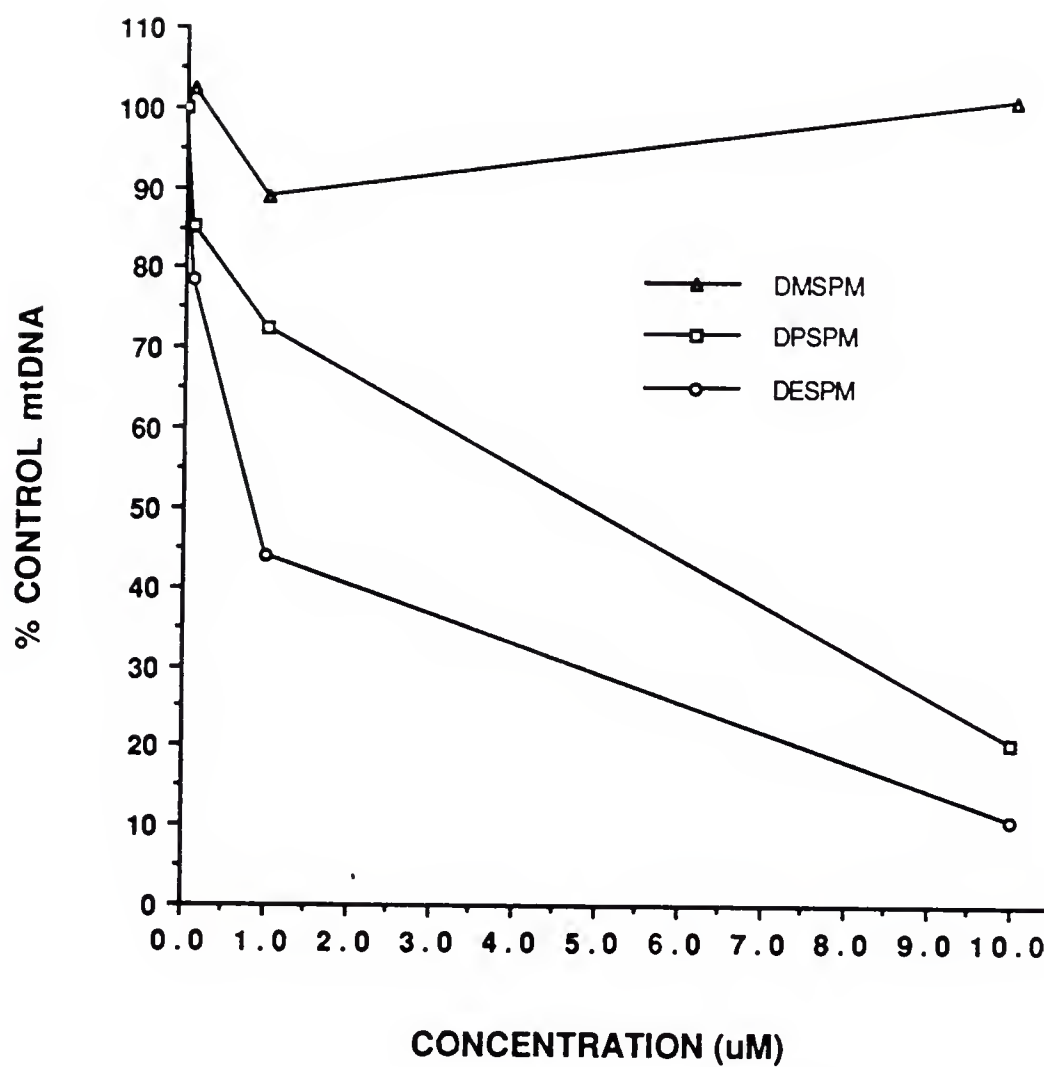
Figure 3-20. Concentration dependence of percent control mtDNA in L1210 cells treated with DENSPM, DESPM or DEHSPM for 72 h.

(Fig. 3-21). Assuming that the total volume of a single L1210 cell is approximately 1000 μm^3, the cellular concentration of DESPM is about 3 mM. What is most interesting is that the total concentration of polyamines, including the analogue, remains approximately the same while the concentrations of the native polyamines spermine, spermidine and putrescine decrease. The greatest relative decrease in polyamine pool occurs in the putrescine level followed next by a decrease in spermidine concentration with the least impact on spermine pool which decreased by approximately 40% in 24 h. It is notable that the impact on polyamine concentrations begins almost immediately. For example, the spermidine pools which have been diminished by 85% at 24 h have already been reduced by 39% at 2 h.

In Vivo Activity

The spermine analogue, DESPM was screened for its ability to inhibit the growth of L1210 ascites tumor growth in DBA/2 mice. Since DESPM is a highly charged, very water soluble compound, it would be expected to be excreted quickly from the body. Therefore it was given in a split dosing schedule over several days. The mice were given the tumor on day 0, and treatment begun 24 h later. The results (Table 3-2) clearly demonstrated a dose-response relationship, with i.p. administration of 15 mg/kg every 8 h for 6 days having the optimum effect of the schedules tested. At this dose animals had an average ILS of greater than 376%, with 60% of the test animals still alive after 60 day and no sign of tumor. Although the 17.5 mg/kg dosing schedule gave a greater ILS and percentage of long term
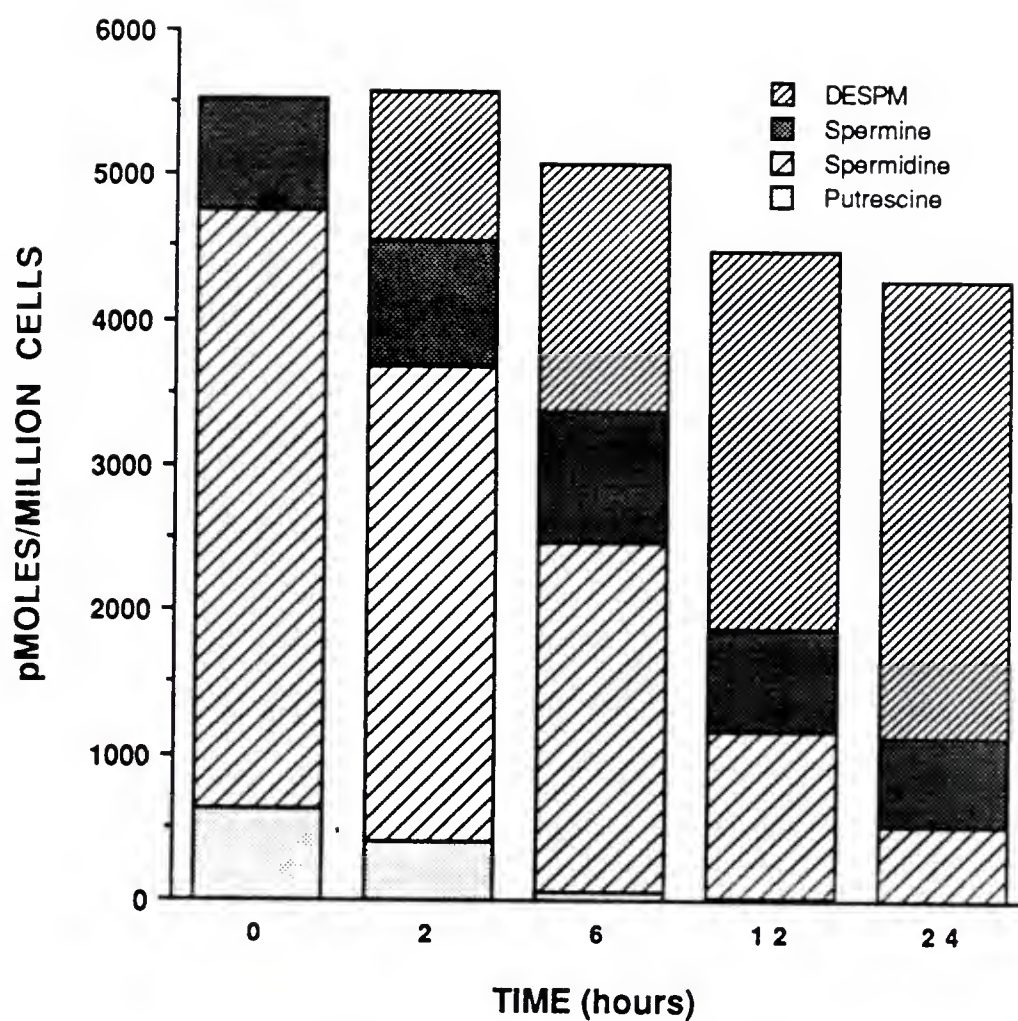
Figure 3-21. Time course for the effect of 100 μM DESPM on polyamine levels in L1210 cells over 24 h.

TABLE 3-2

Activity of N^1,N^{12}-Diethylspermine ·4 HCl Against L1210 Murine Leukemia in DBA/2 Mice

Experiment Number	Treatment[a]	Schedule[b] (Route)	Number of Cells Inoculated (Site)	Days of Death[c]	Mean Survival (days) ± S.D.	%ILS[d]	LTS[e]
1.	5 mg/kg NONE	q8h days 1-6 (IP)	10^5 (IP)	9.5, 10.5, 11.5, 12, 30.5, 13(2), 16.5 8.5, 9(2), 10(2), 10.5, 11(2)	12.3 ± 2.0 9.9 ± 0.9	25	0/8
2.	10 mg/kg NONE	q8h days 1-6 (IP)	10^5 (IP)	13(2), 17(2), 20, 22, 23, 23.5, 24 8.5(3), 9(7), 9.5(2), 10(5), 10.5(2)	34.7 ± 17.5 9.4 ± 0.7	269	5/20
3.	15 mg/kg NONE	q12h days 1-6 (IP)	10^5 (IP)	14(2), 14.5, 15(2), 17 8.5, 9.5(3), 10(3)	14.9 ± 1.2 9.6 ± 0.5	55	0/6
4.	15 mg/kg NONE	q8h days 1-6 (IP)	10^5 (IP)	8, 20, 22, 22.5, 24.5, 28.5, 40, 60(9) 8.5, 9(3), 9.5(2), 10(6), 10.5(2), 11	46.6 ± 17.6 9.8 ± 0.7	376	9/16
5.	17.5 mg/kg NONE	q8h days 1-6 (IP)	10^5 (IP)	8.5, 9.5, 34, 40, 60(4) 9(3), 9.5, 10(4), 11	52.3 ± 11.0 9.7 ± 0.6	439	4/8
6.	45 mg/kg NONE	OD days 1-6 (IP)	10^5 (IP)	7, 7.5, 8, 8.5, 14(2) 9(5), 10, 11(4)	9.8 ± 3.3 9.9 ± 1.0	0	0/6
7.	20 mg/kg NONE	q8h days 1-3 (IP)	10^6 (IP)	13.5, 14(2), 14.5 8.5(2), 9, 10	14.0 ± 0.4 9.0 ± 0.6	57	0/4

119

8.	20 mg/kg	q8h days 1-4 (IP)	10^6 (IP)	14(2), 15(2), 16, 17, 18, 20, 21, 31	18.1 ± 4.9	103	0/10
	NONE			8(2), 9(6), 10	8.9 ± 0.6		
9.	20 mg/kg	q8h days 1-5 (IP)	10^6 (IP)	8, 9, 16(3), 17	13.6 ± 4.0	72	0/6
	NONE			7(3), 8(2), 10.5	7.9 ± 1.3		

[a]Control animals were given no treatment.
[b]Mice given tumor on day 0.
[c]The experiment was ended at 60 days. Animal survival was evaluated on this day, however, animals surviving until this time had no sign of tumor.
[d]Percent increase in life span (%ILS).
[e]Long term survivors, >60 days (LTS).

survivors, there was some significant drug toxicity as indicated by a number of early deaths and an average weight loss of greater than 10%. The animals which recovered, however, appeared normal 4-5 days after the drug treatment was completed. In going from a dose of 5 mg/kg every 8 h for 6 days (a total dose of 90 mg/kg) to 15 mg/kg every 8 h for 6 days (a total dose of 270 mg/kg) we observed an increase from 25% to 376% in life span. The drug dose was only increased 3 times while the life span increased at least 15 times.

The dosing schedule was critical. When the animals received DESPM 20 mg/kg every 8 h for 4 days (a total dose of 240 mg/kg) there was a 103% ILS, while those treated with 10 mg/kg every 8 h for 6 days (a total dose of 180 mg/kg) exhibited a 269% ILS. This is in keeping with observations in cell culture. Irreversibility of cell growth inhibition in culture required that the cells be exposed to the drug for a minimum of 96 h, suggesting that in the short-term dosing experiments the cells were not exposed to the drug long enough to irreversibly inhibit their proliferation.

The initial dosages and treatment schedules of DEHSPM in leukemic mice were based on the original in vivo studies with DESPM, and a consideration of the four-fold greater in vitro antileukemic activity of DEHSPM compared to DESPM at 96 h. The mice were given ascites tumor on day 0. The results with DEHSPM (Table 3-3) clearly demonstrated a dose-response relationship, with i.p. administration of 5 mg/kg every 8 h on days 1-6 having the optimum effect of the

TABLE 3-3

Activity of N^1,N^{14}-Diethylhomospermine ·4 HCl Against L1210 Murine Leukemia in DBA/2 Mice

Experiment Number	Treatment[a]	Schedule[b] (Route)	Number of Cells Inoculated (Site)	Days of Death[c]	Mean Survival (days) ± S.D.	%ILS[d]	LTS[e]
1.	5 mg/kg NONE	OD days 1-6 (IP)	10^5 (IP)	9, 10, 10.5, 12(3) 8, 9(3), 9.5, 10	10.9 ± 1.3 9.1 ± 0.7	20	0/6
2.	10 mg/kg NONE	OD days 1-6 (IP)	10^5 (IP)	12, 17, 24(2), 27 9(3), 9.5, 10	20.8 ± 6.1 9.3 ± 0.4	115	0/5
3.	15 mg/kg NONE	OD days 1-6 (IP)	10^5 (IP)	21, 27, 60(3) 9(2), 9.5(3)	45.6 ± 19.8 9.3 ± 0.3	390	3/5
4.	20 mg/kg NONE	OD days 1-6 (IP)	10^5 (IP)	15, 28, 29.5, 32, 45, 60 8, 8.5(4), 9(5)	34.9 ± 15.6 8.7 ± 0.4	301	1/6
5.	5 mg/kg NONE	q8h days 1-4 (IP)	10^5 (IP)	17, 18, 20, 22(2), 60 9(4), 10, 11(3), 11.5(2)	26.5 ± 16.5 10.2 ± 1.1	160	1/6
6.	5 mg/kg NONE	q8h days 1-5 (IP)	10^5 (IP)	15, 18(2), 23, 31, 39 9(4), 10, 11(3), 11.5(2)	24.0 ± 9.2 10.2 ± 1.1	135	0/6
7.	5 mg/kg NONE	q12h days 1-6 (IP)	10^5 (IP)	26.5, 33, 35, 60(3) 9(4), 10, 11	45.7 ± 15.8 9.5 ± 0.8	381	3/6
8.	10 mg/kg NONE	q12h days 1-6 (IP)	10^5 (IP)	31, 60(5) 9(4), 10, 11(3), 11.5(2)	55.2 ± 11.8 10.2 ± 1.1	441	5/6
9.	1.25 mg/kg NONE	q8h days 1-6 (IP)	10^5 (IP)	10, 12.5, 13(2) 9, 9.5, 10.5, 11.5	12.1 ± 1.44 10.1 ± 1.1	20	0/4
10.	2.5 mg/kg NONE	q8h days 1-6 (IP)	10^5 (IP)	20.5, 22, 23, 32, 60 9(3), 9.5(2)	31.5 ± 16.6 9.2 ± 0.3	242	1/5

11.	5 mg/kg NONE	q8h days 1-6 (IP)	10^5 (IP)	22.5(2), 25, 26, 47, 60(41) 8(3), 8.5(5), 5, 9(6), 9.5(11), 10(4), 10.5(6) 11	56.6 ± 10.4 9.4 ± 0.8	502	41/46
12.	5 mg/kg NONE	q8h days 3-8 (IP)	10^4 (IP)	29(2), 39, 60(3) 9.5(3), 10.0, 10.5, 11.5	46.1 ± 15.5 10.0 ± 0.8	361	3/6
13.	5 mg/kg NONE	q8h days 4-9 (IP)	10^5 (IP)	11(2), 11.5(3), 32 8.5, 9, 9.5(2), 11(2)	14.8 ± 8.4 9.8 ± 1.0	51	0/6
14.	12.5 mg/kg NONE	q12h days 1-6 (IP)	10^6 (SQ)	29, 32.5, 33, 60(3) 8(4), 9, 10	45.8 ± 15.7 8.5 ± 0.8	429	3/6
15.	20 mg/kg NONE	0D days 1-6 (IP)	10^5 (SQ)	12, 13, 14, 21, 39, 58 10(3), 11(2), 20.5	26.2 ± 18.6 12.1 ± 4.2	116	0/6
16.	10 mg/kg NONE	q12h days 1-6 (SQ)	10^5 (IP)	19.5, 22(2), 60(9) 8.5(4), 9(4), 9.5(2), 10	50.3 ± 15.9 9.0 ± 0.5	458	9/12
17.	20 mg/kg NONE	0D days 1-6 (SQ)	10^5 (IP)	21, 60(5) 9(4), 9.5, 10(5)	53.5 ± 15.9 9.6 ± 0.5	457	5/6
18.	20 mg/kg/day NONE	Days 1-6 (SQ PUMP)	10^5 (IP)	7, 13, 14.5, 17.5 7, 9.5(3)	13.0 ± 4.4 8.9 ± 1.2	46	0/4

a Control animals were given no treatment.
b Mice given tumor on day 0.
c The experiment was ended at 60 days. Animal survival was evaluated on this day, however, animals surviving until this time had no sign of tumor.
d Percent increase in life span (%ILS).
e Long term survivors, >60 days (LTS).

123

schedules tested. At this dose animals had an average ILS of greater than 500%, with 90% of the test animals alive after 60 days with no sign of tumor. In going from a dose of 1.25 mg/kg every 8 h on days 1-6 (a total dose of 22.5 mg/kg) to 5 mg/kg every 8 h for 6 days (a total dose of 90 mg/kg) we observed an increase from 20% to 500% in life span. The drug dose was only increased four times while the life span increased at least 25 times. It was found that DEHSPM could be administered every 12 h. At an i.p. dosage every 12 h on days 1-6, 5 mg/kg gave a 381% ILS with half the animals being long term survivors (>60 days), and 10 mg/kg exhibited a 441% ILS with 5/6 of the animals surviving >60 days. Even more surprising was that DEHSPM could be given on a once daily schedule. At the optimum single daily dosage of 15 mg/kg on days 1-6, there were 3/5 long term survivors and a 390% ILS. Administration of DEHSPM by a constant s.c. osmotic pump infusion of 20 mg/kg/day gave poor results (46% ILS) when compared to a single i.p. injection of the same daily dose on days 1-6 (301% ILS).

As with DESPM, the length of treatment time was clearly critical. Animals treated i.p. with 5 mg/kg every 8 h on days 1-4 or 1-5 exhibited only about a 150% ILS, while animals given 2.5 mg/kg every 8 h on days 1-6 had a 242% ILS.

Studies employing a remote site of injection from the tumor site also gave excellent results. When the tumor was inoculated in a s.q. site and DEHSPM administered 12.5 mg/kg on days 1-6 by i.p. injection, there was a 429% ILS and half the mice survived 60 days.

Also, when mice were given i.p. tumor and treated by s.q. injection on days 1-6 with either 10 mg/kg every 12 h or 20 mg/kg once daily, there was a 457% ILS and 75% of the animals living >60 days.

Administration of DEHSPM, 5 mg/kg or 7.5 mg/kg every 8 h for days 1-8, was only moderately effective at inhibiting the growth of the solid B-16 melanoma tumor in C57Bl/6 mice. The mean tumor mass in treated mice at both dosages was 26% of the mass in control mice (26% T/C). The analogue was also shown to be effective at inhibiting the growth of the solid Lewis lung carcinoma in C57Bl/6 mice, exhibiting a 20% T/C at a dose of 5 mg/kg every 8 h for days 1-8.

Serum Levels in Mice

Serum levels of DESPM in CD-1 mice after a single i.p. injection of 25 mg/kg (62 μmoles/kg), indicated rapid adsorption of the drug from the peritoneum reaching peak serum levels of 48 μg/mL (120 μM) in 15 min (Fig. 3-22). Elimination from the serum was very rapid with a serum half-life of about 10 min and levels below detection after 120 min.

Excretion Studies in Rats

In the canulated rat model, DEHSPM was excreted from the body mainly by the kidneys after a single i.p. injection of DEHSP (25 mg/kg) (Fig. 3-23). The drug decreased the urine and bile flow during the first 3 h after injection as compared to control animals so that appreciable sample volumes were not collected until the 6-h fraction and the majority of the analogue was excreted in the 9- and 12-h fractions of the urine. As a dose of 25 mg/kg (58 μmoles/kg)

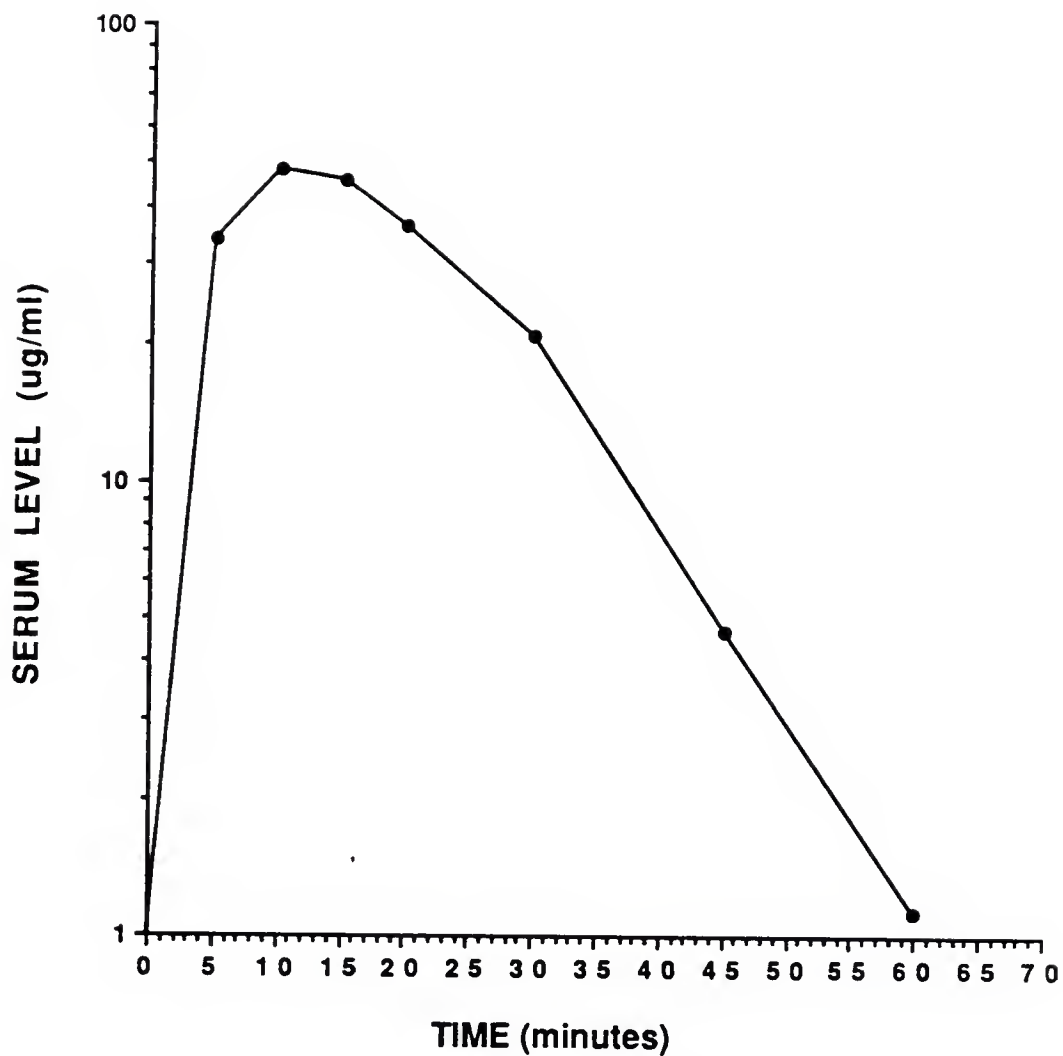Figure 3-22. Serum levels of DESPM in CD-1 mice after a single i.p. injection of 25 mg/kg. Analysis was performed on serum samples from duplicate animals at each time point.
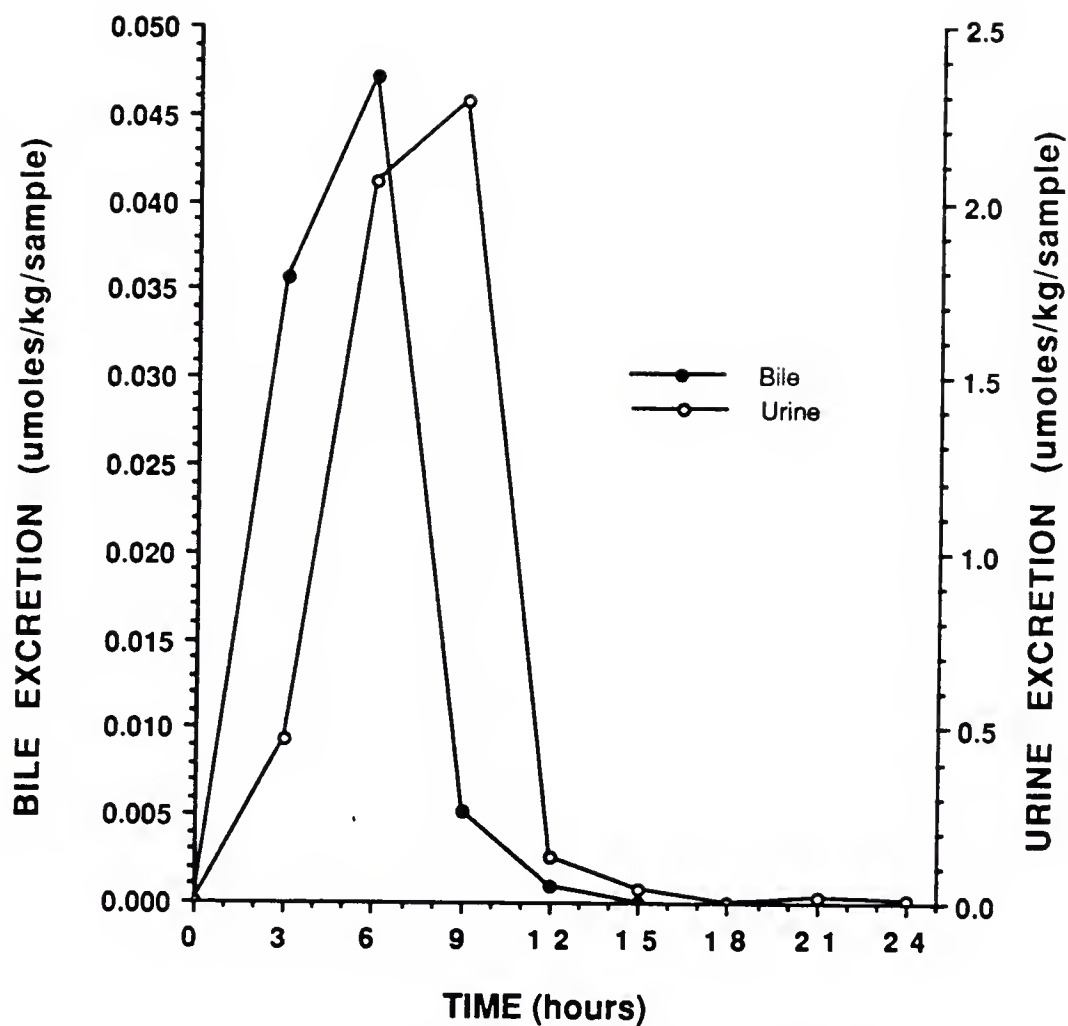
Figure 3-23. Excretion of DEHSPM in rat urine and bile, collected in 3 h fractions, after a single i.p. injection of 25 mg/kg (58 μmoles/kg). Analysis was performed on urine and bile samples from duplicate animals at each time point.

was administered and the mean cumulative excretion in the urine and bile totaled about 5.1 μmoles/kg (Fig. 3-24), less than 10% of the dose administered was excreted unchanged from the body in 24 h.

Toxicity Studies

Acute single-dose i.p. toxicity in CD-1 mice for DESPM (Fig. 3-25) and DEHSPM (Fig. 3-26) was very similar. The LD_{10}, LD_{50} and LD_{90} doses for DESPM were determined to be 200, 385 and 475 mg/kg, respectively, and for DEHSPM, 250, 330 and 475 mg/kg, respectively. Animal deaths, at acute toxic doses for both compounds, occurred by what appeared to be respiratory paralysis within 10 min after administration, and were unrelated to the gastrointestinal toxicity and weight loss seen on chronic administration in the in vivo activity studies.

In chronic 5-day single-dose toxicity studies the i.p. LC_{10}, LD_{50} and LD_{90} doses for DESPM (Fig. 3-27) were determined to be 72, 83 and 100 mg/kg, respectively, and for DEHSPM (Fig. 3-28), 33, 37 and 52 mg/kg, respectively. Severe weight loss (>20% of original weight) was observed on the fifth day of treatment in all animals at toxic doses, and animals at lethal doses either recovered or died within one week of the final injection.

Discussion

The compounds described in this study are all in some way related to the natural products spermidine and spermine. They were designed to evaluate relationships which might exist between the
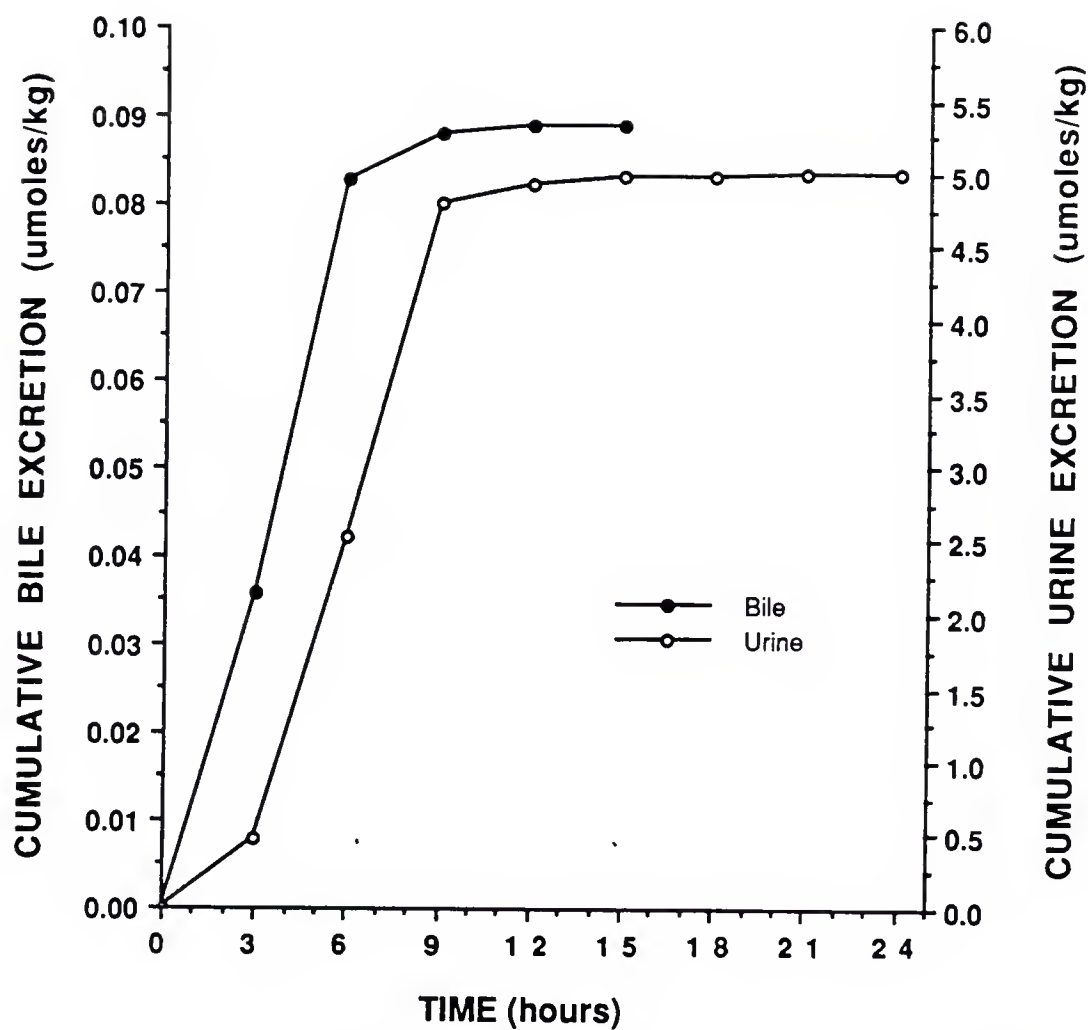
Figure 3-24. Cumulative excretion of DEHSPM in rat urine and bile after a single i.p. injection of 25 mg/kg (58 μmoles/kg).
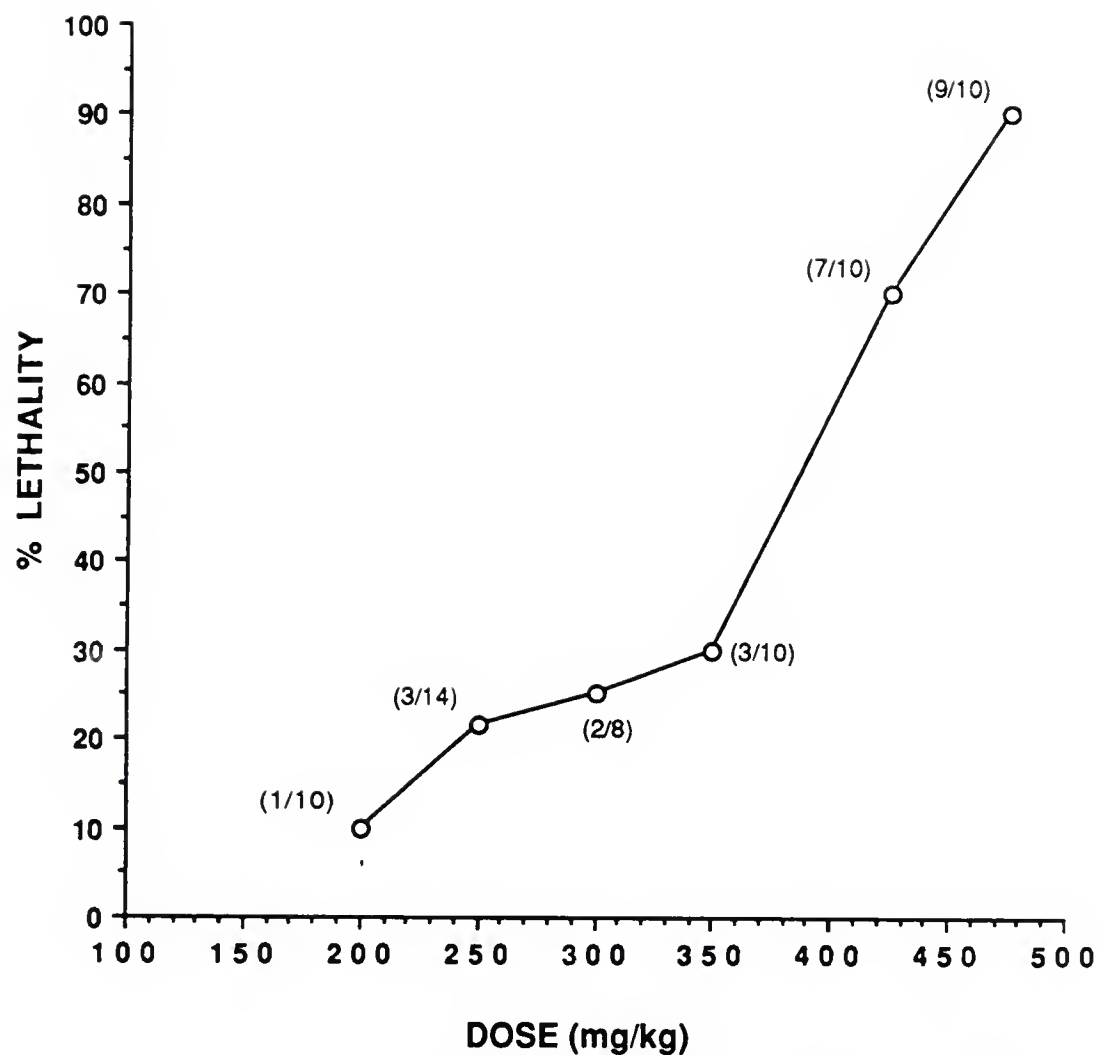
Figure 3-25.   Toxicity of DESPM in CD-1 mice after a single
i.p. injection (number of deaths/total number of animals).
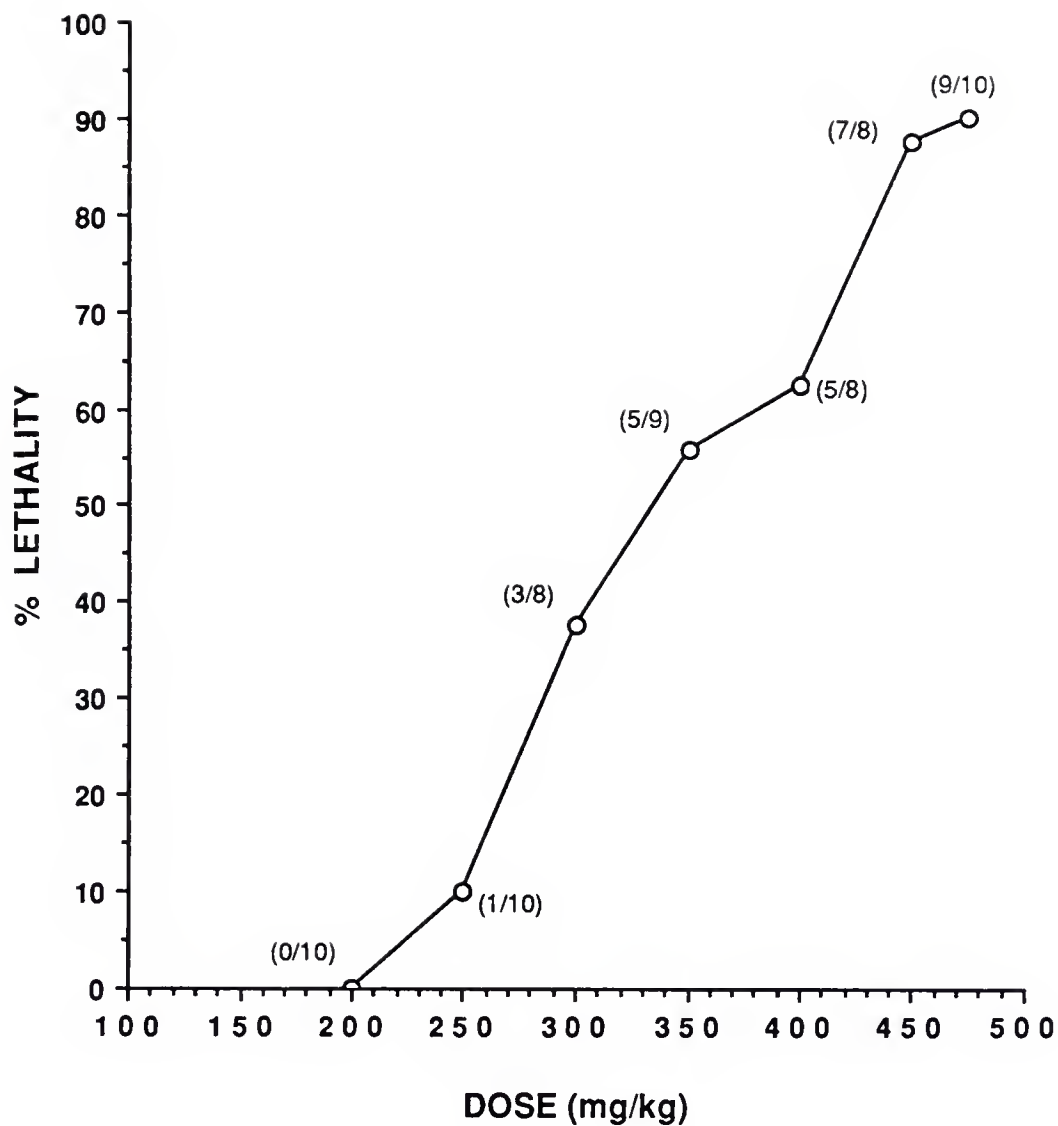
Figure 3-26. Toxicity of DEHSPM in CD-1 mice after a single i.p. injection (number of deaths/total number of animals).
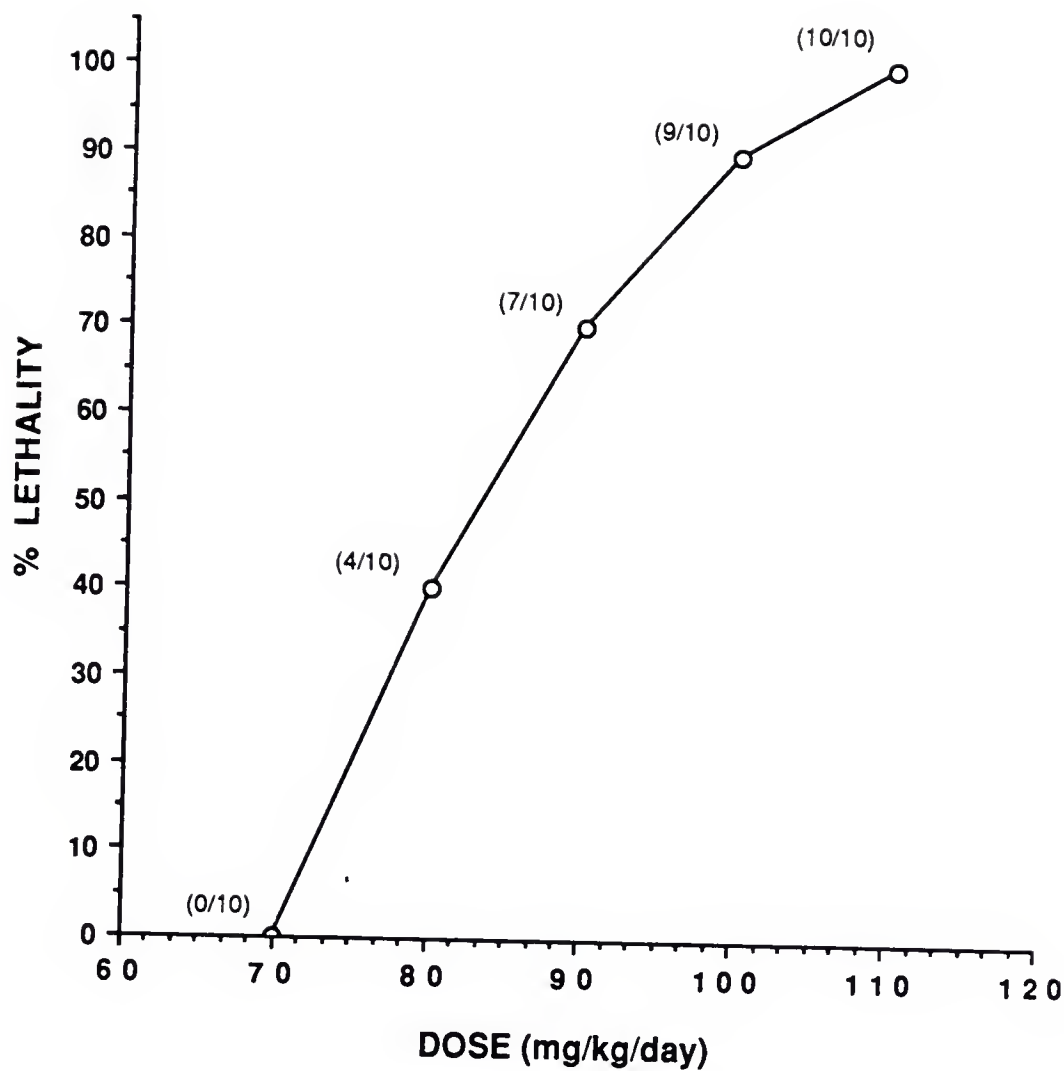
Figure 3-27. Toxicity of DESPM in CD-1 mice after a single daily i.p. injection for 5 consecutive days (number of deaths/total number of animals).
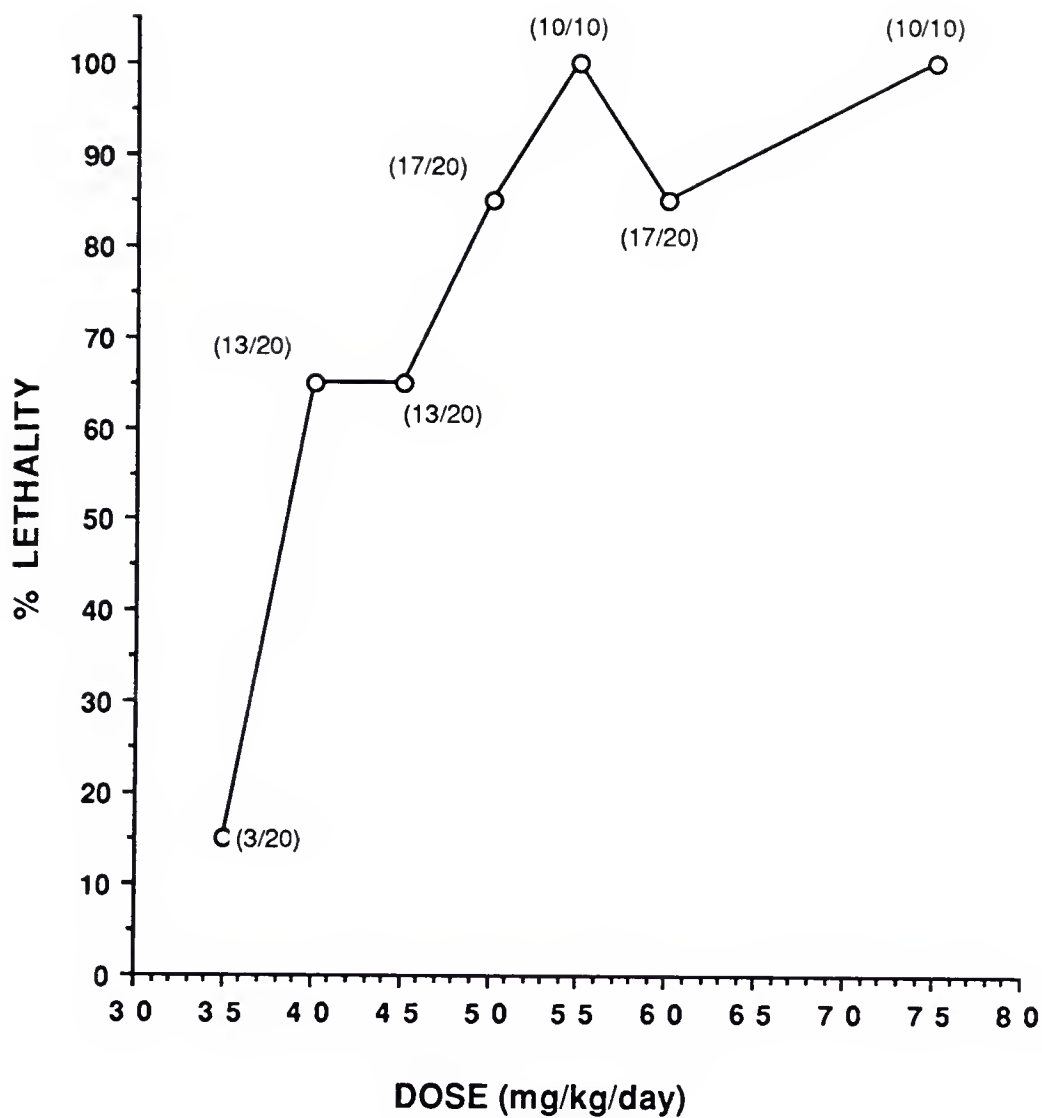
Figure 3-28. Toxicity of DEHSPM in CD-1 mice after a single daily i.p. injection for 5 consecutive days (number of deaths/total number of animals).

structure of various alkylated polyamine analogues and their activity against tumor cells in culture.

Although several of the analogues had 48-h 50% inhibitory concentrations (IC_{50}s) of less than 50 μM, the polyamine analogues generally took a significant period of time to exhibit their maximal effects on cell proliferation. Therefore, the 96 h IC_{50}s were selected for comparison and observed the general activity order: spermine analogues > YANK > spermidine analogues.

In a series of terminally N-alkylated spermidine analogues (Fig. 3-1), it is obvious that the presence of 3 nitrogens which are capable of being protonated at physiological pH, are necessary for activity. When the central nitrogen of the active BESPD is replaced by a methylene unit (BEDAO) or the pKa of the central nitrogen is decreased by the addition of a N^4-p-nitrophenyl group (BEPNPSPD) the antileukemic activity of the analogue is destroyed. These results are consistant with findings which demonstrated that N-acylated spermidine analogues were poor inhibiters of L1210 cell growth (59,65). The effect of N-alkyl chain length on activity showed BESPD > BPSPD. Additionally, the effect of methylene backbone length demonstrated the greater activity of BESPD over BENSPD. N^1,N^8-Diethylspermidine was the most active of the spermidine analogues tested against cultured L1210 cells, and was previously shown to decrease the intracellular concentrations of ornithine decarboxylase and spermidine and putrescine (65,66,69).

In comparing the spermine compounds (Figs. 3-2 and 3-3) with their spermidine counterparts, it is clear that the spermine compounds are substantially more active against L1210 cells. This is in keeping with the findings that DESPM had a far greater impact on polyamine biosynthesis and the polyamine biosynthetic enzymes than the spermidine analogues (100). The spermine compound reduced the level of intracellular polyamine pools as well as decreasing both ODC and AdoMetDC levels.

The results with L1210 cells clearly suggest that monoalkylation of both of the terminal primary nitrogens of spermine is important for antiproliferative activity. The terminally alkylated polyamines DMSPM, DESPM, and DPSPM are all more active than either the tetraalkylated spermine, TESPM, or the internally dialkylated spermine, IDESPM.

The effect of the N-alkyl chain length on the activity of spermine analogues showed ethyl > propyl >> methyl; and the dibenzyl analogue, while cytotoxic at higher concentrations, was not active at lower concentrations. As was observed in the spermidine derivatives, when the basicity of the terminal nitrogens is reduced by the addition of trifluoroethyl groups (FDESPM), there is no substantial activity. Furthermore, when the two central nitrogens of spermine are replaced by methylenes, while each of the terminal nitrogens maintains its alkyl group (DEDAD), there is a substantial loss in activity against L1210 cells even though the distance between the terminal nitrogens is approximately maintained. When the distance

between the two central nitrogens of DESPM is shortened by incorpor-
ating the nitrogens in a 1,4 piperazine system, the compound's anti-
proliferative activity essentially disappears despite the fact that
an analogue with internal tertiary nitrogen atoms, NTESPM, does
retain discernible activity. Extension of the DESPM backbone result-
ing in the hexaamine, YANK, demonstrated L1210 cell growth inhibitory
activity similar to that of DMSPM, DESPM, and DPSPM. Finally, the
role of the methylene backbone in the antiproliferative activity of
the spermine analogues demonstrates DEHSPM > DESPM > DENSPM.

The most active of all compounds tested were the spermine ana-
logues, DEHSPM and DESPM. Both of these polyamine analogues demon-
strated a broad spectrum of activity in the range of 0.1 to 1.0 μM
against several animal and human cultured cell lines, and appeared to
be related to the doubling time of the cells.

The development of drug resistance is often a limiting factor
in cancer chemotherapy and is compounded by the fact that drug-
resistant tumor cells often show cross resistance to structurally
unrelated drugs (101). These multidrug resistant (Mdr) cell lines
apparently utilize an energy dependent system to actively expell the
drug from the cell (102,103). Several of the Mdr cell lines have
been characterized by the increased amount of a 150-170 kd membrane
glycoprotein (P150-170 glycoprotein) and a 140 kb region of amplified
DNA whose level of amplification correlates with the level of drug
resistance (97-99). The Mdr cell lines DC3F/ADX and L1210/DOX-0.6

(96) showed colateral sensitivity with their parental cell lines to DESPM and DEHSPM. The ability of L1210 cells to develop resistance to the polyamine analogues is, apparently, unrelated to the Mdr phenomena as L1210/DES-10 and L1210/HDES-1 cells showed no increase in P140-180 glycoprotein or related amplified DNA regions (96) and were equally sensitive as their parental lines to Adriamycin. This lack of cross-resistance between the polyamine analogues and Mdr-cells may be of some possible clinical significance.

The incubation of 1 mM aminoguanidine, a serum diamine oxidase inhibitor (93), along with DESPM in culture with L1210 cells had no significant effects on cell growth or mtDNA content. It is important that the activity of the polyamine analogues was not decreased by an inhibitor of diamine oxidase. This enzyme catalyzes the catabolism of acetylated spermidine and spermine to oxidation products which have been postulated (104) to be responsible for the antiprolifera-tive activity of the natural polyamines. Presumably, the analogues are not substrates for the enzyme so that the toxic end products, 3-acetamidopropanal and acrolein, were not produced.

Unlike cytotoxic drugs, the dose-response curves for the con-centration dependence of growth inhibition at 48 h (Fig. 3-4) are un-usually flat over a large concentration range for DESPM and DENSPM. The cytostatic nature of the growth inhibition of the two compounds is seen in trypan blue exclusion (Fig. 3-9) and Rh-123 mitochondrial uptake studies (Figs. 3-10 and 3-11). At the approximate 48-h IC_{50} values, DESPM treatment does not exhibit significant cell death until after 96 h, while exposure to DENSPM is not cytotoxic until 144 h.

Even though DEHSPM is much more active over a wider range of concentrations and demonstrates greatly reduced cell viability at 144 h, significant cytotoxicity is not seen until after 96 h of treatment.

Although the analogues did not appear to demonstrate direct cytotoxicity, cells exposed to DESPM and DEHSPM at their 48-h IC_{50}s for greater than 72 h were unable to proliferate when incubated in drug-free medium (Figs. 3-14 and 3-15). This may indicate some earlier lethal event caused by the analogue from which the cells cannot recover.

Flow cytometric analysis of L1210 cells after treatment with 10 μM DESPM for 48 h and 96 h showed cell populations with only slightly decreased S-phase and G_2-phase nDNA content compared with controls (Fig. 3-17). Cells exposed to 30 μM DENSPM or 0.6 μM DEHSPM showed similar changes in nDNA with time. This was not consistent with a decrease in cell growth caused by blocking progression of cells through any particular phase of the cell cycle. It appeared that the cells were slowing throughout the entire cell cycle, as if they no longer had sufficient energy to synthesize DNA and divide. A significant number of cells accumulating at the G_1/S border was seen only after 144 h of treatment.

The relationship between cell doubling and mtDNA content, seen in Figure 3-19, is consistent with a mechanism in which DESPM inhibition of mtDNA replication causes a depletion in mtDNA content with cell division until a quantity insufficient to support continued cell growth remains. Similar results have been obtained in studies of the

action of MGBG on L1210 cells in vitro (105). The resultant decrease in mtDNA due to the polyamine analogues undoubtedly causes secondary effects on cellular energy production. These results suggest that although the cells are alive, they simply do not have sufficient energy to support normal growth and division, although other explanations are certainly feasible. It is possible that secondary effects on energy production contribute to the decrease in cell size with treatment time of the polyamine analogues. It is interesting that the effect on mtDNA occurs while nDNA synthesis is unaffected. Similar differentiated effects on mtDNA have been observed with MGBG (106).

The antiproliferative activity of the polyamine analogues may be related to their ability to inhibit mtDNA, and the analogue's antimitochondrial action may be a better means of assessing the compound's antiproliferative action than cell growth studies. The relative ranking of the IC_{50}s of DMSPM < DESPM < DPSPM is reflected in their antimitochondrial effects as shown in Figure 3-20. It would require approximately 5 times the concentration of DPSPM to see the same reduction in mtDNA as 1 μM DESPM in a 72-h exposure, while DMSPM has little effect at concentrations of up to 10 μM. At 100 μM the less active spermidine analogue, BESPD reduced mtDNA content to only 66% of control L1210 cells after a 72-h incubation.

The striking effects of the polyamine analogues on the mitochondria and growth of the L1210 cells may not be exclusively accounted for by depletion of intracellular polyamine pools and polyamine biosynthetic enzymes. Depletion of intracellular polyamine

pools by DFMO, a specific inhibitor of polyamine biosynthesis, is shown to be apparently unrelated to inhibition of mtDNA synthesis. In addition to being an inhibitor of polyamine biosynthesis, MGBG has been shown to inhibit mtDNA synthesis. This effect may be directly correlated in a dose-dependent manner with selective mitochondrial ultrastructural damage (106), and its antimitochondrial activity, not alterations in polyamine pools, has been postulated as the major antiproliferative effect of MGBG (107).

Incubation of L1210 cells for 48 h with N^1,N^4-bis(ethyl)putrescine (BEP), BESPD and DESPM were found to cause reduced levels of intracellular putrescine, spermidine and spermine (100). The time course for the effect of 100 μM DESPM on cells (Fig. 3-21), however, demonstrates that while the concentrations of the native polyamines spermine, spermidine and putrescine decrease the total concentration of polyamines, including the analogue, remains approximately the same in the 24 h experiment.

The possibility must be considered that the inhibitory effects of the analogues could be due to interference at critical binding sites normally occupied by the native polyamines. It is interesting to speculate on the nature of these binding sites. Numerous electrostatic interactions of polyamines have been reported with macromolecules, including nucleic acids and certain proteins (108,109). Along with the histones, polyamines appear to be present in the nucleus in quantities sufficient to neutralize 15-30% of the nDNA anionic charges (110). Histone acetyltransferases also possess polyamine acetylation activity, and it has been suggested that histone and

polyamine acetylation function in concert to lower the stability and change the conformation of the nucleosome core, thus facilitating replication and transcription (111). Areas of histone acetylation have been correlated with active areas of nDNA replication and transcription (112). Neutralization of cationic charges by acetylation of the natural polyamines may function to lower the stability and allow changes in the conformation of certain critical binding sites, facilitating their normal activity and function. The terminally N-alkylated polyamines, however, are evidently not substrates for the acetyltransferases, since there is no evidence of acetylation of the secondary amines of spermine or spermidine (108). Thus, while polyamine analogues may be able to enter the cell and replace the natural polyamines at their binding sites, they are not acetylated. In this way the polyamine analogues would prevent any structural modifications necessary for normal activity and function of these critical areas, and in a sense, the polyamine analogue would "overstabilize" the site.

It is interesting that BESPD (70) as well as MGBG (113) (which has also been proposed to replace natural polyamines at intracellular binding sites (114) and also would not be a substrate for the acetyltransferases) cause several hundred-fold induction of the N^1-acetyltransferase. It may be proposed that the induction is due to the cell's inability to acetylate and displace the analogue from the critical "overstabilized" site. This increase in acetylase enzyme may also help to deplete intracellular polyamine pools by interconversion pathways of acetylated spermine and spermidine to putrescine and elimination of putrescine from the cell (100).

While nDNA activity does not appear to be affected by the analogues at an early point, the mitochondria may be one site at which

these compounds act to regulate cell growth. Mitochondrial DNA, being circular and without histones (115), may require polyamines to a greater degree than nuclear chromatin for its stabilization, and therefore, may be more sensitive to the effects of the polyamine analogues.

Despite the apparent similarities in cellular effects, the polyamine analogues differ from DFMO and MGBG in important ways. Namely, the analogues do not result in compensatory increases in Ado-MetDC activity as seen with DFMO or increases in ODC activity as is the case with MGBG. Preliminary studies suggest that BESPD (66) and DESPM (116) do not act to inhibit AdoMetDC or ODC activity directly but rather regulate the enzymes at a translational and/or post-translational level by the same mechanisms as spermidine. These points of enzyme regulation may indicate additional sites where natural polyamines may be replaced by the analogues.

The analogues, DESPM and DEHSPM were shown to have significant activity against L1210 ascites tumor growth in DBA/2 mice. The results with DESPM (Table 3-2) clearly demonstrated a dose-response relationship, with i.p. administration of 15 mg/kg every 8 h for 6 days having the optimum effect of the schedules tested. At this dose animals had an average increase in ILS of greater than 376% with 60% long term survivors.

The results with DEHSPM (Table 3-3) clearly demonstrated a dose-response relationship, with i.p. administration of 5 mg/kg

every 8 h on days 1-6 having the optimum effect of the schedules
tested. At this dose animals had an average ILS of greater than
500%, with 90% of the test animals alive after 60 days and no sign of
tumor.

The dosing schedule was critical and possibly related to cell
doubling time. This is in keeping with our observations in cell cul-
ture. Irreversibility of cell growth inhibition in culture required
that the cells be exposed to the drug for a minimum of 96 h. This
suggesting that in the short-term dosing animal experiments the cells
were not exposed to the drug long enough to irreversibly inhibit
their proliferation.

Studies employing a remote site of injection from the tumor
site also gave excellent results. The s.q. treatment of i.p. L1210
tumor, and the i.p. treatment of s.q. L1210 tumor were equally
effective as i.p. tumor treated by i.p. injection of an equivalent
dose of DEHSPM. In addition, DEHSPM was shown to be moderately
effective at inhibiting the growth of the solid B-16 melanoma tumor
and Lewis lung carcinoma in C57B1/6 mice.

Not only was the in vivo activity of DEHSPM shown to be sub-
stantially greater than that of DESPM (on a milligram basis) but
DEHSPM was shown to be a better and safer drug. At dosages of 2.5 to
7.5 mg/kg every 8 h for 6 days, DEHSPM had good activity without
significant toxicity. This demonstrated a wider dosage range of
activity than DESPM, which was active only in the dose range of 10-15
mg/kg every 8 h for 6 days, while 17.5 mg/kg every 8 h for 6 days

showed signs of toxicity. Also, at a constant total dose of DESPM, decreasing the dosing schedule from 3 times daily to twice daily greatly reduced the effectiveness. However, DEHSPM showed significant activity at a constant daily dose whether given on a one, two, or three times daily schedule. While DEHSPM was shown to be more toxic (on a milligram basis) it has a better therapeutic index (toxic dose/active dose) than DESPM. The total dose necessary for the LD_{50} (for the 5-day toxicity) was divided by the total dose of the analogue necessary to produce a significant ILS as a quick indicator of therapeutic index. For example, to produce a 269% ILS required DEHSPM 10 mg/kg every 8 h for 6 days (180 mg total dose) and the total dose for the 5-day LD_{50} was 415 mg, yielding a value of 2.3 as the index for DESPM. To produce a 242% ILS it required DEHSPM 2.5 mg/kg every 8 h for 6 days (45 mg total dose) and the total dose for the 5-day LD_{50} was 185 mg, yielding an index of 4.1. At doses necessary to yield a comparable ILS against the L1210 tumor, DEHSPM had 1.75-2 times better therapeutic index than DESPM.

Preliminary studies have shown that DESPM is rapidly adsorbed from the peritoneal cavity of the mouse, reaching peak serum levels in 15 min. As expected, the water soluble highly charged analogue is rapidly cleared from the serum, exhibiting a serum half-life of approximately 10 min. With these kinetics it was surprising, even though animals were dosed 3 times daily, that the compounds were

active. The excretion studies demonstrate, however, that while some of the drug is eliminated from the body at an early time point (mainly in the urine) it is probably highly tissue bound and a large fraction of the dose administered remains in the animal. Apparent decreased excretion of the analogue due to metabolism to an unknown product is very unlikely in light of present knowledge of polyamine metabolism (108). Further pharmacokinetic, metabolic and organ distribution studies are needed to optimize the dosage schedule of the analogues to maximize effectiveness and minimize toxicity.

CHAPTER IV
CONCLUSION

The microbial iron catecholamide chelators (siderophores) and the N-alkyl polyamine analogues have been shown to be effective agents in controlling the growth of cancer cells.

The hexacoordinate catecholamide chelators, parabactin and vibriobactin, were the most active of the ligands tested. When L1210 and Daudi cells were exposed to the siderophores, parabactin and vibriobactin, cell growth was essentially halted. Both these siderophores have IC_{50} values of less than 2 μM, with reversible cytostatic activity on short-term exposure and cidal activity on long-term exposure.

The siderophores are also shown to be potent antiproliferatives with activity in the micromolar range against a broad range of other cultured cell lines, e.g., murine B-16 melanoma, CHO cells, HL-60 cells and HFF cells.

The catecholamide siderophores demonstrated their ability to control cellular proliferation by inhibiting normal iron utilization by cells. Preliminary studies with the catecholamides had demonstrated their ability to block DNA synthesis through the inhibition of the iron dependent enzyme ribonucleotide reductase. The antiproliferative activity of the chelators has now been clearly associated with their ability to chelate iron. Methylation of the

145

catechol hydroxyl groups of parabactin and vibriobactin, or addition of equalmolar amounts of Fe(III) to the medium along with the chelators resulted in a loss of their cell growth inhibitory activity.

Others have shown that the rate of removal of iron from serum transferrin by iron chelators is relatively slow when compared to the very early inhibitory effects of the catecholamide chelators on L1210 cell growth and DNA synthesis. The ligand's antiproliferative activity and DNA synthesis inhibition, however, is little affected by serum concentrations in the growth medium. These studies provide strong arguments for catecholamide interference with iron utilization by chelation at an intracellular site rather than the extracellular removal of iron from transferrin in the medium.

Flow cytometric analysis reveals that the catecholamide chelators, parabactin and vibriobactin, block DNA synthesis with cells accumulating at the G_1-S border of the cell cycle. On removal of the chelator, the cell cycle block is released resulting in a cell cycle synchronization. Parabactin, a relatively nontoxic microbial iron chelator, was a more potent cell cycle synchronization agent than either hydroxyurea or desferrioxamine, with a portion of the cell population remaining synchronized for 3 cell cycles. Parabactin produces a similar cell cycle block and synchronization in mice with ascites L1210 tumor.

The catecholamides act as potent cell blocking and cell cycle synchronization agents and in proper combination may enhance the

effects of phase-specific antineoplastics such as ara-C, Adriamycin, or BCNU. However, the time frame for the drug combination is critical. This enhancement effect, while offering some potential advantage in the design of combination chemotherapy protocols, has not been demonstrated <u>in vivo</u>. The search for drug combinations which give better differential activity between the antineoplastic alone and antineoplastic in combination with the chelators, as well as the synthesis of a potent water soluble chelator is currently under investigation.

The terminally bis-alkylated polyamines evaluated in this study were highly effective in controlling the growth of rapidly proliferating cells. It is clear that the spermine compounds are substantially more active against L1210 cells than the corresponding spermidine derivatives. DESMP and DEHSPM were the most potent compounds with regard to inhibition of L1210 cells; they were also active against a variety of human and animal tumor cell lines <u>in vitro</u> with IC_{50}s of less than 1 μm in all cases.

The Mdr cell lines showed collateral sensitivity with their parental cell lines to DESPM and DEHSPM. Resistance to the polyamine analogues is, apparently, unrelated to the Mdr phenomena and resistant cells were equally sensitive as their parenteral lines to Adriamycin. This lack of cross-resistance between the polyamine analogues and Mdr-cells may be of some possible clinical significance.

Although the analogues did not appear to demonstrate direct cytotoxicity, the ability of treated cells to proliferate when

incubated in drug-free medium was dependent on time of exposure to the drug. This may indicate some earlier lethal event caused by the analogue from which the cells cannot recover.

Changes in nDNA content of polyamine treated cells were not consistent with a decrease in cell growth caused by blocking progression of cells through any particular phase of the cell cycle.

On exposure of L1210 cells to the active polyamine analogues, mtDNA was depleted. The decrease was consistent with a lack of synthesis coupled with continued cell division in the first few days after treatment. These results suggest that although the cells are alive, they simply do not have sufficient energy to support normal division, although other explanations are certainly feasible. The striking effects of the polyamine analogues on the mitochondria of the L1210 cells may be independent of depletion of intracellular polyamine pools and polyamine biosynthetic enzymes.

Exposure of L1210 cells to polyamine analogues, at concentrations which cause growth inhibition, decreased cell size substantially, a decrease that continued with exposure time. This phenomena may be due to secondary energy effects caused by mtDNA inhibition.

Small changes in the structure of the polyamine analogues, e.g. DENSPM vs. DESPM vs. DEHSPM, and DMSPM vs. DESPM vs. DPSPM, have pronounced effects on the ability of the analogues to control the growth of L1210 cells. An understanding of the differences in activity among the various polyamine analogues is not only likely to help reveal the mechanism of the drug's action, but also to provide

valuable information as to the biochemical role of polyamines in cellular function.

In evaluating the effects of the polyamine analogues on polyamine pools, although the concentrations of the polyamines spermidine, spermine and putrescine are altered over a 24 h exposure, there is an approximate conservation in total cellular polyamine content (spermidine, spermine, putrescine and analogue). Conservation of the total intracellular polyamines is consistant with polyamine analogue replacement of the natural polyamines at intracellular sites.

Furthermore, these compounds were highly effective in extending the life span of DBA/2 mice with murine L1210 leukemia. The analogues, DESPM and DEHSPM, were shown to have significant activity against L1210 ascites tumor growth in DBA/2 mice. The results clearly demonstrated a dose-response relationship in activity. At optimum dosage and treatment schedules both analogues demonstrated significant increases in life span with a large percentage of "cures." Similar activity was seen when the analogue was injected at a site remote from the tumor. DEHSPM was also moderately effective at inhibiting the growth of the solid tumors, B-16 melanoma and Lewis lung carcinoma, in vivo.

Not only was the in vivo activity of DEHSPM shown to be substantially greater than that of DESPM but DEHSPM was also shown to be a better and safer drug. DEHSPM demonstrated a wider dosage range of activity than DESPM, and had significant activity when given as a one, two, or three times daily dosing schedule. While DEHSPM was

shown to be more toxic on a per milligram basis, it has a better therapeutic index than DESPM.

Preliminary studies indicate that the polyamine analogues are rapidly adsorbed from the peritoneal cavity of the mouse and rapidly cleared from the serum. The drugs are eliminated from the body, mainly in the urine, however, they are presumably highly tissue bound.

The activity against mouse tumor models and moderate toxicity of the N-alkylated polyamine analogues qualify them for further study as to the mechanism of action, pharmacokinetics, metabolism and activity against human tumors in mice, and for eventual human clinical testing as antineoplastics.

The catecholamide iron chelators and N-alkyl polyamine analogues have both been shown to be potent agents for the control of neoplastic cell growth. Both classes of agents are currently under investigation for their ability to control growth in other proliferative processes.

REFERENCES

1. Hider, R.C. Structure and Bonding, 58: 25-87 (1984).

2. Neilands, J.B. Ann. Rev. Nutr., 1: 27-46 (1981).

3. Venuti, M.C., Rastetter, W.H., and Neilands, J.B. J. Med. Chem., 22: 123-124 (1979).

4. Neilands, J.B. Ann. Rev. Nutr., 50: 715-731 (1981).

5. Harris, W.R., Carrano, C.J., Cooper, S.R., Sofen, S.F., Avdeef, A.E., McArdle, J.V. and Raymond, K.N. J. Am. Chem. Soc. 101: 6097-6104 (1979)..

6. Schwarzenback, G., Anderegg, G., and L'Eplattenier, F. Helv. Chim. Acta, 46: 1400-1409 (1963).

7. Aisen, P. and Listowsky, I. Ann. Rev. Biochem., 49: 357-393 (1980).

8. Masson, P.L. and Heremans, J.F. Comp. Biochem. Physiol. B., 39: 119-129 (1971).

9. Ducsay, C.A., Buhi, W.C., Bazer, F.W., and Roberts, R.M. Biol. Reprod., 26: 729-743 (1982).

10. Crichton, R.R., Roman, F. and Roland, F. FEBS Lett., 110: 271-274 (1980).

11. Rogers, H.J. Infect. Immun., 7: 445-456 (1973).

12. Heubeb, H.A. and Finch, C.A. Blood, 64: 763-767 (1984).

13. Newman, R., Schneider, C., Sutherland, R., Vodinelich, L. and Greaves, M. Trends Biochem. Sci., 215: 397-400 (1982).

14. Weinberg, E.D. Nutr. and Cancer, 4: 223-233 (1983).

15. Larrick, J.W. and Cresswell, P. J. Supramolec. Struct., 11: 579-586 (1979).

16. Mattia, E., Krishnamurity, R., Shapiro, D.S., Sussman, H.H. and Klansner, R.D. J. Biol. Chem., 259: 2689-2692 (1984).

17. Rao, K., Harford, J.B., Rouault, T., McClelland, A., Ruddle, F.H. and Klausner, R.D. Molec. Cell. Biol., 6: 236-240 (1986).

18. Weinberg, E.D. Physiol. Rev., 64: 65-102 (1984).

19. Garibaldi, J.A. J. Bacteriol., 110: 262-265 (1972).

20. Hann, H.L., Stahlhut, M.W. and Blumberg, B.S. Cancer Res., 48: 4168-4170 (1988).

21. Bergeron, R.J., Streiff, R.R. and Elliott, G.T. J. Nutrition, 115: 369-374 (1985).

22. Amann, R.W., Muller, E., Bansky, J., Schuller, G. and Hacki, W.H. J. Gastroenterol., 15: 733-736 (1980).

23. Hibbs, J.B., Jr., Taintor, R.R. and Vaurin, F. Bioch. Biophys. Res. Comm., 123: 716-723 (1984).

24. Drapier, J.C. and Hibbs, J.B. J. Clin. Invest., 78: 790-797 (1986).

25. Kameyama, T., Takahashi, A., Kurasawa, S., Ishizuka, M., Okami, Y., Takeguchi, T., and Umezawa, H. J. Antibiot. (Japan), 40: 1664-1670 (1987).

26. Reichard, P. and Ehrenberg, A. Science, 221: 514-519 (1983).

27. Thelander, L., Eriksson, S. and Akerman, M. J. Biol. Chem., 255: 7426-7432 (1980).

28. Thelander, L., Graslund, A. and Thelander, M. Biochem. Biophys. Res. Comm., 110: 859-865 (1983).

29. Takeda, E. and Weber, G. Life Sci., 28: 1007-1014 (1981).

30. Bergeron, R.J., Accounts. Chem. Res., 19: 105-113 (1986).

31. Bergeron, R.J., Kline, S.J., Stolowich, N.J., McGovern, K.A. and Burton, P.S. J. Org. Chem., 46: 4524-4529 (1981).

32. Bergeron, R.J., Garlich, J.R. and McManis, J.S. Tetrahedron, 41: 507-510 (1985).

33. Tait, G.H. Biochem. J., 146: 191-197 (1975).

34. Griffiths, G.L., Sigel, S.P., Payne, S.M. and Neilands, J.B. J. Biol. Chem., 259: 2997-3002 (1984).

35. Shindelman, J.E., Ottmeyer, A.E. and Sussman, H.H. Int. J. Cancer, 27: 329-334 (1981).

36. Walker, R.A. and Day, S.J. J. Pathol., 148: 217-224 (1986).

37. Bergeron, R.J., Cavanaugh, P.F., Jr., Kline, S.J., Hughes, R.G., Jr., Elliott, G.T. and Porter, C.W. Biochem. Biophys. Res. Comm., 121: 848-843 (1984).

38. Cavanaugh, P.F., Jr., Porter, C.W., Tukalo, D., Frankfurt, O.S., Pavelic, Z.P. and Bergeron, R.J. Cancer Res., 45: 4754-4759 (1985).

39. Bergeron, R.J., Burton, P.S., McGovern, K.A., St. Onge, E.J. and Streiff, R.R. J. Med. Chem., 23: 1130-1133 (1980).

40. Thelander, L. and Reichard, P. Ann. Rev. Biochem., 48: 133-158 (1979).

41. Hoffbrand, A.V., Ganeshaguru, K., Hooten, W.L. and Tattersall, M.H.N. Brit. J. Haematology, 33: 517-526 (1976).

42. Testa, U., Louache, F., Titeux, M., Thomopoulas, P. and Rochant, H. Brit. J. of Haematology, 60: 491-502 (1985).

43. Cory, J.G. and Fleischer, A.E. Cancer Res., 39: 4600-4604 (1975).

44. Heby, O. Differentiation, 19: 1-20 (1981).

45. Tabor, C.W. and Tabor, H. Ann. Rev. Biochem., 53: 749-790 (1984).

46. Bachrach, U., Kaye, A., Chayen, R. (Eds) Advances in Polyamine Research, Vol. 4, Raven Press, New York, 1983.

47. Janne, J., Poso, H., Raine, A. Biochim. Biophys. Acta, 473: 241-293 (1978).

48. Pegg, A.E. Biochem. J., 234: 249-262 (1986).

49. Pegg, A.E. and McCann, P.P. Am. J. Physiol., 243: C212-C221 (1982).

50. Pegg, A.E. Cancer Res., 48: 759-774 (1988).

51. Russell, D.H. and Durie, B.G.M. (Eds) Progress in Cancer Research and Therapy, Vol. 8, Raven Press, New York, 1978.

52. Seppanen, P., Alhonen-Hongisto, L., Janne, J. Eur. J. Biochem., 110: 7-12 (1980).

53. Sjoerdsma, A., Schechter, P.J. Clin. Pharm. and Therap., 35: 387-300 (1984).

54. Marton, L. Med. Biol., 59: 448-457 (1981).

55. Metcalf, B.W., Bey, P., Danzin, C., Jung, M.J., Casara, P.,
     Vevert, J.P. J. Am. Chem. Soc., 100: 2551-2553 (1978).

56. Seppanen, P., Alhonen-Hongisto, L., Janne, J. Biochim. Biophys.
     Acta, 674: 169-177 (1981).

57. Janne, J., Alhonen-Hongisto, L., Seppanen, P., Simes, M. Med.
     Biol., 59: 448-457 (1981).

58. Alhonen-Hongisto, L., Seppanen, P. and Janne, J. Biochem. J.,
     192: 941-945 (1980).

59. Porter, C.W., Bergeron, R.J. and Stolowich, N.J. Cancer Res., 42:
     4072-4078 (1982).

60. Bergeron, R.J., McGovern, K.A., Channing, M.A. and Purton, P.S.
     J. Org. Chem., 45: 1589-1592 (1980).

61. Bergeron, R.J., Burton, P.S., McGovern, K.A. and Kline, S.J.
     Synthesis, 9: 732-733 (1981).

62. Bergeron, R.J., Stolowich, N.J. and Porter, C.W. Synthesis, 8:
     689-692 (1982).

63. Bergeron, R.J. and Garlich, J.P. Synthesis, 9: 782-785 (1984).

64. Bergeron, R.J., Garlich, J.R. and Stolowich, N.J. J. Org. Chem.,
     49: 2997-3001, 1984.

65. Porter, C.W., Cavanaugh, P.F., Stolowich, N., Ganis, B., Kelly,
     E., Bergeron, R.J. Cancer Res., 45: 2050-2057 (1985).

66. Porter, C.W., Berger, F.G., Pegg, A.E., Ganis, B., Bergeron, R.J.
     Biochem. J., 242: 433-440 (1987).

67. Casero, R., Bergeron, R.J., Porter, C.W. J. Cell. Physiol., 121:
     476-482 (1984).

68. Porter, C.W. and Bergeron, R.J. Science, 219: 1083-1085 (1983).

69. Porter, C.W., Ganis, B., Vinson, T., Marton, L.J., Kramer, D.,
     Bergeron, R.J. Cancer Res., 46: 6279-6285 (1986).

70. Erwin, B.G. and Pegg, A.E. Biochem. J., 238: 581-587 (1986).

71. Casero, R., Go, B., Theiss, H., Smith, J., Baylin, S.B., and Luk,
     G.D. Cancer Res., 47: 3964-3967 (1987).

72. Bergeron, R.J., Elliott, G.T., Kline, S.J. and Ramphell, R. Antimicrob. Agents and Chemo., 24: 725-730 (1983).

73. Chou, T.C. and Talalay, P. Trends in Pharmacol. Sci., 4: 450-454 (1983).

74. Bernal, S.D., Shapiro, H.M. and Chen, L.B. Int. J. Cancer, 30: 219-224 (1982).

75. Thornwaite, J.T., Sugerbaker, E.V. and Temple, W.J. Cytometry, 1: 229-237 (1980).

76. Braylan, R.C., Benson, N.A. and Nourse, V.A. Cancer Res., 44: 5010-5012 (1984).

77. Dolbeare, F., Gratzner, H., Pallavicini, M.G. and Graw, T.W. Proc. Natl. Acad. Sci. U.S.A., 80: 5573-5577 (1983).

78. Becton Dickinson Monoclonal Antibody Sourcebook, Section 3.80.1, Becton Dickinson Immunocytometry Systems, Mountain View, CA.

79. Grabstein, K. and Chen, Y.U., In Vitro Immune Responses, in Selected Methods in Cellular Immunology. B.B. Mishell and S.M. Shiigi (Eds), W.H. Freedman and Co., San Francisco, CA, 1980.

80. Krankoff, I.H., Brown, N.C. and Reichard, P., Cancer Res. 28: 1559-1565 (1968).

81. Frankfurt, O.S., J. Cell. Physiol., 107: 115-122 (1980).

82. Carrano, C.J. and Raymond, K.N. J. Amer. Chem. Soc., 101: 5401-5404 (1979).

83. Konopka, K. and Neilands, J.B. Biochem., 23: 2122-2127 (1984).

84. Lederman, H.M., Cohen, A., Lee, J.W.W., Freedman, M.H. and Gelfand, E.W., Blood, 64: 748-753 (1984).

85. Moran, R.E. and Straus, M.J., Cancer Treat. Rep., 64: 81-86 (1980).

86. Furth, J.J. and Cohen, S.S., Cancer Res., 28: 2061-2067 (1968).

87. Nicolini, C., Biochim. Biophys. Acta, 458: 243-282 (1976).

88. Goodman, L.S. and Gilman, A. The Pharmacological Basis of Therapeutics, 5th ed., Macmillan Publishing Co., Inc., New York, 1975.

89. Bjerkvig, R., Oredsson, S.M., Marton, L.J., Linden, M., and Deen, D.F., Cancer Res., 43: 1497-1500 (1983).

90. Goldin, A., Vende, H. Jim, MacDonald, J.S., Muggia, F.M., Henney, J.E. and Devita, U.T. Jr., Europ. J. Cancer, 17: 129-142 (1981).

91. Skipper, H., Schabel, F.M. Jr. and Wilcox, W.S., Cancer Chemo. Reports, 35: 1-111 (1964).

92. In Vivo Cancer Models, 1976-1982, U.S. Department of Health and Human Services, National Institutes of Health. Publication No. 84-2635, p. 33 (1984).

93. Shore, P.A. and Cohn, V.H. Biochem. Pharmacol., 5: 91-95 (1960).

94. Raynor, L.O., Bortell, R. and Neims, A.H. Fed. Proc. Fed. Am. Soc. Exp. Biol., 46: 1001 (1987).

95. Schwartz, A., Sugg, H., Ritter, T.W. and Fernandez-Repollet, E., Cytometry, 3: 456-458 (1983).

96. Personal communication, Dr. J.L. Biedler.

97. Beidler, J.L., Hansjorg, R., Peterson, R.H. and Spengler, B., J. Nat. Cancer Instit., 55: 671-677 (1975).

98. Beidler, J.L., Chang, T., Meyers, M.B., Peterson, R.H. and Spengler, B.A., Cancer Treat. Reports, 67: 859-867 (1983).

99. Scotto, K.W., Beidler, J.L. and Melera, P.W., Science, 232: 751-755 (1986).

100. Porter, C.W., McManis, J., Casero, R. and Bergeron, R.J., Cancer Res. 47: 2821-2825 (1987).

101. Ames, G.F., Cell, 47: 323-324 (1986).

102. Skovsgaard, T., Cancer Res., 38: 1785-1791 (1978).

103. Inaba, M., Kobayashi, H., Sakurai, Y. and Johnson, R.K., Cancer Res., 39: 2200-2203 (1979).

104. Seiler, N., Bolkenius, F.N. and Rennert, O.M., Med. Biol., 59: 334-346 (1981).

105. Bortell, R., Raynor, L.O. and Neims, A.H., Fed. Proc. Fed. Am. Soc. Exp. Biol., 46: 999 (1987). Detailed manuscript in preparation.

106. Feuerstein, B., Porter, C.W. and Dave, C., Cancer Res., 39: 4130-4137 (1979).

107. Pleshkewych, A., Kramer, D.L., Kelly, E. and Porter, C.W., Cancer Res. 40: 4533-4540 (1980).

108. Seiler, N., Can. J. Physiol. Pharmacol., <u>65</u>: 2024-2035 (1987).

109. Marton, L.J. and Feuerstein, B.G., Pharm. Res., <u>3</u>: 311-317 (1986).

110. McCormick, F. In: <u>Advances in Polyamine Research</u>, R.A. Campbell, D.R. Morris, D. Bartos, G.D. Daves, Jr. and F. Bartos (Eds.), Vol. 1, Raven Press, New York, 1978.

111. Morgan, J.E., Blankenship, J.W. and Matthews, H.R., Biochemistry, <u>26</u>: 3643-3649 (1987).

112. Simpson, R.T., Cell, <u>13</u>: 691-699 (1978).

113. Pegg, A.E., Erwin, B.G., and LoPersson, Biochem. Biophys. Acta, <u>842</u>: 111-118 (1985).

114. Block, J.B., Field, M. and Oliverio, V.T., Cancer Res. <u>24</u>: 1947-1951 (1964).

115. Fink, I. and Petijohn, D.E., Nature (Lond.), <u>253</u>: 62-63 (1975).

116. Porter, C.W. and Bergeron, R.J. In: <u>Advances in Enzyme Regulation</u>, G. Weber (Ed.), Vol. 27, Pergamon Press, Inc., New York, 1988.
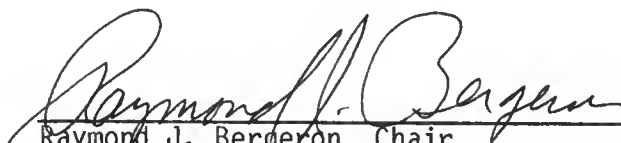
BIOGRAPHICAL SKETCH

Michael J. Ingeno was born in Upper Darby, Pennsylvania, in 1953. After receiving his B.Sc. in chemistry from the Philadelphia College of Pharmacy and Science, he went on to receive his M.Sc. at the Institute of Paper Chemistry in Appleton, Wisconsin. He obtained his B.Sc in pharmacy from Philadelphia College of Pharmacy in Philadelphia, where he practiced as a staff pharmacist for four years and was a member of the nutritional support team.

Among the awards he has received are the Freshman and Junior chemistry awards, and the American Chemical Society Philadelphia Section's Scholarship Achievement Award while graduating with "meritorious honors." During his graduate studies he was a finalist in the Excellence in Graduate Research Award and has numerous publications.

After completion of his Ph.D. in medicinal chemistry from the University of Florida, Michael J. Ingeno and family will reside in Basel, Switzerland, while he is holding a postdoctoral position with Ciba-Geigy Ltd.
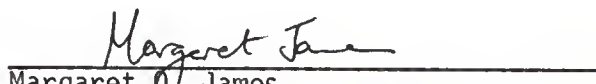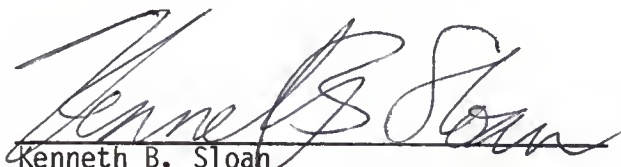
I certify that I have read this study and that in my opinion it conforms to acceptable standards of scholarly presentation and is fully adequate, in scope and quality, as a dissertation for the degree of Doctor of Philosophy.

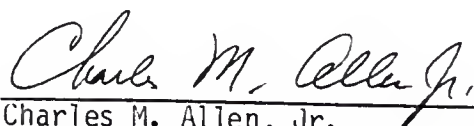Raymond J. Bergeron, Chair
Professor of Medicinal Chemistry

I certify that I have read this study and that in my opinion it conforms to acceptable standards of scholarly presentation and is fully adequate, in scope and quality, as a dissertation for the degree of Doctor of Philosophy.

Richard R. Streiff
Professor of Medicinal Chemistry

I certify that I have read this study and that in my opinion it conforms to acceptable standards of scholarly presentation and is fully adequate, in scope and quality, as a dissertation for the degree of Doctor of Philosophy.

Margaret O. James
Associate Professor of Medicinal
Chemistry

I certify that I have read this study and that in my opinion it conforms to acceptable standards of scholarly presentation and is fully adequate, in scope and quality, as a dissertation for the degree of Doctor of Philosophy.

Kenneth B. Sloan
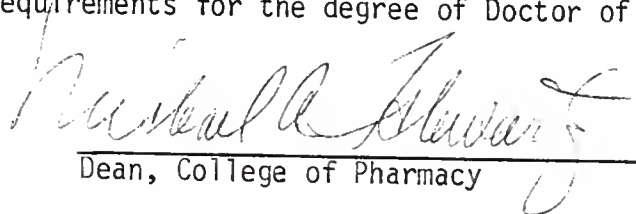Associate Professor of Medicinal
Chemistry

I certify that I have read this study and that in my opinion it conforms to acceptable standards of scholarly presentation and is fully adequate, in scope and quality, as a dissertation for the degree of Doctor of Philosophy.

Charles M. Allen, Jr.
Professor of Biochemistry and Molecular Biology

This dissertation was submitted to the Graduate Faculty of the College of Pharmacy and to the Graduate School and was accepted as partial fulfillment of the requirements for the degree of Doctor of Philosophy.

December 1988

Dean, College of Pharmacy

Dean, Graduate School